HYDRAULIC PROPERTIES OF AGGREGATED OIL SAND MATERIAL FROM THE ATHABASCA DEPOSIT

A Thesis

Submitted to the College of Graduate and Postdoctoral Studies

In Partial Fulfillment of the Requirements for the Degree of

Master of Science

In the Department of Soil Science

University of Saskatchewan

Saskatoon

By

Eric John Neil

PERMISSION TO USE

In presenting this thesis in partial fulfillment of the requirements for a Postgraduate degree from the University of Saskatchewan, I agree that the libraries of the university may make it freely available for inspection. I further agree that permission for the copying of this thesis in any manner, in whole or in part, for scholarly purposes may be granted by the professor who supervised the thesis work or, in their absence, by the Head of the Department or the Dean of the College in which the thesis work was completed. It is understood that due recognition shall be given to the author(s) and to the University of Saskatchewan in any scholarly use of any material in this thesis. It is also understood that any copying, publication, or use of this thesis or parts thereof for financial gain, is prohibited without the author's written permission. Requests for permission to copy or to make other use of the materials in this thesis, in whole or in part, should be addressed to:

Head of the Department of Soil Science

University of Saskatchewan

51 Campus Drive

Saskatoon, Saskatchewan

S7N 5A8 Canada

DISCLAIMER

Reference made in this thesis to any specific commercial product, process, or service by trade name, trademark, manufacturer, or otherwise, does not constitute or imply its endorsement, recommendation, or favouring by the University of Saskatchewan. The views and opinions of the author expressed herein do not reflect those of the University of Saskatchewan, and shall not be used for advertising or product endorsement purposes.

ABSTRACT

Of crucial importance to the reclamation of oil sands mining-affected areas, is creation of a soil medium capable of supporting a target ecosystem. A considerable portion of these landscapes contain coarse-textured soils, which have poor water retention. Furthermore, many soils naturally contain oil sand, and little is known of its effects on the surrounding soils. The key objectives of this thesis were to assess the soil water repellency (WR) and infiltration rates of aggregated oil sand material (AOSM) and surrounding soils from the Athabasca region, to understand their potential to modify the soil water dynamics of reclamation ecosystems. To evaluate the efficacy of discreet and composite salvaging techniques, the effects of salvage depth on the hydraulic properties of AOSM were also examined.

A correlation exists between AOSM salvage depth and extent of weathering, where near-surface deposits contain fewer petroleum hydrocarbons (PHC)s than at depth. This relationship confirms onion-skin weathering, where exposure to weathering and degradation is greater in the near-surface of the profile and on the surface of individual aggregates. The WR of AOSM was significantly greater than the surrounding soils, indicating potential for reduced absorption and conductivity. This was confirmed by an infiltration study, which showed AOSM have significantly lower infiltration rates than the surrounding soils. Therefore, AOSM may slow the flow of water through the profile, increasing water storage and providing additional plant-available water, potentially modifying the soil water regime and enabling the establishment of relatively productive ecosites. As salvage depth of AOSM increased (weathering decreased), PHC content and WR increased while infiltration rate decreased. Similarly, PHC content and WR increased with depth into individual AOSM. These results suggest interstitial PHCs are responsible for the enhanced WR and reduced infiltration rates. Therefore, as AOSM continues to weather and its PHCs are degraded and/or removed, its hydraulic properties will likely become more similar to that of the surrounding soils. The results of this study imply the benefits of discreet salvaging, where deep deposits containing relatively high levels of PHCs remain at depth after reclamation, avoiding the excessive drying and expression of WR often experienced in the near-surface.

ACKNOWLEDGEMENTS

I would like to extend my most sincere thanks to my supervisor, Dr. Bing Si. Your guidance and support throughout our time together has not only contributed to the development of my professional skills, but to who I am as a person. The mentorship and opportunities you have provided me have enriched my life and instilled in me, what I'm sure will be, a lifelong passion for science and research.

I would like to thank my graduate committee members Drs. Ian Fleming, Ken van Rees, and Derek Peak, whose steadfast efforts have undoubtedly improved the quality of my research and my contributions to the academic community. My thanks is also extended to Marty Yarmuch for his guidance in preparing and conducting my research activities. Also to Dr. Jeff Shoenau, who has always readily provided a friendly ear and kind advice, thank you.

A special thank you to those graduate students and researchers who have become near and dear to me over the past several years, and assisted me in countless ways – Trent Pernitsky, Mark Sigouin, Henry Chau, Carolyn Murray, Wei Hu, Katya Gudkova, Min Li, and Ivanna Faucher. Your friendship, and the memories of our time together, will be with me wherever I go.

Most importantly, my deepest appreciation goes out to my family – my parents Diane and Jack, and siblings Jaycie and Garrett. Your love, friendship, support, and encouragement have been with me every step of the long journey that has been my education. Words cannot convey the love and admiration I have for each of you.

Finally, to Kristen Nicole Dubé, my soulmate and life partner, who has shown me what I truly cherish in life, thank you for everything you do and everything you are to me.

TABLE OF CONTENTS

LIST OF TABLES

LIST OF FIGURES

LIST OF NOMENCLATURE

α	Inverse capillary length scale
θ_v	Volumetric soil water content
Ψ	Pore suction
ANOVA	Analysis of variance
AOSM	Aggregated oil sand material
ASCS	Aurora Soil Capping Study
ATR-FTIR	Attenuated total reflectance Fourier transform infrared
B/C	Blended B/C horizons salvage
Bm	Upper subsoil Bm horizon salvage
BTEX	Benzene, toluene, ethylene, xylene
CA	Contact angle
CCME	Canadian Council of Ministers of the Environment
COSIA	Canada's Oil Sands Innovation Alliance
CV	Coefficient of variation
EtOH	95% ethanol
FC	Field capacity
K_{fs}	Field-saturated hydraulic conductivity
PAH	Polycyclic aromatic hydrocarbon
PHC	Petroleum hydrocarbon
SS	Composite subsoil salvage
TDR	Time domain reflectometry
TOC	Total organic carbon
WDPT	Water drop penetration time
WR	Water repellency

1. INTRODUCTION

1.1 Background

As conventional oil and gas reserves become depleted, other energy sources must be obtained and utilized (Hein et al., 2016). Four of the major unconventional energy resources which are available in North America are heavy oil, bitumen sands, oil shales, and coal-bed methane (Hein et al., 2016). Of the total global resources of bitumen sand or "oil sand", the vast majority (>70%) are located in the Western Canada Sedimentary Basin of Alberta and Saskatchewan (Hein et al., 2016). For Canada, as well as the rest of the world, this is an enormous resource which faces considerable challenges regarding sustainable development, especially in light of the potential for greenhouse gas emissions and other economic and environmental concerns (Hein et al., 2016).

The oil sands region of Northern Alberta contains the vast majority of Canadian oil sands resources and consists of the Athabasca, Peace River, and Cold Lake areas which contain a total of fifteen individual deposits that are estimated to hold 27 billion m^3 (170 billion barrels) of crude oil reserves, underlying an area of approximately 142,000 km^2 (Fig. 1.1) (Gosselin et al., 2010; Government of Alberta [GOA], 2016). Large scale commercial mining operations commenced in the region in the late 1960's and have since grown considerably (Gosselin et al., 2010). The removal of oil sand material is accomplished either through in situ extraction or open pit surface mining (Johnson & Miyanishi, 2008; GOA, 2009). Deep deposits, which account for approximately 80% of the available oil sands, are accessible only through in situ extraction methods such as cyclic steam stimulation and steam-assisted gravity drainage, which use steam to heat and liquefy the oil, allowing it to be pumped to the surface (GOA, 2009; GOA, 2016). The remaining shallow materials can be reached through surface mining, and are limited to a region within the Athabasca deposit, near Fort McMurray, AB (Fig. 1.1) (GOA, 2016). In recent years, in situ extraction has been the prevalent method, accounting for 57% of the total oil sands oil production in 2015 (GOA, 2016). The in situ processes are energy expensive, but beneficial due to the relatively small ecological footprint (GOA, 2016). Historically

however, surface-mining has been responsible for the majority of oil production in the oil sands region, and is the method that has the most complete and long-term impact on ecosystems (Johnson & Miyanishi, 2008). Although in situ methods are gaining popularity, surface-mining continues to be an active practice. In 2015, surface-mining was responsible for 43% of the total oils sands oil production, and is projected to experience a 49% increase in overall production by 2030 (GOA, 2016).

Figure 1.1. Map of the Oil Sands Region of Western Canada. (http://appstore.capp.ca/oilsands/page/oil-sands-2012-01-23-03-01-45)

The near-surface deposits which are accessible through surface-mining underlie approximately 4,800 km^2 of land surface (GOA, 2016). As of August, 2016, over 900 km^2 of this land had been disturbed by oil sands mining operations (GOA, 2016). In accordance with Alberta's Environmental Protection and Enhancement Act, oil sands mining companies are mandated to reclaim disturbed land and ensure land capability equivalent to that which existed prior to disturbance (Cumulative Environmental Management Association, 2006). One of the requisite components of reclamation is the placement of appropriate substrate and soil capping materials. These may include tailings sands that are recovered during the bitumen extraction process, as well as the overburden materials which

have been previously removed in order to access the oil sand reserves (Rooney & Bayley, 2011). A soil survey performed on dominantly coarse-grained Brunisolic soils of over 1,000 oil sands sites in the Athabasca oil sands region revealed that petroleum hydrocarbon (PHC)-affected materials (oil sand), in the form of aggregates and layers, are naturally present in the upper three meters of the soil profile at approximately half of the sites (Leskiw et al., 2006). Because the available reclamation materials may originate from the near-surface, they have the potential to contain portions of oil sand. These PHC-bearing materials may have the ability to hinder the recovery and maintenance of reclamation ecosystems by suppressing plant roots, soil organisms, and soil processes (Visser, 2008b).

In a recent study based in the Athabasca oil sands region, Fleming (2012) found that the potential for oil sand aggregates to cause hydrocarbon contamination and toxicity of soils and surrounding water bodies was limited. In almost all cases, PHC concentrations of saturated and drained soils and leachate were well within acceptable limits for soils and groundwater, according to the Canadian Council of Ministers of the Environment (CCME) (2008) Canada-Wide Standard for Petroleum Hydrocarbons in Soil (Fleming, 2012). Although there appears to be limited potential for PHC toxicity of soils and groundwater, it is possible that other soil physical and hydrological processes may be affected by the presence of oil sand inclusions. It has been observed that areas above oil sand-affected soils seem to experience increased soil water contents (Leskiw et al., 2006; Fleming, 2012). Furthermore, it has been speculated that, depending on the location of oil sand aggregates or layers within the soil profile, the soil water retention in the rooting zone may either increase or decrease as a result (Leskiw, 2005; Leskiw et al., 2006; Visser, 2008b; Fleming, 2012). There are two mechanisms that are thought to contribute to this phenomenon: (i) a reduction in pore space due to intrapore PHCs; and (ii) hydrophobicity due to the chemical composition of the PHCs. The PHCs within the pore structure of the oil sand are naturally immobile and reduce pore space, and as a result can greatly inhibit the flow of fluid through the material (Mossop, 1980). It is also thought that, because oil sand from the region is typically composed of relatively recalcitrant and insoluble PHCs, hydrophobicity may be present (Leskiw et al., 2006; Fleming, 2012). Both of these characteristics would enable PHC-

affected soils to act as a zone of low hydraulic conductivity, slowing the flow of water through the soil profile and increasing the residence time of water in the overlying soils.

1.2 Hypothesis and Objectives

It is hypothesized that oil sand aggregates (aggregated oil sand material [AOSM]) from the Athabasca oil sands region, have lower infiltration rates and greater hydrophobicity (water repellency) than the surrounding coarse-textured soils. Furthermore, AOSM which are nearer to the soil surface receive more exposure to weathering and degradation.

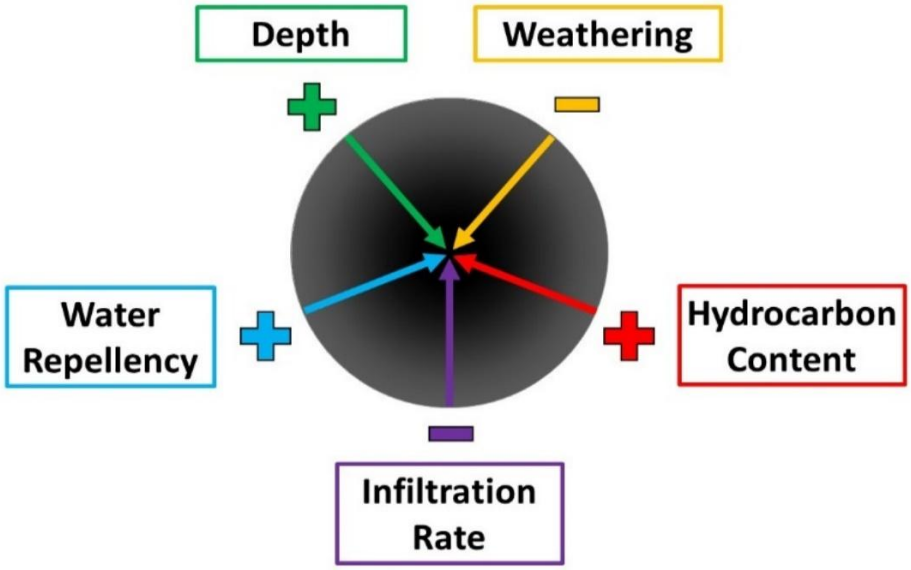

Figure 1.2. Proposed model for onion-skin weathering and hydraulic properties of aggregated oil sand material.

Therefore, it is also hypothesized that AOSM express onion-skin patterns of weathering and hydraulic properties, where PHC content and water repellency increase and infiltration rate decreases, with increasing salvage depth as well as with increasing depth into individual aggregates (Fig. 1.2). To address these questions, the following objectives were outlined:

1. Characterize the water repellency of AOSM and soils from various salvage depths.
2. Identify the infiltration rates of AOSM and soils from various salvage depths.
3. Evaluate the effects of salvage depth and depth of sampling into individual aggregates on the PHC content, hydrophobicity, and infiltration rates of AOSM.

1.3 Organization of Thesis

This thesis is composed in manuscript style, as a collection of articles submitted to peer-reviewed journals. Following this introduction is Chapter 2, the Literature Review, which outlines some of the challenges associated with oil sands mining reclamation and the materials found therein. Chapters 3 and 4 address Objectives 1 and 2 respectively, as well as provide insight into Objective 3. In Chapter 3, the degree and persistence of hydrophobicity of AOSM are determined through measurements of sessile drop contact angle (CA) and water drop penetration time (WDPT). Chapter 4 evaluates the infiltration rates of AOSM and surrounding soils through water and ethanol infiltration studies. Chapter 5, Synthesis and Conclusions, includes a summary and synthesis of the findings of Chapters 3 and 4, as well as relevant implications for the reclamation industry and recommendations for future research. For reader convenience and to minimize redundancy, Chapter 6 includes a single, combined list of works cited for all chapters in this thesis. The effects of AOSM inclusions in reclamation soils are briefly discussed in an auxiliary study included in Appendix B., The Effects of Aggregated Oil Sand Material on the Saturation, Drainage, and Field Capacity of Reclamation Soils, and are also touched upon in Chapters 3 through 5.

2. LITERATURE REVIEW

2.1 Athabasca Oil Sands Region

2.1.1 Climate and Soils

The oil sands of Northern Alberta reside within the Boreal Forest Natural Region of Alberta. This region experiences a cold continental climate, with short summers in which the average daily temperature exceeds 15 °C for only one or two months, and long, cold winters with daily temperatures below -10 °C for four months or more in most Natural Subregions (Natural Regions Committee, 2006). Precipitation follows a summer-high continental pattern, where 60 to 70% of the annual precipitation is received between April and August, with peak rainfall occurring in July (Natural Regions Committee, 2006). Extensive portions of the post-glacial landscape are composed of glaciofluvial and aeolian deposits, resulting in the development of coarse-textured Brunisolic and Luvisolic forest soils throughout much of the region (Natural Regions Committee, 2006). Additionally, many of these soils naturally contain portions of oil sand. The presence of oil sand in the near-surface is generally thought to be the result of erosional and depositional processes, which occurred approximately nine to ten thousand years ago during the drainage of glacial Lake Agassiz (Leskiw et al., 2006; Visser, 2008b). Its rapid draining resulted in the removal of oil sand from the McMurray Formation and subsequent deposition in glacial lakes and ponds which eventually receded, leaving behind soil materials with oil sand inclusions (Leskiw et al., 2006; Visser, 2008b).

2.1.2 Mine Site Reclamation

Due to the large-scale nature of the mining activities in the region, reclamation will involve the reconstruction of landforms and ecosystems at a landscape scale (Johnson & Miyanishi, 2008) (Fig. 2.1). In order to ensure equivalent capability of reclaimed areas, a number of factors are taken into consideration including landscape features such as landform, slope, aspect, hydrology, and soil stability, as well as the composition of the reclamation soils, and the revegetation and land-use targets

(Visser, 2008a). The goal in engineering new ecosystems from mining-disturbed land is not to re-create the landscape as it was pre-disturbance, but rather to construct a landscape which will provide habitat for living organisms, allowing them to sustainably develop (Johnson & Miyanishi, 2008). In the case of the oil sands region, primary land-uses are commercial timber production and wildlife habitat (Visser, 2008a), but may also include recreation as well as sources of traditional foods and medicinal plants (Oil Sands Vegetaion Reclamation Committee, 1998).

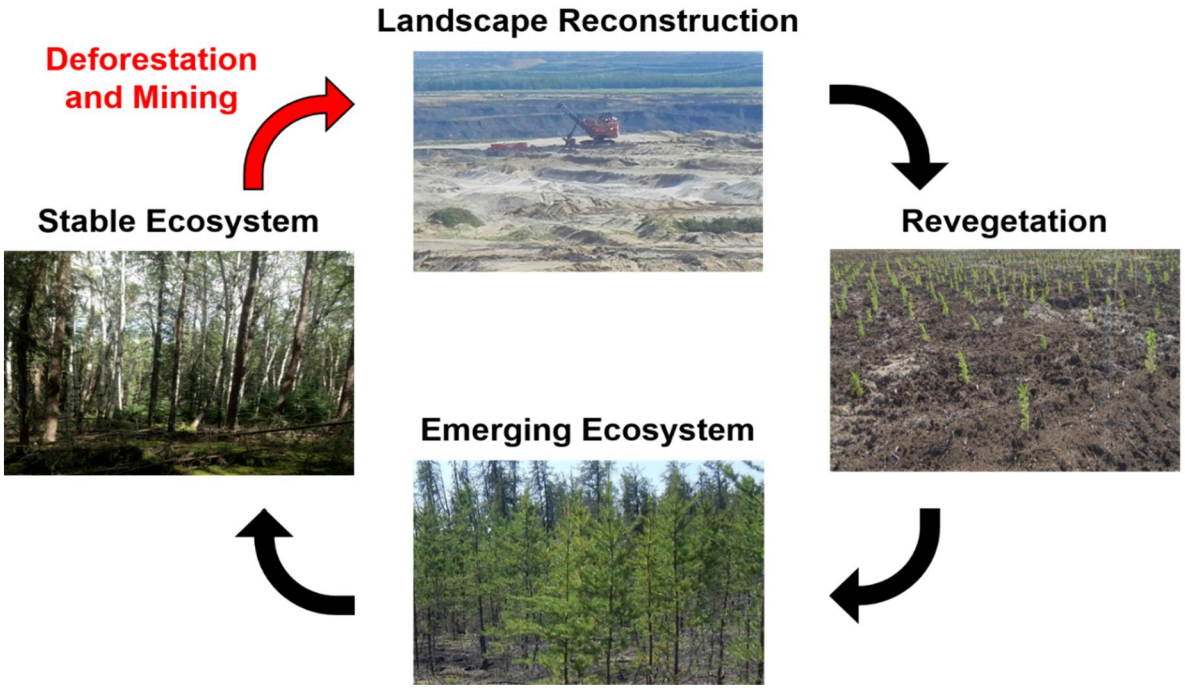

Figure 2.1. Oil sands surface mining and reclamation processes.

A fundamental component of reclamation is the creation of a soil medium which has the nutrient and water retention necessary to support a target ecosystem (Leatherdale et al., 2012). Soil materials available for reclamation can be arranged in various combinations, called prescriptions (Leatherdale et al., 2012). In order to optimize the effectiveness of soil prescriptions the compositions, depths, and sequence of layering must be considered (Huang et al., 2011b). Following extraction, oil sand bitumen can be upgraded to synthetic crude oil by removing carbon and sulfur and adding hydrogen (Johnson & Miyanishi, 2008; GOA, 2009). During processing and upgrading, several by-products are created including fluid fine tailings, sand tailings, petroleum coke, and elemental sulfur (Gosselin et al., 2010).

While tailings are one of the materials abundantly available for reclamation, they typically make an inappropriate medium for plant growth. This is due to its low water and nutrient holding capacities, as well as undesirable soil chemistry arising from residual bitumen compounds such as petroleum hydrocarbons (PHC)s and heavy metals (Naeth et al., 2011; Rooney & Bayley, 2011). Therefore, soil prescriptions must be composed of more suitable soil materials such as the lean oil sand, subsoil, topsoil, and peat which are removed in order to reach the oil sand deposits (Naeth et al., 2011).

2.2 Recreating Landscapes and Ecosystems

2.2.1 Reclamation Challenges

Due to the glacial and post-glacial history of the region, many of the materials overlying the oil sand reserves are coarse-textured glaciofluvial and aeolian deposits. As such, a considerable portion (20%) of the final reclaimed landscapes in the region will be composed of these materials (Huang et al., 2011b). Coarse-textured soils typically have high infiltration rates and hydraulic conductivities and low water-holding capacities (Leatherdale et al., 2012). Consequently, these materials also have relatively low nutrient-holding capacities, which could further limit the potential productivity of emerging and stable reclamation ecosystems. These properties make coarse-textured soils suitable for certain vegetation types such as jack pine, but less suitable for white spruce and trembling aspen for example, which require relatively high soil water contents (Zettl et al., 2011). Furthermore, because the majority of the precipitation in this region is received during the warmest months of the year, evapotranspiration may exceed precipitation, increasing the potential for soil water depletion and deficit.

Although many of the soils are consistently coarse-textured, they naturally exhibit a range of soil water and nutrient contents, and associated forest stand types (Zettl et al., 2011). These regions have traditionally supported a range of ecosite phases from relatively unproductive ‘a’ ecosites characterized by low nutrient holding capacities and subxeric moisture regimes, to that of more highly productive ‘d’ ecosites with submesic moisture and medium nutrient regimes (Beckingham & Archibold, 1996). The characteristics of the soils and relatively dry climate in the region present reclamation challenges with respect to supporting more highly productive ecosites. The wide range of

moisture regimes found in the naturally occurring coarse-textured soils suggests there are natural mechanisms controlling the moisture availability and associated forest stands which develop (Zettl et al., 2011). To ensure that reclamation soil prescriptions are capable of replicating the same range of moisture regimes and associated ecosites that existed prior to mining disturbance, these natural mechanisms must be understood (Zettl et al., 2011).

2.2.2 Aggregated Oil Sand Material

As mentioned, due to the depositional history in the region, many of the near-surface soils contain portions of oil sand. Because many of the available reclamation soils originate from the near-surface, they also have the potential to contain these PHC-affected materials. Aggregated oil sand material (AOSM), previously referred to as tarballs, are portions of oil sand that are naturally present in surface soils and subsoils, typically at depths of 50 cm to > 100 cm (Visser, 2008b). They are present as distinct balls or aggregates, typically millimeters to tens of centimeters in diameter, but may be up to several meters (Fleming, 2012). They also exists as bands which are millimeters to tens of centimeters in thickness and extend from centimeters to several meters in length (Fleming, 2012). AOSM from the Athabasca oil sands region are frequently similar in texture to their surrounding soils (Leskiw et al., 2006; Rosso, 2016); although, Fleming (2012) found they can contain significantly ($P < 0.05$) elevated silt and clay contents. Using the Canadian System of Soil Classification (Soil Classification Working Group, 1998), soils from the region are commonly classified as sand textured, but may be as fine as loamy sand (Fleming, 2012; Rosso, 2016). The total mass-based PHC content of AOSM from the Athabasca oil sands region is typically < 10%, with the majority (95%) composed of highly recalcitrant, high molecular weight hydrocarbons from the F3 (Carbon $[C]_{>16}$ - C_{34}) and F4 ($C_{>34}$) fractions, and the remainder from the relatively low molecular weight F2 ($C_{>10}$ - C_{16}), F1 (C_6 – C_{10}), and volatile (benzene, toluene, ethylene, and xylene [BTEX]) fractions (CCME, 2008) (Leskiw et al., 2006; Visser, 2008b, Fleming, 2012). However, Fleming (2012) also found that some AOSM samples contain “rich cores”, where the concentrations of all hydrocarbon fractions are orders of magnitude greater than that of typical AOSM.

Oil sand, particularly that from northern Alberta, has many unique structural and chemical properties compared to most other conventional oil reserves around the world. Oil sand bitumen is a mixture of molecular species consisting primarily of highly condensed polycyclic aromatic hydrocarbons (PAH) (Gosselin et al., 2010). In comparison to conventional and heavy oils, bitumen PHCs have a relatively high molecular weight, lower hydrogen to carbon ratio, and higher levels of sulfur, nitrogen, and metals such as nickel and vanadium (Gosselin et al., 2010). High grade Athabasca oil sands have porosities of 25 to 35%, which is considerably higher than most petroleum reservoir sandstones (Mossop, 1980). This high porosity is generally attributed to the lack of mineral cement, which in most sandstones, occupies a considerable amount of void space (Mossop, 1980). This lack of consolidation is why these deposits are called oil sands rather than oil-bearing sandstones (Mossop, 1980). Many oil sand deposits around the world are oil wet, meaning that the oil is in intimate contact with the mineral grain surfaces; whereas the Alberta oil sands are referred to as water wet (Mossop, 1980). These water wet deposits are composed of mineral grains surrounded by thin films of connate water, followed by the bitumen which protrudes into the pore spaces created by the mineral grain structure (Mossop, 1980; Takamura, 1982). The interstitial location of the PHCs suggests there may be potential for reduced porosity and pore connectivity, in comparison to PHC-free soil materials. Additionally, the highly recalcitrant and insoluble nature of the bitumen further increases the potential for hydrophobicity and soil water repellency (WR) (Page et al., 2000; Reid et al., 2000). Regardless of the mechanism(s), it is known that the bitumen in Alberta oil sand inhibits the flow of fluids through the porous medium created by its mineral grain structure (Mossop, 1980).

These qualities suggest that oil sand inclusions may have the ability to considerably modify the soil water dynamics of reclamation soil profiles through increased WR and reductions in absorption, conductivity, and storage of soil water. These oil sand inclusions could further complicate reclamation efforts and hinder the establishment of target ecosystems. It therefore, becomes important to understand the hydraulic properties of oil sand materials in order to prepare effective reclamation prescriptions.

2.2.3 Aurora Soil Capping Study

For years, oil sands mining companies have been making earnest efforts to prepare for post-mining reclamation. Many companies have launched research programs to improve our understanding of reclamation ecosystem development and sustainability (Johnson & Miyanishi, 2008). Among the most recent and significant contributors has been Canada's Oil Sands Innovation Alliance (COSIA). COSIA is a group of ten oil sands companies from the region, whose goal is to develop and share experience and intellectual property regarding the environmental sustainability and reclamation of oil sands impacted ecosystems.

In 2012 Syncrude Canada Ltd., a contributing member of COSIA, established a reclamation research site called the Aurora Soil Capping Study (ASCS). The site is located within the Athabasca oil sands region, at the Syncrude Canada Ltd. Aurora North Mine, north of Fort McMurray, AB (57° 19′ 20″ N, 111° 30′ 24″ W). The ASCS is a long-term, instrumented watershed research site designed to test the efficacy of various reclamation prescriptions which utilize coarse-textured, PHC-affected soil materials. This site provides several unique research opportunities. It is a landscape-scale site composed of multiple substrates and soil prescriptions, with the capability to instrument and monitor at landscape-scales over relatively long time spans (years to decades). Additionally, the ASCS incorporates soils which were salvaged and replaced in various depth increments. These different salvaging approaches were used to test the performance of various layering schemes, but also to compare the effects of discreet and composite salvaging techniques on the success of reclamation soil profiles.

Discreet salvaging is the removal and replacement of soil layers in relatively small, distinct soil horizons (e.g. 0-15 cm, 15-50 cm, 50-100 cm, 100-200 cm). Composite salvaging is the removal of relatively large portions of the soil profile with little consideration for material composition (e.g. 15-200 cm). It was thought that because the composition of the soils are fairly consistent with depth throughout large portions of the soil profiles, discreet salvaging may be unnecessary. In this case, composite salvaging and replacement may provide a reclamation option which is not only effective in promoting reclamation success, but is also economically and environmentally efficient. Composite salvaging

allows for a reduction in the activity of heavy machinery, which conserves resources as well as minimizes the ecological footprint of reclamation efforts through a reduction in associated green house gas emissions.

To address the objectives of the current study, the hydraulic properties of soils and AOSM from various discreet and composite salvages of the ASCS were determined. Not only will this provide an indication of the effects of AOSM on the soil water dynamics of reclamation soils, but also evaluates the effects of soil salvage depth and thickness (i.e. discreet vs. composite salvaging).

2.3 Soil Water Dynamics of AOSM-Affected Reclamation Soils

2.3.1 Soil Layering

By controlling the various factors which naturally affect water and nutrient availability, there is potential to customize reclamation prescriptions to suit desired ecosystems. There are several design strategies which may be used to optimize the water- and nutrient-holding capacities in primarily coarse-textured soils including textural layering (Huang et al., 2011a; Huang et al., 2011b; Zettl et al., 2011), soil compaction (Naeth et al, 2011; Pernitsky et al., 2016), and the addition of organic matter (Hudson, 1994).

Due to the availability of multiple soil materials in the region (subsoil, topsoil, peat, and lean oil sand overburden), there is an opportunity and in many cases a necessity, to include layering and textural/structural contrasts within the reclamation soil profiles. In recent years, layered systems have received considerable attention due to their popularity in engineered cover systems used in waste containment and mine waste storage (Huang et al., 2011a). Many soil reclamation designs also utilize textural layering in order promote the formation of flow barriers (Huang et al., 2011). Flow barriers are created in natural and reclaimed soils, under unsaturated conditions, as a result of textural and/or structural contrasts (Si et al., 2011). These contrasts produce discontinuities in soil hydraulic properties, potentially limiting the downward flow of water and chemicals (Si et al., 2011). Furthermore, by reducing percolation, flow barriers act to increase soil water storage capacity of the overlying soils, which is often beneficial for both natural and post-reclamation ecosystems in semi-arid regions such

as portions of the Alberta oil sands region (Huang et al., 2011a; Si et al., 2011). An increase in soil water storage is particularly beneficial when dealing with predominantly coarse-textured reclamation materials, which have high infiltration rates and saturated hydraulic conductivities and low soil water storage capacities. In the Athabasca oil sands region, the layering and resulting textural contrasts of coarse-textured soils of natural sites has shown to considerably enhance the available soil water-holding capacity, and provides the ability of texturally similar materials to support a wider range of moisture regimes and associated ecosite types as compared to texturally homogeneous soil profiles (Huang et al., 2011a; Huang et al., 2011b; Zettl et al., 2011). In addition to increasing the residence time of water in the soil, this decreased flow rate can lead to reduced nutrient loss from the soil profile and can also minimize the potential for groundwater contamination (Si et al., 2011).

Flow barriers can be further distinguished as hydraulic barriers and capillary barriers. Capillary barriers may form in soils with textural contrasts, such as where fine-textured soil is underlain by a coarser-textured soil (Naeth et al., 2011; Si et al., 2011). They may also form in texturally similar materials, where a more highly compacted layer overlies a less compacted layer (Naeth et al., 2011). In oil sands reclamation for example, capillary barriers form where tailings sand is capped with other finer-textured soils (Naeth et al., 2011). Water in the relatively small pores of the finer-textured capping material is held at high suction and will not permit flow into the larger pores of the underlying coarse-textured tailings sand where pore suction is lower (Naeth et al., 2011). As a result, water will be held in the finer, overlying soil layer until the water content is high enough (suction low enough) for water to flow into the underlying tailings (Naeth et al., 2011). In areas with soil water deficits (precipitation < potential evapotranspiration), capillary barriers can be beneficial to plant communities by limiting percolation out of the root zone and increasing plant available water (Naeth et al., 2011).

Hydraulic barriers can form where a coarse-textured soil is underlain by a finer-textured, or more highly compacted, soil. Typically, the finer-textured (or highly compacted) layer will have a lower hydraulic conductivity than that of the overlying coarse (lightly compacted) layer (Scott, 2000; Si et al., 2011). During infiltration, when the wetting front reaches the layer interface, the hydraulic conductivity decreases to that of the limiting (fine-textured; highly compacted) layer (Scott, 2000; Si et al., 2011).

Over time, water will accumulate just above the layer interface, resulting in an increased residence time of water within the overlying layer (Scott, 2000; Si et al., 2011). The hydraulic barrier effect can; therefore, provide plant available water in coarse soils where water is typically unavailable (Scott, 2000; Si et al., 2011). For example, in reclamation soil prescriptions composed of coarse-textured subsoils overlying highly compacted lean oil sand from the Athabasca oil sands region, Pernitsky et al. (2016) observed a considerably lower hydraulic conductivity in the lean oil sand layer, which resulted in an increase in soil water storage in the overlying subsoil.

In addition to the layering of various soils, the inclusion of PHC-affected materials such as AOSM could also create flow barriers and hydraulic discontinuities within the reclamation soil profiles. Furthermore, the bitumen within AOSM may be hydrophobic and promote soil water repellency, which could also create or contribute to hydraulic discontinuities.

2.3.2 Soil Water Repellency

Hydrophobic compounds in soils such as organically derived oils, are known to have the potential to produce soil water repellency, a surface property that reduces or prevents the absorption or infiltration of water into the soil (Dang-Vu et al., 2009; Müller & Deurer, 2011; Diehl, 2013). Depending on the location and site specific conditions, hydrophobic compounds may either enhance or diminish the soil water retention and hydraulic conductivity of the affected soil, and consequently affect the ecosystem present (Diehl 2013). Currently, our understanding of the causes of WR is still incomplete and appears as though its development is influenced by site-specific conditions. However, there seems to be a consensus that WR is most commonly caused by an accumulation of hydrophobic organic substances on the surfaces of soil particles (Müller & Deurer, 2011). It is well known that, in comparison to fine-textured soils, coarse-textured soils are particularly vulnerable to WR due to the relatively small surface area-to-volume ratio of their soil particles (Doerr et al., 2000). In other words, in coarser-textured soils, when introduced to a given amount of hydrophobic material, a greater volume of the soil particles may become coated and consequently exhibit WR. Finer-textured materials have a greater surface area to distribute the hydrophobic substances across and; therefore, smaller

volumes of the soil are affected. In addition to hydrophobic coatings, WR may also be caused by hydrophobic interstitial matter (Bisdom, 1993; Doerr et al., 2000). One hydrophobic compound which can both coat soil particles and fill soil pores, are petroleum hydrocarbons such as those contained within oil sand bitumen (Walker et al., 1976; Roy & McGill, 2000; Quyum et al., 2002; Buczko et al., 2006; Brassington et al., 2007; Adams et al., 2016). As mentioned, many of the available reclamation materials in the Athabasca oil sands region are coarse-textured, and furthermore, often contain coarse-textured oil sand inclusions (i.e. AOSM). In addition to their vulnerability due to their coarse texture, AOSM have an increased risk of hydrophobicity due to the chemical composition and interstitial location of the bitumen within.

Water repellency is a dynamic property because the soil water content can alter the wetting properties of the soil. In other words, WR changes with changing water content (i.e. wetting and drying). Typically, as a water repellent soil becomes drier, it becomes increasingly hydrophobic until reaching a maximum level at or near drought conditions (Doerr et al., 2000; Müller & Deurer, 2011; Diehl, 2013; Tillman et al., 1989). Similarly, water repellent soils experience a decrease in WR with time and exposure to water (Tillman et al., 1989). Because WR is dynamic, there are multiple properties that should be known in order to accurately predict WR, among the most important of which are the degree and persistence (Müller & Deurer, 2011). The sessile-drop contact angle (CA) of a water droplet on an air-dry material surface is a measure of the degree of WR, and represents the maximum WR that the material may experience after prolonged drought periods (Dekker & Ritsema, 1994; Müller & Deurer, 2011; Diehl, 2013). The persistence of WR refers to the time required for the WR to diminish and water to infiltrate (Müller & Deurer, 2011). During the wetting of a dry soil, the time required for the maximum CA of water on the soil surface to gradually decrease to zero and allow complete infiltration, is known as the persistence of WR (Müller & Deurer, 2011). The measurement of the time required for complete infiltration is often referred to as the water drop penetration time (WDPT) test (Dekker & Ritsema, 1994; Müller & Deurer, 2011). The critical water content is an additional criterion which can provide important information about the water repellent behaviour of the soil. The critical water content is the soil water content below which the degree and persistence of WR

are functions of the soil water content (Müller & Deurer, 2011). In other words, it is the soil water content below which the soil is hydrophobic and above which it is hydrophilic.

2.3.3 Hydraulic Properties of Aggregated Oil Sand Material

It is hypothesized that AOSM shows onion-skin patterns of weathering and hydraulic properties. Onion-skin weathering arises from greater exposure to weathering and degradation in materials located in the near-surface of the soil profile as well as on the outer portions of aggregates, resulting in near-surface aggregates and outer portions of individual aggregates which contain relatively small quantities of PHCs (i.e., drier in regards to PHC content). Because exposure of the aggregates to weathering progressively decreases with increasing depth into the soil profile as well as with increasing depth into the centers of aggregates, the materials contain progressively greater quantities of PHCs with depth into the soil profile and with depth into individual aggregates (i.e., wetter in regards to PHC content). Fleming's (2012) observations of AOSM with rich cores would also suggest this is the case, where the total amount of all PHC fractions were higher in the cores than the outer portions of the AOSM. This would indicate that, compared to the inner portions, the outer AOSM will likely have increased porosity (fewer interstitial PHCs) and reduced WR (fewer insoluble/water repellent PHCs), leading to an increase in hydraulic conductivity. Because the PHCs within Athabasca oil sand are present throughout the pore spaces of the material, pore connectivity may be limited. The plugging of soil pores typically results in decreased water infiltration rates (Gray, 1970) and heterogeneity in water content, where the inner portions are often wetter, resulting in lower pore-water suction and the promotion of anoxic conditions (Gerke & Kohne, 2002). In the case of oil sand materials, anoxic conditions within the AOSM would limit biodegradation of the inner bitumen, while aerobic conditions on the surface would promote it (Frontera-Suau, 2000; Gu, 2006; Zhao & Machel, 2011). This pattern of breakdown would further enhance the difference in hydraulic conductivity of outer and inner aggregate portions, by modifying the relative abundances of light (hydrophilic) and heavy (hydrophobic) PHCs within the respective layers of the AOSM. Therefore, onion-skin weathering patterns should be present, and may even become more pronounced with subsequent weathering and

degradation. However, there are several mechanisms which could potentially modify these patterns in AOSM including heterogenous distributions of PHCs and pore water, and the formation of low conductivity surface seals and precipitates.

The rich cores observed by Fleming (2012) contain elevated concentrations of heavy PHCs which should promote hydrophobicity and decrease hydraulic conductivity. However, the inner portions also contain greater concentrations of light PHCs which could increase hydrophilicity (reduce hydrophobicity) and consequently increase the hydraulic conductivity of the affected portions, contradicting the onion-skin weathering hypothesis. Visser (2008b) found that the heterogeneity in the distribution of PHCs within AOSM samples was inversely related to the total PHC content. Based on the coefficients of variation (CV) for the PHC contents in each fraction in each AOSM sample, AOSM with relatively low PHC contents had highly heterogeneous or patchy distributions of PHCs (CV = approximately 60-65%); whereas, AOSM with high PHC contents were found to be far less variable in distribution (CV < 10%) (Visser, 2008b). It is possible that AOSM which contain a relatively low PHC content and highly heterogeneous distribution of PHCs will also express heterogeneity in WR. In the case of AOSM with rich cores, it is possible that WR will be far more variable on the outer portions of the aggregate where PHC content is lower, and become more consistent with depth into the material. This could potentially result in weak or unexpected trends among WR, hydraulic conductivity, and depth.

It is known that soil water content is inversely related to WR, so as water content decreases, WR increases until reaching its maximum under drought conditions (Doerr et al., 2000). Therefore, an increased water content on the inner portions of AOSM could reduce the expression of WR of its inner portions, giving rise to a negative correlation between WR and depth into AOSM, contradicting the onion-skin weathering and hydraulic property hypothesis. Portions of the AOSM which are not connected to the atmosphere through soil pores (due to interstitial PHCs) are protected from the evaporative demand of the surrounding air, effectively reducing the water vapour pressure gradient, and allowing pore water to remain relatively unmodified. Additionally, if the pore connectivity is limited, the likelihood of the material being isolated will increase with increasing depth into the aggregate.

Therefore, it is possible that inner, isolated portions of some AOSM deposits may consistently remain wetter than their outer portions. Additionally, when hydrophobicity is present, pores may trap and hold water once it has infiltrated, resulting in reduced evaporation and loss of water (Müller & Deurer, 2011). This can occur if the surface of a porous material becomes sufficiently dry to express hydrophobicity, shielding the inner waters from evaporation (Müller & Deurer, 2011). Furthermore, it has been speculated that the presence of light PHCs within rich cores of AOSM may indicate that heavy PHCs within the outer portions are providing shielding or protection, which promotes the accumulation of light PHCs by preventing their further modification and/or removal (Fleming, 2012). These heavy PHCs may also act to shield and trap water within the inner portions of the oil sand. The increase in the number of light PHCs within the inner portions may also increase the hydrophilicity (decrease hydrophobicity) of those portions, leading to negative correlations between hydraulic properties and depth into aggregates.

A process called slaking, may also promote the formation of surface seals which can decrease the hydraulic conductivity of the affected material. Slaking promotes the breakdown of soil structure and enhancement of surface sealing, and occurs when soil aggregates are structurally unable to withstand the stresses produced by differential swelling, the pressure of entrapped air, the rapid release of heat during wetting, and the mechanical action of moving water (Liu et al., 2011). The effects of slaking are greatly controlled by the water content and wetting rate, where aggregate slaking decreases with antecedent water content and increases with wetting rate (Liu et al., 2011). Therefore, AOSM which are closer to the soil surface and typically have a lower antecedent water content, are more vulnerable to soil slaking processes than those found at depth. Similarly, inner portions of AOSM which are relatively protected from the surrounding environment, should also contain higher water contents and; therefore, undergo less slaking and associated pore sealing than outer portions of AOSM. This pattern of exposure to slaking could contribute to atypical trends in hydraulic conductivity with depth, and contradict the onion-skin weathering hypothesis.

Salt precipitates and surfactants may also have the ability to considerably modify the expected relationships among WR, hydraulic conductivity, and sampling depth of AOSM. Previous studies have

shown the presence of intra-pore salt precipitates, such as calcite and calcium sulfate, can significantly reduce soil hydraulic conductivity (González-Delgado, 2011; Nicot, 2012). AOSM from the Athabasca oil sands region contain relatively high concentrations of sulfur, which could potentially combine with other substances to form precipitates. In fact, salt precipitates have often been observed on and around AOSM deposits throughout the region (Leskiw et al., 2006; Visser, 2008). It is also possible that sulfate, or other chemical species contained within the oil sand, may combine with organic substances to form a surfactant (Jafvert and Heath, 1991; Zhou and Zhu, 2005). Depending on the surfactant that forms, the WR and absorption potential of the material may be enhanced or diminished as a result (Zhou and Zhu, 2005).

2.3.4 Observations of AOSM-Affected Soils

The impact of oil sand materials on the overall soil water regime is largely unknown; however, field observations have revealed that areas above oil sand-affected soils are noticeably wetter than the surrounding soils (Leskiw et al., 2006; Fleming, 2012). An increase in soil water storage will likely increase ecosystem productivity and could aid in the establishment of reclamation ecosystems, by providing additional plant-available water (Leskiw et al., 2006). It has been speculated that differences in particle size and/or pore size distributions between AOSM and their adjoining soils may be contributing to the observed increases in soil water storage above AOSM (Leskiw et al., 2006; Fleming, 2012). Fleming (2012) found that AOSM can contain a significantly ($P<0.05$) greater silt and clay content than the surrounding soils, which could account for differences in pore size distributions. It is also possible that in texturally similar materials, the interstitial PHCs within the oil sand decrease it's pore size distribution in relation to the surrounding PHC-free soils. Regardless, a decrease in pore size distribution would likely reduce the hydraulic conductivity of the oil sand, resulting in the formation of a hydraulic barrier at the interface of the oil sand and the overlying soil. It is also possible that WR, due to the presence of hydrophobic PHCs, is contributing to a reduction in the hydraulic conductivity of the oil sand.

If oil sand is located beneath the rooting zone, there is potential for increased water storage within the overlying rooting zone. In addition to providing more plant-available water, this reduced hydraulic conductivity and increased residence time of water in the rooting zone also inhibits deep percolation and reduces the input of hydrocarbon leachate to groundwater (Leskiw, 2005; Fleming, 2012). However, an oil sand layer near the surface of the soil profile has the potential to reduce soil water storage by limiting infiltration (Leskiw et al., 2006). Reduced infiltration can result in additional adverse effects including reduced groundwater recharge, increased runoff and erosion, and the subsequent contamination of surrounding surface water bodies through excessive sediment and nutrient loading.

Just as hydrophobic oil sand may act to increase soil water storage in the rooting zone, so too may hydrophilic oil sand inclusions. In a study performed by Fleming (2012) it was found that AOSM contain significantly higher water contents than the surrounding soil matrix. Typically, coarse-textured materials have coarse pore-size distributions and low water holding capacities. However, as mentioned, coarse-textured oil sand may contain a finer pore size distribution than the surrounding soil due to interstitial PHCs. This could result in an accompanying increase in water retention under relatively high pore water suctions. Therefore, by retaining more water than the surrounding PHC-free soils, hydrophilic oil sand inclusions are capable of increasing overall soil water storage. Additionally, because of it's finer pore size distribution it is possible for a capillary barrier to form on the underside of the AOSM, which would limit the percolation of water out of the AOSM into the underlying coarse-textured soils, resulting in greater soil water storage within the AOSM and overlying soils.

Anecdotal accounts from personnel who have worked with oil sand aggregates suggest that the majority of accumulations are hydrophilic, while only some are hydrophobic (Fleming, 2012). It is possible that the observed hydrophilic nature of many AOSM may have arisen from the weathering and/or degradation of the interstitial PHCs (Fleming, 2012). It is unknown whether this reduction in hydrophobicity is caused from a change in the relative number of light (hydrophilic) and heavy (hydrophobic) interstitial PHCs or from a reduction in the total number of PHCs. For the former, the ratio of light to heavy PHCs would have to decrease through the degradation and/or removal of heavy PHCs, exposing a greater proportion of light PHCs. This seems unlikely, as light PHCs are less

complex and more soluble in solution than heavy PHCs and; therefore, have a greater chance of degradation and/or removal from the oil sand (Fleming, 2012). For the latter, the removal of PHCs from the oil sand may expose more of the mineral grain surfaces, leading to a decrease in hydrophobicity. Please recall that unweathered oil sand from Northern Alberta contain layers of connate water surrounding their mineral grains (Mossop, 1980; Takamura, 1982). This suggests that the mineral components are hydrophilic by nature (Mossop, 1980; Takamura, 1982; Gu, 2006). It therefore, stands to reason that once the hydrophobic PHCs are removed and the hydrophilic mineral grains exposed, the oil sand will express little to no WR. Given these considerations, it is expected that the WR of oil sand will be positively correlated with it's total PHC content.

Due to the widespread occurrence of oil sand-affected soils in the region, and their potential to considerably alter the hydrology and consequently the ecosystems that develop, it is important to identify oil sand hydraulic properties and their effects on soil water dynamics. Addressing the objectives in this study will improve our understanding of these materials, and enhance our ability to make accurate predictions and models of the various reclamation scenarios which incorporate oil sand-affected soils.

3. EXPOSURE TO WEATHERING REDUCES THE WATER REPELLENCY OF AGGREGATED OIL SAND MATERIAL FROM SUBSOILS OF THE ATHABASCA REGION[1]

3.1 Preface

Near-surface oil sand materials are naturally present throughout many of the soils of the Alberta oil sands region. Due to differences in their depositional location, and subsequent history of weathering and degradation, these materials display a range of chemical and physical properties. Because oil sand contains petroleum hydrocarbons, water repellency is one such property that is present, to varying extent, in the majority of these materials. In order to provide an indication of the potential for near-surface oil sand inclusions to alter the hydrology of an affected area, this chapter examines the magnitude and variability of the water repellency of oil sand inclusions.

3.2 Abstract

This study assesses the water repellency (WR) of aggregated oil sand material (AOSM) from the Athabasca region, Canada, and evaluates the onion-skin weathering hypothesis, which postulates that with increasing depth into the soil profile or into individual AOSM samples, the exposure to and extent of weathering of AOSM decreases and petroleum hydrocarbon (PHC) content and WR increase. WR and PHC content were determined for outer and inner portions of AOSM from depths of 15–200 cm. Results show AOSM displays a wide range of WR, in terms of both contact angle (CA) (0° to 129°) and water drop penetration time (WDPT) (0 to > 3600 s). As salvage depth or depth into AOSM increases, PHC content and WR increase, confirming onion-skin weathering. These findings imply the benefit of discreet salvaging into separate layers, as opposed to composite salvaging of shallow and deep soils. Deep materials, which contain relatively high PHC contents, can be salvaged and replaced

[1] This work has been previously published in Neil, E.J., and Si, B.C. (2018), Exposure to weathering reduces the water repellency of aggregated oil sand material from subsoils of the Athabasca region. Published in Can. J. Soil Sci. doi: 10.1139/CJSS-2017-0087. Minor modifications have been made for consistency.

as deep layers to avoid the excessive drying and expression of WR which may occur in the near-surface. By controlling the location of AOSM within the soil profile, water storage in the rooting zone may be increased, allowing the establishment of relatively productive ecosystems.

3.3 Introduction

Northern Alberta, Canada is home to the world's largest and richest oil sand reserves, consisting of the Athabasca, Peace River, and Cold Lake deposits, which underlie an area of approximately 142,000 km^2 [Government of Alberta (GOA) 2016]. Oil sand, or bitumen, deposits are present in over 80 locations worldwide (Meyer et al. 2007), with more than 70% of these resources located within the Alberta oil sands (Hein 2006). The shallow portions of this region which are accessible through surface mining comprise an area of 4,800 km^2 near Fort McMurray, AB (GOA 2016). The Alberta government requires oil sands mining companies to reclaim disturbed land and recreate self-sustaining, maintenance-free watersheds and ecosystems with capabilities equivalent to or better than the pre-disturbance conditions (Cumulative Environmental Management Association 2006). The reconstruction of soil profiles is a critical component of any reclamation plan, because the ultimate capability of a reclaimed area is controlled largely by the quality of the reconstructed soil (Oil Sands Vegetation Reclamation Committee 1998). Creation of the soil medium requires selection of an appropriate soil layering prescription, which includes depths, composition, and configuration of reclamation materials (Huang et al. 2011). In order to effectively prepare reclamation prescriptions, an understanding of each of the available materials is essential.

A soil survey performed in the Athabasca oil sands region shows that considerable quantities of petroleum hydrocarbon (PHC) affected soils are present in the form of aggregates and layers within the top three meters of these dominantly coarse-grained Brunisolic soils (Leskiw et al. 2006). One of the most common surficial hydrocarbon deposits of the region is aggregated oil sand material (AOSM), previously referred to as "tarballs" (Fig. 3.1). These aggregates are PHC-impregnated materials with a similar texture to that of the surrounding soil, and are typically millimeters to tens of centimeters in diameter (Fleming 2012). The materials available for reclamation in this region may originate from the

near-surface horizons of the profile and; therefore, have the potential to contain AOSM, which may or may not inhibit the plant roots, soil organisms, and soil processes required for the recovery and maintenance of a stable ecosystem (Visser 2008). Several studies have shown that PHCs, such as those contained within oil sand bitumen, are often associated with WR (Walker et al. 1976; Roy and McGill 2000; Quyum et al. 2002; Buczko et al. 2006; Brassington et al. 2007; Adams et al. 2016), and it has been hypothesized that the weathering of PHCs will typically shift their chemical composition toward relatively recalcitrant products with greater hydrophobicity (Walker et al. 1976; Brassington et al. 2007).

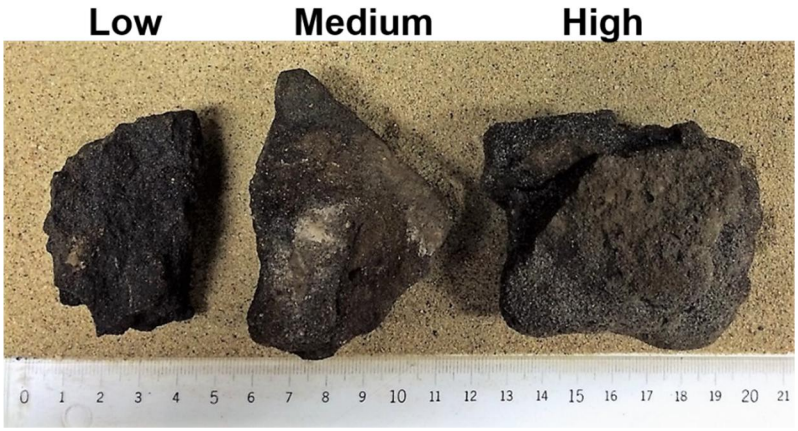

Figure 3.1. Aggregated oil sand material (AOSM) from three stages of weathering (low, medium, and high), placed on top of their surrounding sandy subsoil. Measurement scale in centimeters.

Polycyclic aromatic hydrocarbons (PAH) are a common class of PHC present in oil sand bitumen, and have the potential to produce hydrophobicity and soil water repellency (Cerniglia 1992; Zhou and Zhu 2005). Typically, low molecular weight PAHs such as naphthalene and phenanthrene are rapidly degraded in sediments and soils, whereas high molecular weight PAHs such as benz[a]anthracene, chrysene, and benzo[a]pyrene, which are relatively insoluble and highly resistant to degradation, may persist indefinitely (Cerniglia 1992). This is largely due to the decreasing enzymatic capability of soil microorganisms to degrade PHCs of increasing complexity (Walker et al. 1976). Although microbial degradation of heavy PAHs may occur, there are a limited number of species of microorganisms that

are capable of complete mineralization (Cerniglia 1992; Zhou and Zhu 2005), making it unlikely that all of the PHCs within AOSM would be degraded by means of microbial degradation. Additionally, as molecular size increases, solubility and mobility decrease, which further promotes the depletion of light PHCs and enrichment of heavy PHCs within the weathered oil sand material (Mossop 1980; Eastcott et al. 1988; Fleming 2012). Generally, low-molecular-weight PHCs are preferentially degraded, volatilized, and leached from bitumen, resulting in the accumulation of heavier, more complex PHCs over time (Mossop 1980; Brunner et al. 1987; Cerniglia 1992).

Previous investigations have confirmed that typical AOSM from the Athabasca oil sands region is composed primarily of relatively heavy hydrocarbons, such as those from the F3 (Carbon $[C]_{>16}$ - C_{34}) and F4 ($C_{>34}$) fractions of the classification system provided by the Canadian Council of Ministers of the Environment (CCME) (2008) in their Canada-Wide Standards for Petroleum Hydrocarbons (PHC) in Soil (Fleming 2012). Volatile hydrocarbons, including benzene, toluene, ethylene, xylene and other low molecular weight hydrocarbons such as those from the CCME (2008) F1 (C_6 – C_{10}) fractions, are typically undetectable; whereas, F2 ($C_{>10}$ - C_{16}) hydrocarbons are slightly more abundant with concentrations above detectable limits (Fleming 2012). Exceptions have been found in AOSM with “rich” cores, which can contain total PHC contents that are orders of magnitude greater than typical AOSM, including elevated levels of the relatively light F1 and F2 hydrocarbons (Fleming 2012). Under normal field conditions, the F1 and F2 fractions are relatively soluble and easily transported in water, whereas the heavier F3 and F4 fractions are nearly insoluble (Fleming 2012). The ability to readily dissolve in water indicates that the F1 and F2 PHCs are hydrophilic, and the relative insolubility of the F3 and F4 fractions suggests hydrophobicity (Page et al. 2000; Reid et al. 2000). Typically, the PHCs remaining in AOSM are relatively heavy in composition, so differences in WR will likely be due to differences in the total PHC content as opposed to differences in PHC composition. Roy et al. (2003) showed that total PHC content was positively correlated with soil water repellency in 12 petroleum-contaminated sites in central Alberta.

The Alberta oil sands are somewhat unique in composition: the bitumen is not in direct contact with the mineral particle portions of the oil sand; upon formation there is a thin lens of connate water

surrounding the mineral particles, separating the mineral particles from the bitumen contained within the centers of the pores (Mossop 1980; Takamura 1982). This physical arrangement has two important implications for WR: (i) mineral particles are originally surrounded by water and are; therefore, considered hydrophilic (Mossop 1980; Takamura 1982; Gu 2006); and (ii) water that is introduced to the pore structure of the oil sand is in direct contact with the exposed interstitial bitumen rather than the sheltered mineral portions, suggesting that the water repellent nature of the oil sand will be primarily, if not exclusively, controlled by the water repellent characteristics of the bitumen within. Depending on the location and site specific characteristics, the WR of oil sand inclusions may enhance or diminish the level of WR present at the site, affecting the soil wettability, soil water retention and water storage, and consequently the ecosystem (Diehl 2013). Therefore, when attempting to reclaim a hydrocarbon-affected area such as the Alberta oil sands, it is important to understand the potential soil WR of the available reclamation materials. Aggregated oil sand material is one such potentially water repellent material, which is present in many of the soils in this region, and is composed primarily of sand and PHCs, both of which are prone to WR.

Since the PHCs remaining in the AOSM are thought to cause WR, the water repellent behaviour of the material should be directly related to the extent of weathering, and consequently the amount of PHC remaining. As biodegradation occurs and hydrophobic molecules are broken down, water repellency is reduced (Bisdom et al. 1993; Dekker and Ritsema 1994). The limited biodegradation of the heavy hydrocarbon fractions (F3 and F4) which are present in oil sand, is most likely a biotransformational process which can render larger, more complex PHCs into several smaller “daughter” PHC compounds (Fleming 2012). These daughter compounds are more easily dissolved in soil solution and leached from the AOSM than the parent compounds. It is also known that the presence of oxygen typically increases the biodegradation rate of crude oil constituents (Cerniglia 1992; Frontera-Suau 2000; Gu 2006; Zhao and Machel 2011). Based on the above it stands to reason that the outer portions of AOSM, which are more exposed to weathering and degradation agents, should contain fewer PHCs and exhibit less WR than the more protected inner portions. The AOSM with rich cores that were observed by Fleming (2012) also suggest this. Similarly, near-surface AOSM

deposits should be more exposed to weathering, contain fewer PHCs, and exhibit less WR than deeper deposits.

We hypothesize that AOSM undergoes onion-skin weathering, where the amount of weathering or degradation decreases and consequently the PHC content and WR increase, with increasing depth from the soil surface as well as with increasing depth into individual AOSM samples. To test these hypotheses, the WR of AOSM from various salvage depths and apparent stages of weathering were determined. The objective of this study is to evaluate the onion-skin weathering hypothesis of AOSM, to better understand the dynamics of oil sand weathering and its effects on soil hydraulic properties such as WR.

3.4 Materials and Methods

3.4.1 Study Site and Reclamation Materials

The study area is located in the Central Mixedwood Natural Subregion within the Boreal Forest Natural Region of Alberta (Natural Regions Committee 2006). The area may be further distinguished into smaller components called ecosite phases, based on moisture and nutrient regimes, as outlined in Beckingham and Archibald (1996). The study region has been known to support portions of ‘a’, ‘b’, and ‘d’ ecosite phases (Zettl et al. 2011), characterized by subxeric, submesic, and mesic moisture regimes respectively, and by poor (‘a’ ecosites) and medium (‘b’ and ‘d’ ecosites) nutrient regimes (Beckingham and Archibald 1996). Parent materials in the area are composed primarily of glaciofluvial sands and gravels, giving rise to coarse-textured Brunisolic soils (Leskiw et al. 2006). These soils most commonly support the ‘a1’ ecosite phase, which is characterized by a subxeric moisture regime and poor nutrient regime, with jack pine (*Pinus banksiana* Lamb) and lichen (*Cladina* spp. and *Cladonia gracilis*) as the dominant tree and understory species (Beckingham and Archibald 1996). Prior to surface mining, the forest vegetation, soils, and lean oil sand overburden are removed to depths of up to 100 m in order to reach the desired oil sand reserves (Johnson and Miyanishi 2008). The excavated overburden and soil materials are then stored in stockpiles. These materials, and potentially additional

peat and soils collected from neighboring undisturbed areas, are available for later use in reclamation (Johnson and Miyanishi 2008).

In order to test the efficacy of utilizing various soil reclamation prescriptions, as well as to explore the potential impacts to ecological receptors (i.e. vegetation, microbial communities, surface and ground waters, etc.) that may occur in hydrocarbon-affected reclamation soils, a long-term instrumented watershed research site called the Aurora Soil Capping Study (ASCS) was established in 2012 at Syncrude Canada Ltd.'s Aurora North Mine, north of Fort McMurray, AB. The ASCS site contains 36 one-hectare plots, consisting of 12 reclamation treatments repeated in triplicate. The treatments are composed of various combinations of hydrocarbon-affected soil materials that were collected from the area prior to surface mining. Soils and subsoils containing AOSM were collected from the following materials of the ASCS:

- Upper Subsoil Bm horizon salvage (15 – 50 cm): Surface soil was removed (LFH layer, A horizon, and a portion of the top of the B horizon which totals approximately 15 – 20 cm), then the remaining Bm horizon was salvaged to a depth of 50 cm.
- Blended B/C horizons salvage (50 – 100 cm): Surface soil and upper subsoil Bm horizon were removed (0 – 50 cm), then the remaining B horizon and a portion of the C horizon were salvaged to a depth of 100 cm.
- Composite Subsoil salvage (15 – 200 cm): Surface soil was removed (LFH layer, A horizon, and a portion of the top of the B horizon which totals approximately 15 – 20 cm), then the remaining Bm horizon and a portion of the C horizon were salvaged to a depth of 200 cm.

The three soil salvage types will be referred to as Bm, B/C, and SS respectively. The soils were originally salvaged by Syncrude Canada Ltd. in various depth ranges and intervals, in order to compare the effects of discreet and composite salvaging techniques on the success of reclaimed soil profiles. Discreet salvaging involves the removal (prior to mining) and replacement (during reclamation) of soil layers in distinct soil horizons, such as those of the Bm and B/C salvages. Composite salvaging is the removal and replacement of relatively large sections of the soil profile, with

little concern for material composition, as in the case of the SS salvage. It was posited that, due to the relatively uniform composition of the soils throughout the depth of the soil profiles in the region, discreet salvaging may be unnecessary. If so, composite salvaging would provide an alternative technique which promotes reclamation success, but that is superior in terms of economic and environmental efficiency. Composite techniques minimize the use of heavy machinery, consequently conserving resources, and mitigating the ecological footprint of mining and reclamation activities by reducing green house gas emissions.

In-tact AOSM samples, ranging from centimeters to decimeters in diameter, were chosen randomly from each of the available salvage materials and lightly brushed to remove the excess sand matrix adhering to their outer surfaces. Aside from periods of active testing, which were performed at 20 °C and 30% relative humidity, the AOSM was stored at 4 °C to minimize microbial degradation. Prior to testing, the AOSM was air dried at 20 °C and 30% relative humidity, for a period of several days to weeks, until reaching a constant mass.

In addition to their salvage type, the majority of the AOSM samples were categorized into one of three relative weathering stages (low, medium, or high), based on physical stability, visual appearance, and odour (Table 3.1).

Table 3.1.
Weathering stage determination for aggregated oil sand material.

Weathering stage	*Colour	Petroleum odour	Physical fragmentation requirements
Low	black	Strong	hammer and chisel
Medium	dark grey	Mild	by hand
High	light grey	None	soft-bristled paint brush

*Light coloured surface precipitate indicates a greater stage of weathering.

To assess the physical stability of the AOSM, the relative force required to cause the sample to physically fragment, or break, was determined. Firstly, the sample was brushed with a soft-bristled paint brush, and if fragmentation occurred then the sample was considered highly weathered in terms

of physical stability. Secondly, if the sample did not fragment with the use of a paint brush, but could be broken by hand, it was considered to be at a medium stage of weathering. Lastly, if fragmentation of the sample required the use of a steel hammer and chisel, it was classified as low-weathered. The visual signs of weathering were based on the colour of the sample, as well as whether it contained a light-coloured precipitate on portions of it's surface, where the presence of a precipitate indicated a higher stage of weathering. The level of petroleum odour was determined simply by smelling the sample while it was approximately 5 cm from the assessor's nose. A clear and strong odour of petroleum indicated a low stage of weathering, a faint odour indicated a medium stage, and the absence of a petroleum odour indicated a high stage of weathering. Generally, AOSM would receive the same classification (low, medium, or high) using each of the three criteria (visual appearance, physical stability, and odour). For samples where one of the three weathering criteria came to a different conclusion, the weathering stage was based on the majority (i.e. weathering stage indicated by the two criteria with matching conclusions). For samples where all three weathering criteria suggested a different weathering stage, the sample was classified as medium weathered.

A Horiba LA-950 particle size analyzer was used to determine the particle size distributions of the AOSM and soil matrix (Horiba Scientific, Edison, NJ, USA). This type of apparatus is known to overestimate the size of small particles, particularly clay sized particles, present in soil samples. To ensure the AOSM and soil matrix were of sufficient coarseness for accurate testing using a laser particle size analyzer, the texture of several samples were determined using the pipette method based on Stokes' Law as outlined in Dane and Topp (2002). The results of the pipette method showed the materials contained only minute amounts of clay sized particles (< 2% by mass), making them suitable for the LA-950 laser analyzer. Particle sizes were categorized into soil separates using the classification systems of the Canadian Soil Survey Committee and United States Department of Agriculture, which define soil separates as sand (< 2000 μm to 50 μm), silt (< 50 μm to 2 μm), and clay (< 2 μm) (Dane and Topp 2002). The soil textures were determined using the Canadian System of Soil Classification (Soil Classification Working Group 1998). The mass-based total organic carbon (TOC) contents of AOSM and soil matrix from the three salvage types were determined using a LECO

C-632 dry combustion carbonator (LECO Corp., St. Joseph, MI, USA) (Wang and Anderson 1998). Because these soil materials contain limited soil organic matter, it can be assumed that the measured TOC is primarily of petroleum origin (i.e., PHCs).

The most common type of hydrophobic substance causing WR in sands are amphiphilic molecules, polar organic molecules containing both hydrophilic and hydrophobic portions (Doerr et al. 2000; Diehl 2013). For such a case, the affected material may act in a hydrophobic or hydrophilic manner, depending on the antecedent water content as well as pH and temperature (Doerr et al. 2000; Diehl 2013). Furthermore, soils affected by WR may change their behaviour from hydrophobic to hydrophilic during wetting, and vice versa during drying (Dekker and Ritsema 1994; Doerr et al. 2000). This is certainly the case in the Athabasca oil sands region, where studies by Hunter (2011) and Chau et al. (2014) have illustrated the dependence of wetting duration on the WR of both natural (undisturbed) and reclamation (disturbed) soil materials.

3.4.2 Measurement of Water Repellency

Due to the temporally transient nature of WR in the study region, both the degree and persistence of WR of the AOSM were determined. The degree of WR of air-dry soil materials can be used to determine the maximum or potential WR that may be experienced after prolonged drought periods (Müller and Deurer 2011). The sessile drop CA between a water droplet and the material surface represents the degree of WR and provides a measurement at a fixed point in time (Dekker and Ritsema 1994; Diehl 2013). The WDPT represents the persistence of WR and provides measurements through time (Dekker and Ritsema 1994; Müller and Deurer 2011). This indicates whether the potential for WR, as indicated by the CA, will have a substantial effect on water absorption and conductivity of AOSM.

The degree of WR of the AOSM was determined via sessile drop CA analysis, using a PG-X pocket goniometer (FIBRO Systems AB, Hägersten, Sweden). The PG-X delivers a controlled volume of water to the surface of the material. In the current study, this procedure utilized 3 μL deionized, de-aired water droplets. Once a water droplet was applied and its equilibrium position reached, the on-

board camera was used to take photographs of the water droplet on the surface of the material. The photographs were used in conjunction with ImageJ software (Rasband 1997-2012) and the Low Bond Axisymmetric Drop Shape Analysis method outlined by Stalder et al. (2010), to determine the water contact angles. Several AOSM samples from each of the available soil salvage types were tested (Bm = 27; B/C = 21; SS = 11), for a total of 59 samples. Each sample was tested three to six times on relatively flat portions of its outer surface, with measurement locations spaced approximately equidistantly across the surface of the sample. The mean CA for each AOSM sample was then obtained to account for variability within samples. There are three general scenarios that can arise when examining CA: spontaneous wetting or infiltration (hydrophilic or wettable) where CA = zero; partial wetting (subcritical WR) where 0° < CA ≤ 90°; and non-wetting (critical WR or hydrophobic) where CA > 90° (Müller and Deurer 2011). When the CA is above 90° water should theoretically never infiltrate, but when it is 90° or less, capillary forces will draw water into the sample (Dekker and Ritsema 1994). This information provides insight into the stability of water repellency and is another indication of its persistence (Dekker and Ritsema 1994). Therefore, the times for the CAs of the AOSM to become ≤ 90° were also determined for samples from each salvage type (Bm = 23; B/C = 21; SS = 11), which totalled 55 samples. It is important to note; however, that water will not always infiltrate when CAs are less than 90°. The geometry or shape of soil particles can affect the interactions between solid surfaces and liquids, and prevent infiltration into seemingly subcritically water repellent surfaces (CA < 90°) (Shirtcliffe et al., 2010). For example, a curved or fibre-like structure can suspend a liquid, or prevent infiltration, when its sessile CA is between 0° and 90° (Shirtcliffe et al., 2010). Additionally, particle size can have an effect on the infiltration of water into subcritically water repellent soils, such that soils with liquid CAs < 90° may exhibit incomplete wetting or non-wetting behaviours (Hamlett et al., 2011). Hamlett et al. (2011) found that the smaller the diameter of soil particles, the smaller the liquid contact angles could be while still preventing infiltration. In other words, the critical contact angle, or the largest contact angle at which infiltration commences, decreases as particle size decreases (Hamlett et al., 2011). Therefore, although a CA of 90° is being used as an indication for the likely threshold between partially wettable and non-wettable surfaces in this study, there may be exceptions

to this rule. Due to this uncertainty, the times for the CAs to become less than 90° should be considered as merely a possible indication of WR rather than an absolute measure, and the initial sessile drop CAs and WDPTs should be treated as the primary representations of WR in this study.

The persistence of WR was also determined using the CA goniometer. As the 3 μL water droplets infiltrated the AOSM surface, additional CA images were taken at various times throughout infiltration. These changes in CA over time, from maximum CA to zero, represent the WDPT. In addition to the goniometer measurements, persistence was measured on several samples using another form of the WDPT test. Water droplets (40 μL) were introduced to the AOSM using an autopipette, and the time for complete infiltration was recorded. The WPDT measurements were performed on samples from each of the soil salvage types (Bm = 35; B/C = 24; SS = 13), providing a total of 72 samples. As with the CA testing, the WDPT measurements were performed on reasonably flat locations and spaced roughly equally across the surface of the sample. Each sample was measured approximately 10 times and the mean WDPTs of each sample determined, in order to account for variability within samples. The WDPT classification scheme of Bisdom et al. (1993) was then used to categorize the AOSM samples into repellency classes.

As mentioned, the onion-skin weathering hypothesis states that with increasing depth from the soil surface and with increasing depth into individual AOSM samples, the extent of weathering or degradation of AOSM decreases and; consequently, the PHC content and WR increase. In order to test the former portion of the onion-skin weathering hypothesis, the degree and persistence of WR were measured on the outer surfaces of AOSM samples from multiple salvage depths (Bm, B/C, SS salvages). To test the latter portion of this hypothesis, the WR of the inner portions of several samples were determined in addition to the outer surface measurements. To access the inner portions of these samples, a steel dental pick and spatula were used to remove material to a desired depth. Material was removed in 10 mm diameter holes in depth increments of 3 to 10 mm. The sample was then air dried before performing the WDPT measurements. This was completed at one to three depths per test location to a total depth of 3 to 24 mm, depending on individual AOSM sample thickness.

3.4.3 Infrared Measurement of AOSM Surface Precipitate

A select number of AOSM samples contained a light-coloured (white) precipitate on their outer surface, which is consistent with previous studies of oil sand material. It has been observed that salt precipitates often form on and around the outer surfaces of AOSM (Visser 2008). The high concentrations of sulfur (800 to 1200 mg kg^{-1}) within AOSM would suggest the precipitate is likely a sulfate salt, possibly calcium sulfate, that forms from sulfur entering soil solution and traveling to the surface of the AOSM where it precipitates with calcium (Visser 2008). The high suphur content of AOSM and the existence of precipitates on many of the aggregates suggests the presence of a sulfate compound. To explore this possibility, attenuated total reflectance Fourier transform infrared (ATR-FTIR) spectroscopy was performed to test for the presence of sulfate within the outer and inner portions of the four AOSM samples that were WR tested at multiple depths. The ATR-FTIR experiments were performed using a Bruker Optics Equinox 55 FTIR spectrometer (Bruker Optics, Milton, ON, Canada), which was equipped with an N_2-cooled mercury cadmium telluride detector and a single bounce ZnSe diamond coated crystal ATR accessory. The background spectrum of the crystal was collected and later subtracted from the sample spectra prior to data analysis. Material was collected from the outer and inner portions of each of the four AOSM samples, ground into a fine powder, and individually pressed onto the diamond crystal surface for measurement. The ex-situ FTIR spectra of the various samples were then determined over a wavenumber range of 4000 to 700 cm^{-1}. Each of the obtained spectra are the result of 512 co-added scans taken at a resolution of 4 cm^{-1}.

3.4.4 Statistical Analysis

Pearson's r was used to explore potential linear correlations among soil texture, TOC, CA, WDPT, and measurement depth. Analysis of variance (ANOVA) were performed to explore differences in the tested variables, where differences in means were considered significant at $P < 0.05$.

3.5 Results and Discussion

3.5.1 Physical Properties of Reclamation Materials

The weathering classification of AOSM showed that the low weathering class primarily included AOSM from the deep salvage (B/C); the medium class was composed of all salvage types (Bm, B/C, and SS); and the highly weathered class included materials from the shallowest depths (Bm and SS) (Fig. 3.2, Table 3.2).

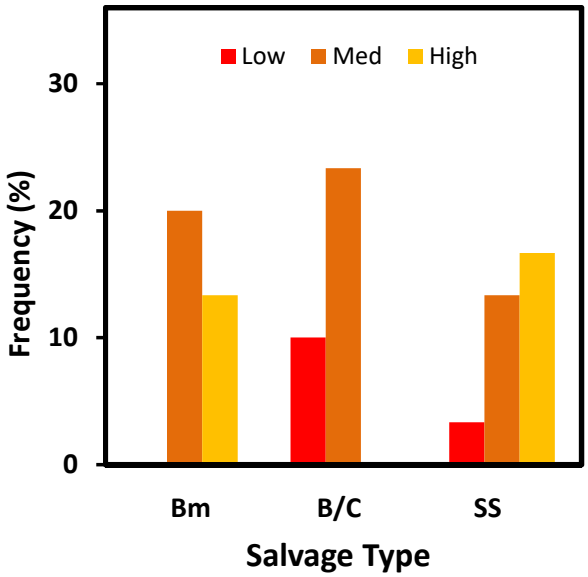

Figure 3.2. Weathering classification (low, med, high) of AOSM from three soil salvage types: Bm (15-50 cm), B/C (50-100 cm), and SS (15-200 cm).

Soil matrix and AOSM from each of the salvage types are sand textured soils, with the exception of two AOSM samples which are somewhat finer and classified as loamy sand. ANOVA showed that AOSM have a significantly ($P = 2.8 \times 10^{-6}$) lower amount (i.e., mass) of clay sized particles than the surrounding soils (Table C.1); however, neither the AOSM (0.0%) nor the soil matrix (0.4%) contain substantial amounts of clay. ANOVA also revealed that outer and inner potions of AOSM are not significantly different ($P > 0.1$) in texture (soil separates) (Tables C.2, C.3, and C.4).

Table 3.2.
Mean and (standard deviation) of total organic carbon content in % by mass of soil matrix, outer AOSM, and inner AOSM from three soil salvage types.

Salvage Type	Depth (cm)	AOSM Weathering	Total Organic Carbon (%)		
			Soil Matrix	AOSM	
				Outer	Inner
Bm	15-50	Med-High	0.6 (0.09)	6.3 (2.1)	7.9 (2.1)
B/C	50-100	Low-Med	0.4 (0.03)	9.7 (5.4)	11.2 (3.1)
SS	15-200	Med-High	0.7 (0.06)	6.5 (2.0)	6.6 (1.0)

†AOSM = aggregated oil sand material

The mean TOC contents with standard deviations, of the soil matrix, outer AOSM, and inner AOSM are presented in Table 3.2. ANOVA revealed the TOC contents of the outer and inner portions of AOSM are significantly different (P = 0.028), where the inner material (9.6%) has a greater mean TOC content than the outer (7.5%) (Table C.5). The low weathered AOSM contained significantly greater TOC contents (13.0%) than the high (6.5%) and medium (6.4%) classes (Fig. 3.3), where P = 1 x 10^{-5} (highly weathered) and P = 3 x 10^{-16} (medium weathered) (Tables C.6 and C.7). Furthermore, there is a positive correlation between TOC content and depth into AOSM samples (Fig. 3.3).

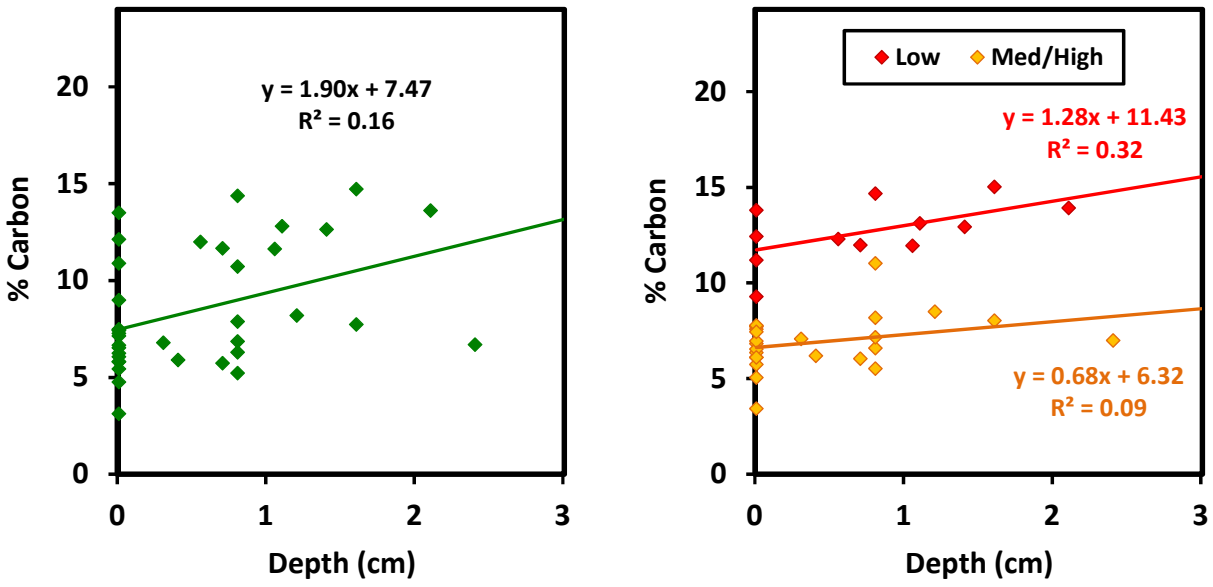

Figure 3.3. Total mass-based carbon content at various depths into individual AOSM for all samples (left) and samples from various weathering classes (low; medium and high combined) (right).

3.5.2 Degree and Persistence of Water Repellency

The maximum CAs of the air-dry AOSM samples measured anywhere from 0° (hydrophilic) to 129° (hydrophobic), where ≥ 75% showed some level of water repellency (CA > 0°) and the remainder were wettable (CA = 0°) (Fig. 3.4). The mean (μ) maximum CA for all samples was 47° with a coefficient of variation (CV) of 96%. The shallow salvage (Bm) primarily showed wettability or subritical WR (μ = 28°; CV = 115%), while the SS salvage was predominantly hydrophobic (μ = 96°; CV = 36%). The B/C salvage showed a range of water repellent behaviour, which included hydrophilic, subcritically water repellent, and hydrophobic materials (μ = 47°; CV = 100%). Similarly, the WR of salvage materials also depended on the degree of weathering: AOSM of medium (μ = 53°; CV = 94%) and high (μ = 49°; CV = 101%) degree of weathering varied from wettable to hydrophobic, while all materials of a low (μ = 105°; CV = 17%) degree of weathering were hydrophobic.

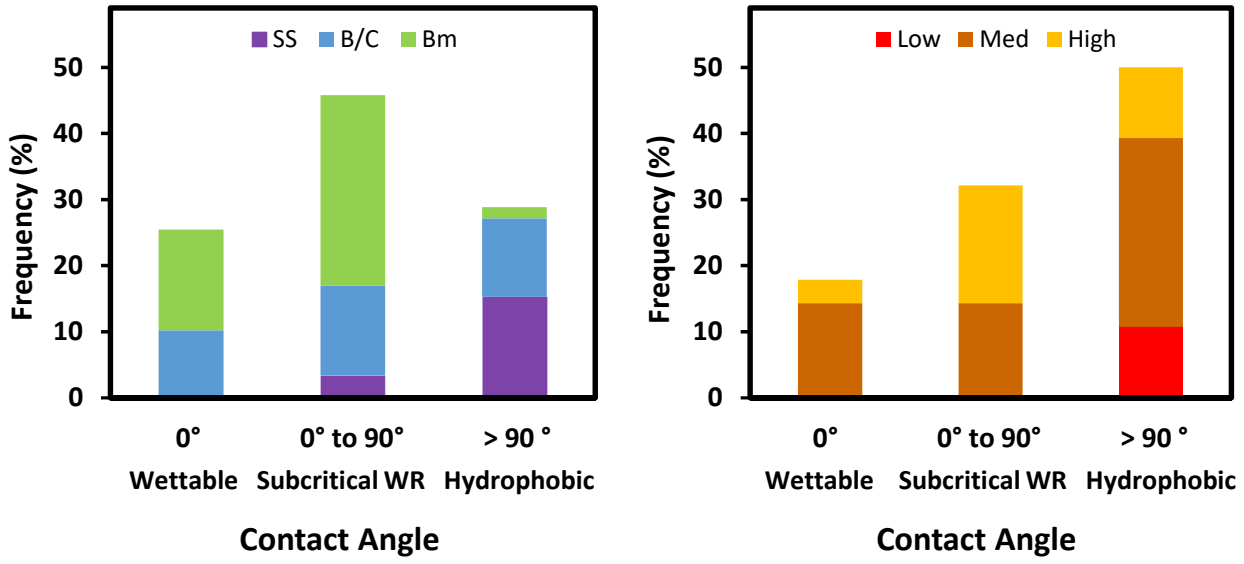

Figure 3.4. Mean degree of water repellency of AOSM, grouped by soil salvage type (left) and extent of weathering (right).

When observing the contact angles through time, more than 70% of the droplets had CA ≤ 90° within 5 s of contact, and the remainder was divided approximately equally between droplets with CA ≤ 90° within 60 s, and those greater than 60 s (Fig. 3.5).

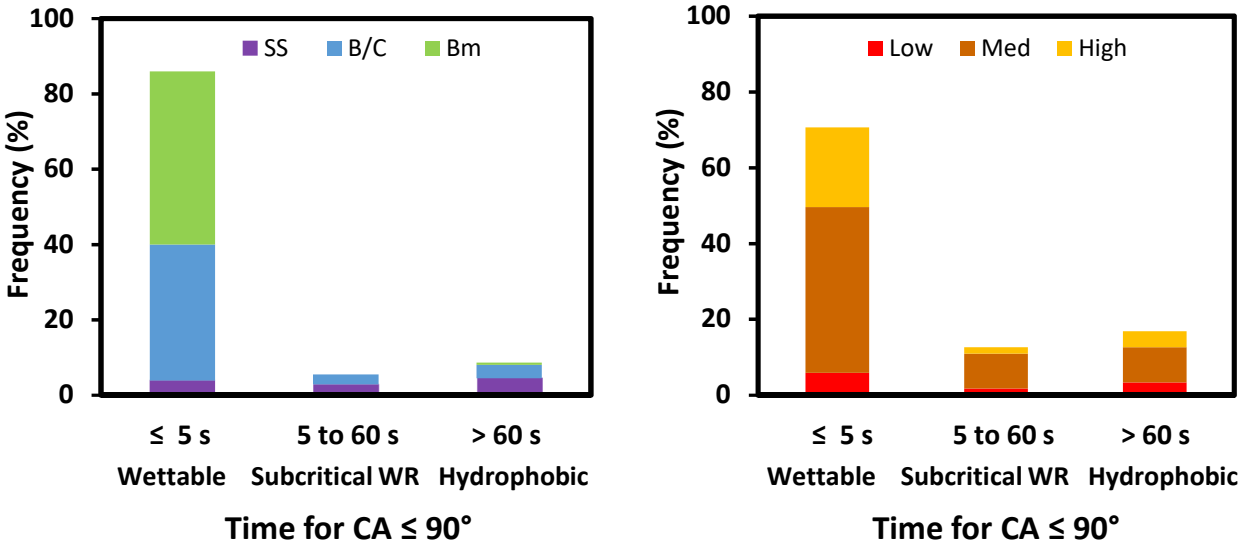

Figure 3.5. Time for the AOSM water contact angles to become ≤ 90°, grouped by soil salvage type (left) and extent of weathering (right).

The WDPTs from both the goniometer and autopipette testing were combined and presented in Figure 3.6. The mean WDPT for all samples was 824 s with a CV of 221%. Approximately 1/3 of the samples are classified as hydrophilic with WDPTs ≤ 5 s, less than 1/3 are slightly water repellent with WDPTs from 5 to 60 s, and more than 1/3 are strongly to extremely water repellent with WDPT ≥ 60 s. Similar to the CA results, the SS salvage predominantly showed extremely water repellent WDPTs (μ = 3250 s; CV = 90%), the Bm was mainly wettable to slightly water repellent (μ = 270 s; CV = 381%), and the B/C showed a range of WDPTs (μ = 331 s; CV = 156%). Furthermore, the degree of weathering also affected soil water repellency, where AOSM with a low degree of weathering (μ = 3775 s; CV = 95%) showed strong to extreme WR, a high degree of weathering (μ = 903 s; CV = 227%) resulted in mainly wettable to strongly water repellent materials, and the medium weathered (μ = 659 s; CV = 231%) AOSM showed a range of WR from wettable to severely water repellent.

The degree and persistence of WR of the AOSM are related, where there is a linear correlation (r^2 = 0.81) between CA and the natural logarithm of WDPT. There also appears to be a correlation between WR and salvage depth (Fig. 3.4; Fig. 3.6), where greater salvage depth generally results in a greater degree (CA) and persistence (WDPT) of WR (B/C and SS > Bm).

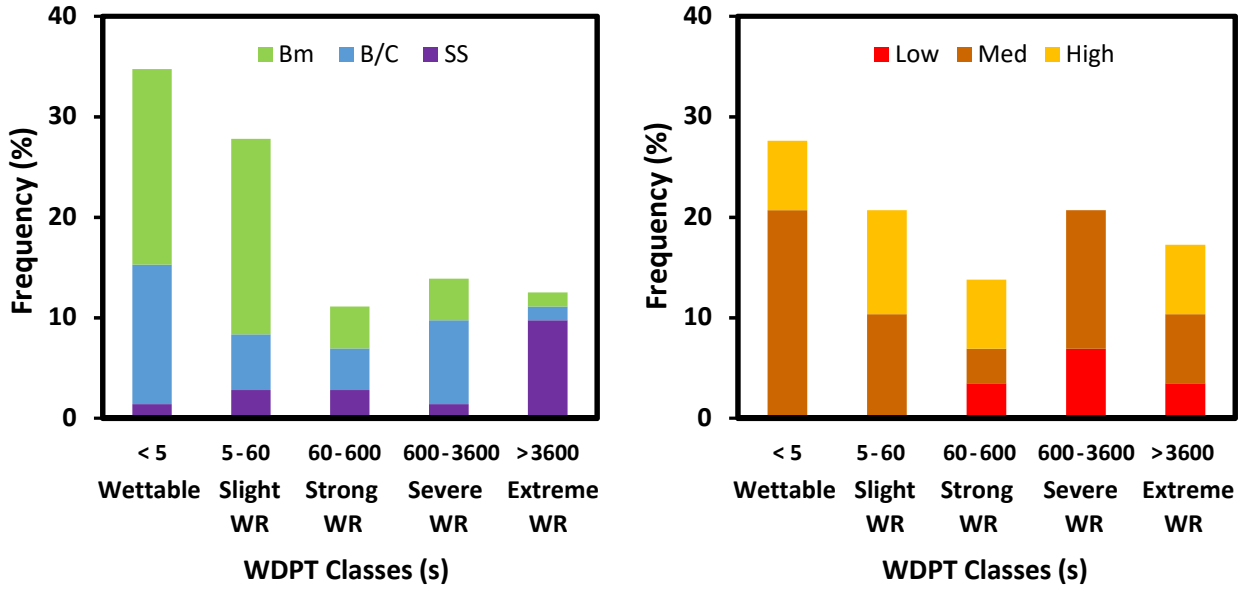

Figure 3.6. Mean persistence of water repellency of AOSM, grouped by soil salvage type (left) and extent of weathering (right).

The WDPTs indicate that the majority of the AOSM will allow infiltration within the first minute of exposure, another portion within 10 min, and some that are severely or extremely water repellent with WDPTs greater than 10 min. Hunter (2011) investigated the WR of soils from several hydrocarbon-affected reclamation sites and natural 'a' ecosites in the Athabasca oil sands region. The sites showed similar WR, with WDPTs ranging from 0 to 122 s and CAs from 0° to > 110°, where the variability was high in both land types with coefficients of variation often exceeding 200%. Although the magnitude of WR in the soils tested by Hunter (2011) was generally lower than the AOSM in the current study, a high level of variability was present in both materials, indicating that the spatial variability of WR in the AOSM from the current study is comparable to that of other natural soil materials in the region.

The WR of the tested AOSM showed a strong dependence on wetting duration. Although repellency is present to some extent in much of the AOSM, according to the CA analysis, over half of the material will wet either immediately (hydrophilic) or eventually if given adequate time (subcritically water repellent) (Fig. 3.4). The remainder are hydrophobic and theoretically may never have the capability of wetting and allowing infiltration in their current condition. The results of Hunter (2011) and Chau et al. (2014) confirm the dependence of wetting duration on the WR of natural and reclaimed hydrocarbon-affected soils, where CA and WDPT were negatively correlated with antecedent soil water content. In addition to the CA and WDPT values themselves, the time it takes for a soil CA to change from > 90° to ≤ 90° also has important implications. In the current study, very few samples (< 20%) had a CA > 90° for longer than one minute, suggesting that the vast majority (> 80%) of the AOSM began to allow at least some infiltration within one minute of contact with water, and are thus considered to be either hydrophilic (WDPT = 0 s) or subcritically water repellent (WDPT > 0 s). This is also consistent with Hunter (2011) who found that the majority of hydrocarbon-affected soils, in both natural and reclaimed sites, are wettable or subcritically WR according to CA analysis.

These results are also consistent with water repellency theory. Some material surfaces are seemingly water repellent (CA > 90°) when first introduced to water, but with time and exposure to water, their amphiphilic molecules reorient themselves to a hydrophilic position which enables infiltration (Dekker and Ritsema 1994; Doerr et al. 2000). This is typically what is observed in the highly weathered or shallow AOSM. In other cases; however, surfaces can be so WR (typically when CA > 90°) that the molecules are unable to reorient themselves within a reasonable or observable time frame, if ever, and are thus considered hydrophobic (Dekker and Ritsema 1994; Doerr et al. 2000), which is what is observed in the low weathered or deep salvage AOSM. This is also consistent with the observed linear correlation (r^2 = 0.81) between CA and WDPT of AOSM in the current study. However, it is important to note that CA and WDPT are not always related. Bachmann et al. (2007) found a significant relationship between the CA and WDPT when the CA was > 90°; whereas, for smaller CAs (≤ 90°) the WDPT was found to be < 5 s, and it was concluded that the measurement of WDPT is insensitive to differences in wettability throughout the entire range from wettable to

hydrophobic. This phenomena is also exhibited in a study performed by Chau et al. (2014) on soils from undisturbed 'a' ecosites and reclaimed sites in the Athabasca oil sands region, which showed that CA and WDPT can be, but are not always, correlated.

The wettable or subcritical nature of the WR in AOSM has been verified by the results of an accompanying tension-controlled infiltration experiment performed on the same AOSM samples used in the current study. The majority of the AOSM allowed infiltration to occur under negative pore water pressures ranging from -20 to -0.1 cm (Neil and Si, 2018b), indicating subcritical WR with CAs ≤ 90° (Bauters et al. 2000). However, the infiltration of 95% ethanol was also determined, under pressure conditions equivalent to those used for water (i.e. the height of ethanol in the infiltration column was adjusted based on the difference in densities of water and ethanol) (Neil and Si, 2018b). The results showed that ethanol infiltration was significantly ($P < 0.05$) higher than that of water, indicating that WR is indeed producing some appreciable effect on the absorption and conductivity of water in the AOSM (Neil and Si, 2018b).

3.5.3 Water Repellency with Depth

There were clear differences in WR between outer (surface; depth = 0 cm) and inner (below surface; depth > 0 cm) portions of the AOSM. The inner material showed a greater degree (CA) and persistence (WDPT) of WR than the outer material, with few exceptions. There is a linear correlation between measurement depth and WDPT, with an $r^2 = 0.61$ (Fig. 3.7). The AOSM sample, of medium to high weathering, from the B/C horizons salvage (B/C-1) had a poor depth–WDPT relationship with an $r^2 = 0.03$; however, the remaining samples (B/C-2, SS-1, and Bm-1) showed strong to moderate correlations with r^2 values of 0.93, 0.69, and 0.62 respectively. A clear difference can be seen between the AOSM of different weathering classes (Fig. 3.7). The least weathered AOSM has the greatest WR and the best relationship between depth and WDPT ($r^2 = 0.93$); the medium AOSM have intermediate WR and reasonable depth–WDPT relationships ($r^2 = 0.69$ and 0.62); and the highly weathered AOSM is generally the least water repellent and has the weakest relationship with depth ($r^2 = 0.03$).

The CA and WDPT increased with salvage depth (Fig. 3.4; Fig. 3.6) and; therefore, there is a positive correlation between WR and salvage depth. This is because shallow AOSM deposits, which are nearer to the soil surface and more exposed to weathering agents prior to salvage, should have a smaller amount of hydrophobic PHC material than AOSM from deeper deposits. The Bm horizon salvage which contains materials from 15 to 50 cm depth, had less TOC than the B/C horizons salvage originating from 50 to 100 cm depth (Fig. 3.2; Table 3.2). The SS salvage contains materials between 15 to 200 cm, where one would expect a greater abundance of low-weathered AOSM; however, the TOC results suggest it contains mainly highly weathered AOSM. This may indicate that AOSM from the SS salvage used in this study originated primarily from shallow depths. In other words, the SS salvage is composed mainly of AOSM from the Bm horizon (15 to 50 cm) and very few from the 50 to 200 cm range. Therefore, there is clearly a dependence of both WR and TOC (i.e., PHCs) on salvage depth.

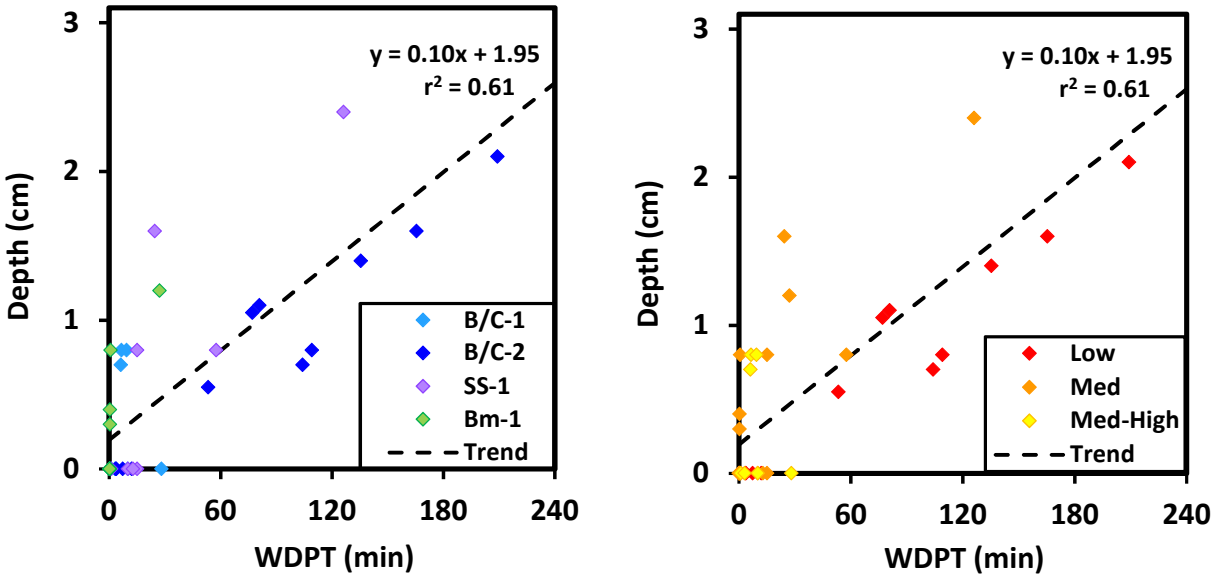

Figure 3.7. WDPT at various depths into four AOSM samples, grouped by soil salvage type (left) and extent of weathering (right).

There is also a negative correlation between WR and the AOSM stage of weathering (Fig. 3.4; Fig. 3.6). Samples from the lowest stage of weathering were more likely to have the greatest WR and include AOSM from the deep salvage (B/C); medium weathered AOSM showed a range of WR and included all salvages (Bm, B/C, and SS); and the highly weathered AOSM are the least water repellent and found in the shallowest material (Bm and SS) (Fig. 3.2; Fig. 3.4; Fig. 3.6). However, due to the unknown pre-disturbance depths of the individual AOSM samples, further analysis of this relationship is not feasible. A similar result was reported by Zhao and Machel (2011) for a site in the Athabasca oil sands region, where the biodegradation of oil sand bitumen was found to decrease with depth.

3.5.4 Onion-Skin Weathering

The relationships among WR, weathering, salvage depth, and TOC (PHC) content confirm the onion-skin weathering hypothesis. As salvage depth increases, exposure to weathering and biodegradation decreases, and consequently PHC content and WR increase. Additionally, WDPT and PHC content are correlated with depth into AOSM samples (Fig. 3.3; Fig. 3.7). Aside from the WDPT results of sample B/C-1, these results also confirm the onion-skin weathering hypothesis, where PHC content and WR increase with depth into the AOSM. The onion skin weathering of AOSM is similar to the spheroidal weathering of rock. Spheroidal weathering results in concentric layers of intact, weathered rock to form sequentially around a central corestone, through fracturing due to mineralogical, chemical, and mechanical processes (Hirata et al. 2016). Typical weathering agents include reactants such as oxygen and water, which advance toward the inside of the corestone (Hirata et al. 2016). In a study focused on the weathering of charnockitic bedrock, Behrens et al. (2015) found that primary minerals are initially removed, leaving behind secondary minerals and crystalline oxides as well as increased porosity. As weathering proceeds, the increase in porosity further increases the ability of reactive substances to penetrate the inner portions of the rock, resulting in enhanced weathering (Behrens et al. 2015). It appears that the removal of PHCs from AOSM may be a similar process: as weathering proceeds, PHCs are removed from the outer portions of the AOSM, increasing porosity and allowing further penetration of weathering agents. This suggests that the spheroidal

weathering and removal of PHCs in AOSM are responsible for the decrease in PHC content and increase in WR, with depth into the soil profile as well as with depth into individual AOSM samples.

3.5.5 AOSM Surface Precipitate

The outer surface of sample B/C-1 differed from the other three WDPT–depth samples, based on visual assessment. It contained extensive cracking, a lighter colour including the presence of a white precipitate on some portions, and a seemingly lower PHC content as was suggested by the colour and by the absence of a strong petroleum odour. These characteristics are indications of strong weathering. However, the surface of this AOSM exhibits substantial WR, contradicting the strong inverse relationships between WR and the degree of weathering and depth into the AOSM. It is possible that the WDPT–depth relationship, which is considerably stronger for other samples, has been modified in sample B/C-1 by the presence of a sulfate compound. The ATR-FTIR results from the outer portions of sample B/C-1 showed a peak absorbance at a wave number of approximately 1100 cm^{-1} (Fig. A.1), which indicates the presence of sulfate (Peak et al. 1999). The outer and inner positions of the other three AOSM samples showed no peak absorbance at 1100 cm^{-1}, with the exception of a portion of the outer surface of sample Bm-1 (Fig. A.1). The outer surface of Bm-1 also contained portions that were similar in appearance to that of B/C-1. However, the previous WDPT–depth measurements of this sample were not performed on the surface(s) which contained the sulfate precipitate, which may explain why Bm-1 did not show a poor WDPT–depth relationship like that of sample B/C-1. Furthermore, additional WR tests confirmed that the portions of Bm-1 which contained sulfate, had a greater mean CA and WDPT on its outer portions (83°, 87 s) than inner (77°, 15 s).

It is possible that sulfate combined with organic substances to form a surfactant (Jafvert and Heath 1991; Zhou and Zhu 2005). Surfactants have the ability to increase the solubility of hydrophobic organic compounds and decrease water repellency, and are a typical means of remediation for various hydrophobic environmental contaminants including PAHs (Jafvert and Heath 1991; Zhou and Zhu 2005). However, depending on the type of surfactant, precipitation and sorption of the surfactant may occur on soil particles, leading to the persistence or exacerbation of hydrophobicity (Zhou and Zhu

2005). For example, strongly sorbed non-ionic surfactants are known to have a strong retention capability for hydrophobic organic compounds, resulting in the reduced availability of hydrophobic substances for degradation and removal (Zhou and Zhu 2005). Therefore, it is possible that a non-ionic sulfate surfactant formed on the surfaces of samples B/C-1 and Bm-1, altering the WR of the affected materials.

3.5.6 Implications for Reclamation

As mentioned, the WR–depth relationship that was observed in the majority of the AOSM is consistent with onion-skin weathering. This has important implications for the salvaging of soil cover materials as well as their re-placement. Because AOSM from deep soils is at a low stage of weathering and thus has the potential for a high level of WR, discreet salvage or salvage by depth, such as the Bm and B/C horizons salvages, will create a natural separation of materials into two classes: ASOM from the Bm (shallow) is predominantly wettable or subcritically water repellent, while the B/C salvage (deep) contains a much greater proportion of water repellent AOSM. For the former, AOSM may still absorb and store water even when experiencing excessive drought, but on the whole the latter may not. Therefore, depending on the site specific conditions, separate placement may be advantageous (i.e., when soils are excessively dry). In such a case, AOSM from the Bm salvage could be placed in the near surface (i.e., rooting zone) and AOSM from the B/C salvage placed deeper in the profile (i.e., below rooting zone). This arrangement will promote hydrophilic conditions by preventing the relatively water repellent AOSM of the deeper salvage from undergoing excessive drying and; therefore, alleviating the potential for the AOSM to become highly water repellent. The presence of excessively dry, highly water repellent oil sand material in the near surface or on the soil surface could limit the infiltration of water into the soil profile and; consequently, reduce soil water storage. This may be particularly relevant when considering the construction of a sloping landscape, where water repellent AOSM placed in the near surface has the potential to reduce infiltration and promote the occurrences of overland flow and erosion.

WR increases with depth into the AOSM. This suggests that it may be beneficial to conduct soil salvaging, stockpiling, and placement in a manner which minimizes or avoids excessively breaking up the AOSM, so that the relatively water repellent inner portions of the material are not overly exposed. The more hydrophilic outer portions will likely absorb a greater amount of water than the highly water repellent inner portions and; therefore, when AOSM are in-tact their outer portions will more often contain water, which may make it easier for the highly water repellent inner portions to also absorb and store water. Handling of the AOSM during cold weather (i.e., winter) would minimize its breakup because under low temperatures the oil in the AOSM is extremely viscous, making these materials relatively rigid.

Several CA measurements were also made by Rosso (2016) on soil matrix from a sand textured B/C horizons salvage collected from the ASCS area. The results showed maximum CAs ranging between 11° and 45°, classifying the soil as subcritically water repellent. Cross-comparison between AOSM from our study and soil matrix from Russo (2016), as well as Hunter et al. (2011), suggests that AOSM is more water repellent than the surrounding soil matrix. This could result in a slower drainage of water through AOSM deposits. Given the current information, it is difficult to predict whether the incorporation of the more water repellent AOSM in reclamation soils will have a positive or negative effect on improving soil water storage. More information, such as the water infiltrability of AOSM in reclamation soils, in addition to the maximum potential water repellency obtained from this study, is needed in order to answer this question.

3.6 Conclusions

It seems likely that AOSM weathers in an onion-skin manner, in terms of both salvage depth and depth into individual AOSM samples: there is a greater degree of weathering and lower PHC content and WR in the shallow salvage materials, and similarly a greater degree of weathering and lower PHC content and WR on the surface of individual AOSM than at depth.

It is apparent that AOSM show a range of water repellent behavior in terms of both degree and persistence. Regardless, the subcritical nature of the WR in AOSM suggests that water absorption will

still occur, albeit relatively slowly. The majority of the samples allowed infiltration to commence within one minute of exposure, indicating that repellency will likely persist only during periods of extensive drought, and only in the small portion of materials that show a severe or extreme persistence of WR. However, this small amount of hydrophobic material has the potential to significantly impact the hydrology of an affected area. The results from previous studies appear to support this, which show that sandy soil matrix from the study area has a considerably lower degree of WR and absorbs water more effectively than the AOSM from our current study. Nonetheless, the ability of the AOSM to allow at least some infiltration will minimize the negative effects of WR-related phenomena.

4. INTERSTITIAL HYDROCARBONS REDUCE THE INFILTRATION RATES OF COARSE-TEXTURED RECLAMATION MATERIALS FROM THE ATHABASCA OIL SANDS[2]

4.1 Preface

Reclamation in the Alberta oil sands is facing many challenges, among the most prominent of which are those associated with coarse-textured soils. Typically, these soils have poor water and nutrient retentions, which can limit the potential productivity of emerging ecosystems. Previous studies have shown that textural/structural layering in natural and reclamation soils have the ability to increase soil water storage and provide additional water for plant uptake. It has been speculated that the inclusion of oil sand materials within the near-surface of the soil profile may also contribute to this effect, by reducing percolation and increasing the residence time of water within the overlying soils. This reduction in water flow is thought to be the result of reduced porosity due to the presence of interstitial petroleum hydrocarbons (PHC)s. Furthermore, Chapter 3 confirmed that near-surface oil sand inclusions exhibit hydrophobicity, which reduces the absorption of water in these materials. These near-surface oil sand inclusions may; therefore, have the ability to modify the soil water regime and associated ecosystems which emerge in these areas. To improve our understanding of the soil water dynamics of oil sand-affected coarse-textured soils, the current chapter examines the water infiltration rates of oil sand inclusions and their surrounding soils.

4.2 Abstract

In the Alberta oil sands, many soils available for reclamation contain portions of oil sand referred to as aggregated oil sand material (AOSM). The objective of this study was to determine the infiltration rates of soils and AOSM from various salvage depths and with various concentrations of interstitial

[2] This work has been previously included in Neil, E.J., and Si, B.C. (2018), Interstitial hydrocarbons reduce the infiltration rates of coarse-textured reclamation materials from the Athabasca oil sands. Accepted in Catena. Minor modifications have been made for consistency.

petroleum hydrocarbons (PHCs). The water infiltration rates of AOSM and surrounding soil were determined using a miniaturized infiltrometer, revealing that the soil allows significantly ($P < 0.05$) greater infiltration than the AOSM. Furthermore, highly-weathered AOSM which originate from the near-surface, exhibit significantly lower PHC contents and greater infiltration rates than medium- and low-weathered AOSM, which are found at depth. The infiltration of 95% ethanol indicates water repellency (WR) is present in both the AOSM and surrounding soil; however, the ethanol results also suggest that the reduced water infiltration rates of AOSM in comparison to the soil, are primarily due to structural differences such as reductions in total porosity and pore connectivity resulting from interstitial PHCs. The diminished infiltration of water into AOSM indicates the ability to slow the downward flow of water and increase the residence time of water in overlying coarse-textured soils, potentially altering the soil water regime and associated ecosite.

4.3 Introduction

The shallow oil sand deposits of northern Alberta, which are economical for open pit mining, consist of a 4,800 km^2 region near Fort McMurray, AB (Government of Alberta, 2016). These near-surface oil sand deposits are accessed by first removing vegetation from the landscape as well as peat, soils, subsoils, and lean oil sand overburden. Once mining operations are complete, reclamation in these areas will require the reconstruction of landforms and ecosystems at a landscape scale (Johnson & Miyanishi, 2008). One key to successful mine reclamation involves the design of a soil medium which has sufficient water and nutrient retention for the development of a desired plant community (Leatherdale et al., 2012). Within the oil sands region, approximately 20% of the final reclaimed landscape will be composed of layered, coarse-textured glaciofluvial and aeolian deposits (Huang et al., 2011). Regardless of their relatively uniform textural classifications, these mining affected areas naturally support a range of boreal forest ecosite and forest stand types, over a range of moisture regimes (Zettl et al., 2011). In order to recreate ecosite assemblages and spatial arrangements similar to those present prior to disturbance, soil treatments capable of supporting various moisture regimes and ecosite phases are required.

Many of the surface soils and subsoils in the Athabasca oil sands region naturally contain portions of oil sand, in the form of discreet accumulations and layers (Leskiw et al., 2006; Visser, 2008). During salvaging and stockpiling activities, these oil sand inclusions often become further fragmented and mixed into the soils. One of the most abundant forms of oil sand inclusions are aggregated oil sand materials (AOSM), which have been previously referred to as “tarballs”. AOSM are discrete accumulations of oil sand of various shapes, ranging from a few centimetres up to several metres in diameter (Fleming, 2012). Limited information is currently available on oil sand aggregates and layers in the root zone of this boreal forest ecosystem; however, it has been frequently observed that in profiles with significant quantities of oil sand within the subsoil, the soil just above was consistently wetter than the surrounding soil (Leskiw et al., 2006; Fleming, 2012). This is likely explained by a change in water conducting porosity, resulting in a prolonged residence time of water in the root zone. Consequently, if an oil sand layer is found within the subsoil material beneath the rooting zone, there may be significant opportunity for increased soil water content, which may result in altered vegetative cover compared to that of an oil sand-free soil (Leskiw, 2005). However, it has also been observed that the presence of an oil sand layer, on or near the soil surface, may limit water storage and plant rooting depth, presumably due to reduced water entry caused by physical sealing or hydrophobicity (Leskiw et al., 2006). It is apparent that further investigation into the cause(s) of modified water contents in hydrocarbon-affected soils is necessary in order to optimize the effectiveness of reclamation prescriptions.

The Alberta oil sand deposits are structured such that, upon formation there is a thin layer of water located between the mineral grains and bitumen, resulting in the protrusion of bitumen into the centers of the pores (Mossop, 1980; Takamura, 1982). Not surprisingly, these bitumen accumulations are known to substantially impede the flow of fluid through the material (Mossop, 1980). This may be due to a reduction in effective porosity, resulting from the presence of the interstitial bitumen. Additionally, water introduced to oil sand will be in direct contact with interstitial bitumen as opposed to mineral grain surfaces, which suggests that the ability of the oil sand to absorb and conduct water will be largely controlled by the surface chemistry and associated hydraulic properties of the bitumen itself.

The composition of bitumen is diverse and complex, containing a multitude of petroleum hydrocarbon (PHC) compounds with various chemical and physical properties (Eastcott et al., 1988; Frontera-Suau, 2000; Gu, 2006). Oil sand bitumen may be modified by physical, chemical, and biological weathering agents, which in turn affects the composition, availability, and distribution of PHCs within the environment (Brassington et al., 2007). At this stage in its weathering, AOSM from the Athabasca oil sands region contains mainly high-molecular-weight or "heavy" PHCs and little or no "light" PHCs (Visser, 2008; Fleming, 2012). AOSM is typically composed of heavy hydrocarbons from the F3 (Carbon $[C]_{>16}$ - C_{34}) and F4 ($C_{>34}$) fractions, some F2 ($C_{>10}$ - C_{16}), and little or none of the F1 (C_6 – C_{10}) and volatile fractions (Canadian Council of Ministers of the Environment, 2008) (Visser, 2008; Fleming, 2012). Fleming (2012) found exceptions to this, where AOSM with "rich" cores contained total PHC contents that were orders of magnitude greater and included elevated levels of the lighter F1 and F2 fractions. The low abundance of light PHCs, in typical AOSM, is due to a combination of factors: light or low-complexity PHCs are biodegraded preferentially to heavy, high-complexity PHCs (Mossop, 1980; Brunner et al., 1987; Cerniglia, 1992); light PHCs are more soluble and mobile in soil solution and, consequently, have a greater chance of removal from the AOSM (Eastcott et al., 1988; Visser, 2008) and; heavy PHCs are often degraded into smaller "daughter" PHCs, which may have a greater solubility and, therefore, a greater probability of removal in soil solution (Fleming, 2012). The relative solubilities of the different hydrocarbon fractions suggest that light PHCs are relatively hydrophilic whereas heavy PHCs are hydrophobic. Neil and Si (2018a) found that AOSM have onion-skin weathering and water repellency (WR) patterns, with increases in total organic carbon (TOC), which is used as an estimate of PHC content, and increases in WR with increasing salvage depth and with depth into individual samples. In other words, AOSM which are presumably more exposed to weathering, such as near-surface deposits and the outer portions of individual aggregates, typically contain fewer PHCs and are less water repellent than portions which are relatively protected, such as deep deposits and inner portions of individual aggregates. This indicates that the WR, and perhaps other hydraulic properties of AOSM, are a factor of its degradational history and resultant PHC distribution.

Neil and Si (2018a) observed a range of water repellent behaviour in AOSM. Due to the heterogeneous and dynamic nature of the WR within AOSM, it is difficult to predict based solely on WR, whether or not other hydraulic properties of the material will be significantly impacted. Properties such as hydraulic conductivity or infiltration rate can provide valuable insight into how a material will behave on a larger scale and how it may impact it's host soil profile and ecosystem through such phenomenon as reduced infiltration, runoff and erosion, preferential flow, and reduced soil water storage (Dekker and Ritsema 1994; Doerr et al. 2000). Because the PHCs within oil sand reduce pore space and promote WR, and the TOC (i.e., PHCs) and WR are correlated with salvage depth and depth into individual samples, we hypothesize that the infiltration rates of AOSM decrease with increasing salvage depth and depth within individual samples, and consequently with increasing PHCs and WR. In addition, we hypothesize that the infiltration of water into AOSM will be significantly reduced in comparison to the texturally similar surrounding soil matrix, due to the presence of interstitial PHCs. To test these hypotheses, infiltration experiments were performed on coarse-textured subsoils of various salvage depths, and on the outer and inner portions of AOSM inclusions from soil salvages of various depths and relative stages of weathering. The objective of this study was to determine the infiltration rates of coarse-textured subsoils and the PHC-affected oil sand aggregates contained within, and to evaluate the effects of PHC content, WR, and salvage depth on these values. This will provide insight into the potential effects of AOSM on the soil water dynamics of reclamation soils.

4.4 Materials and Methods

4.4.1 Study Site and Reclamation Materials

The Aurora Soil Capping Study (ASCS) site at the Syncrude Canada Ltd. Aurora North Mine, north of Fort McMurray, AB, was chosen for this study. The ASCS is a long-term instrumented watershed research site, used to evaluate the performance of various reclamation prescriptions utilizing hydrocarbon-affected soils and lean oil sand overburden. The ASCS consists of 36 one-hectare plots composed of soil reclamation materials containing oil sand aggregates in varying

proportions. There are 12 treatments repeated in triplicate, with the treatments ranging in soil cover design (i.e., one or two soil horizons) and in total reclamation capping thickness. Coversoil (i.e., reclaimed topsoil) materials used in the ASCS are composed of peat salvaged from lowland bogs and fens within the mine development footprint, and of surface soil from upland forest areas containing LFH, A horizon material, and potentially a portion of the B horizon. Subsoil materials consist of mineral soils which contain AOSM, that are salvaged at various depths after the salvage of upland surface soil.

The parent materials for these salvaged soils are primarily of glaciofluvial and aeolian origins, resulting in the subsequent formation of coarse-textured Brunisolic soils (Leskiw et al., 2006). The site is part of the Central Mixedwood Natural Subregion within the Boreal Forest Natural Region of Alberta (Natural Regions Committee, 2006), and its soils typically support an a1 ecosite phase, characterized by a subxeric moisture regime and poor nutrient regime, with jack pine (*Pinus banksiana* Lamb) and lichen (*Cladina* spp. and *Cladonia gracilis*) as the dominant tree and understory species (Beckingham & Archibald, 1996). AOSM-affected soil was collected from the following salvaged subsoil materials composing the ASCS, as described in Chapter 3:

- Upper Subsoil Bm horizon salvage (15 – 50 cm): Surface soil was removed (LFH layer, A horizon, and a portion of the top of the B horizon which totals approximately 15 – 20 cm), then the remaining Bm horizon was salvaged to a depth of 50 cm.
- Blended B/C horizons salvage (50 – 100 cm): Surface soil and upper subsoil Bm horizon were removed (0 – 50 cm), then the remaining B horizon and a portion of the C horizon were salvaged to a depth of 100 cm.
- Composite Subsoil salvage (15 – 200 cm): Surface soil was removed (LFH layer, A horizon, and a portion of the top of the B horizon which totals approximately 15 – 20 cm), then the remaining Bm horizon and a portion of the C horizon were salvaged to a depth of 200 cm.

The soil salvage types will be abbreviated as Bm, B/C, and SS respectively. AOSM was chosen from each of the available reclamation materials, with sizes ranging from centimeters to decimeters in diameter. The AOSM were categorized into one of three weathering stages or classes (low, medium, or highly weathered) based on physical stability, colour, and odour, as outlined in Chapter 3 (Table 3.1). The AOSM was stored at 4 °C to minimize degradation, except during preparation and testing, which occurred at 20 °C and 30% relative humidity.

The particle size distributions of the soils and AOSM were determined using a Horiba LA-950 particle size analyzer (Horiba Scientific, Edison, NJ, USA). The TOC contents of the AOSM and surrounding soil matrix were determined using a LECO C-632 dry combustion carbonator (LECO Corp., St. Joseph, MI, USA) (Wang & Anderson, 1998). Since PHCs are composed largely of carbon, the TOC contents were used as a quick means of estimating the relative PHC contents of the various salvage materials. The soil matrix was sieved to a diameter of 2 mm and packed into metal cores with a length and inner diameter of 5.08 cm, at a gravimetric water content of 0.05 g g^{-1} and bulk density of 1.6 g cm^{-3}. Prior to testing, the soil cores and AOSM were air dried at 20 °C and 30% relative humidity until reaching constant mass.

4.4.2 Miniaturized Infiltrometer

In order to determine the infiltration rates and hydraulic parameters (field-saturated hydraulic conductivity, K_{fs}, and inverse capillary length scale, α) of the AOSM and its host soil matrix, a tension-controlled infiltration experiment was performed using a miniaturized infiltrometer. The experimental setup was a modified version of that used by Leeds-Harrison et al. (1994). The most notable differences were those of the infiltrometer tip and liquid reservoir. The infiltrometer tip design from Chau et al. (2012) was used, which consists of a modified 200 μL pipette tip with an inner diameter of 2 mm and a selectively permeable nylon membrane fixed upon it's end using cyanoacrylate adhesive (superglue). The nylon membrane has an air entry value of approximately -3 kPa or -30 cm water pressure head, which restricts the flow of air at suctions (Ψ) of 3 kPa or less, but allows the passage of liquid. This enables the measurement of liquid flow into materials under negative pore pressure

conditions. The liquid reservoir used in the current study was a form of “Mariotte’s bottle”. This type of apparatus allows fluid to exit the reservoir at a constant water pressure head, regardless of a changing height of fluid in the reservoir (McCarthy, 1934). This provides the capability to conduct infiltration measurements at a constant, known water pressure head throughout the course of an experiment as water is removed from the reservoir.

During testing, the AOSM and soil matrix cores were individually placed on a height-adjustable stand and raised until contact was made between the sample and the infiltrometer tip. During infiltration liquid was drawn out of the reservoir, through the tubing, and into the sample, which registered as a change in mass on an analytical balance. The infiltration rate could therefore, be determined by recording the change in mass in the reservoir over time. During infiltration the mass of the reservoir was recorded at 10 s intervals for the first five minutes and 60 s intervals thereafter. Measurements were conducted sequentially from low to high pressure heads, at values of –20, –13, –7, –3, –1.5, and –1.2 or –0.1 cm. As the pore water pressure conditions were increased (suction decreased), progressively larger soil pores were being accessed in addition to those that were already participating in the infiltration. This is due to the inverse relationship between pore water suction and pore size. The suction values listed above were chosen to provide an indication of the flow of water through macropores (≥ 1 mm pore diameter; pressure heads ≥ -3cm or suctions ≤ 3cm), as well as that of mesopores and micropores (< 1 mm pore diameter; pressure heads < -3cm or suctions > 3cm). The infiltration rate, or liquid flux, from the tip of the infiltrometer was calculated according to the following:

$$q_i = \frac{m_i}{A t_i \rho_f} \tag{4.1}$$

where q_i is the flux or infiltration rate ($L^3\ L^{-2}\ T^{-1}$), A is the contact surface area (L^2), t_i is the time interval of infiltration (T), ρ_f is the liquid density ($M\ L^{-3}$), and m is the mass of liquid infiltrated (M) during time interval t_i.

The majority of the AOSM samples used in this study were previously tested for water repellency (Chapter 3). Once the water repellent characteristics of the AOSM had been determined, the samples were once again air dried and then infiltrations completed on the same locations. The infiltration testing included 22 AOSM samples of various weathering stages, and consequently of various levels of WR, which were chosen randomly from the collected salvage materials. In addition to the AOSM, six soil matrix samples were also tested. The water infiltrations were performed on multiple locations (two to four) on the outer surfaces of each of the AOSM to account for variability within samples. From the 22 AOSM samples, four were chosen for extensive testing on their inner portions (i.e., at various depths within aggregates) in addition to their outer surfaces. Similarly, the WR measurements on the inner portions were completed at multiple depths, and the samples air dried prior to performing the infiltration tests at the same locations and depths.

Additional water infiltration testing was performed on the outer portions of three AOSM samples that were air dried between individual infiltrations. In other words, when the water infiltration rate decreased in response to a decrease in suction (or increase in water pressure head), the AOSM was air dried and the experiment resumed at the suction showing the reduced values.

Once the water infiltrations were complete, the unknown hydraulic parameters were estimated using Wooding's (1968) equation for steady-state infiltration under a shallow circular pond:

$$q(h) = \left(1 + \frac{4}{\alpha \pi r_d}\right) K_{fs} \exp(\alpha h) \tag{4.2}$$

where $q(h)$ is steady-state infiltration rate (L T^{-1}), h is pressure head (L), r_d is the contact radius (L), α is the inverse capillary length scale (L^{-1}), and K_{fs} is the field-saturated hydraulic conductivity (L T^{-1}). The α and K_{fs} parameters were estimated through non-linear regression of q as a function of h, using curve fitting and the least squares method. Wooding's (1968) model and the fitted hydraulic parameters can be used in future modelling and estimation of infiltration rates under various antecedent soil water content or pore suction conditions.

In addition to the various water infiltrations, four AOSM samples and several soil matrix cores were also tested using 95% ethanol. Ethanol has a substantially lower surface tension than water and as a result is virtually not affected by water repellent surfaces (Tillman et al., 1989). Essentially, the ethanol infiltration rate represents the maximum water infiltration rate that could be achieved by the sample if water repellency were not present. Furthermore, because ethanol ignores the effects of repellency, it can provide information about the pore connectivity of water repellent materials (Tillman et al., 1989). Because it was known that the PHCs within the AOSM may be solubilized and removed by the ethanol solution, thereby changing the structure of the AOSM, infiltration times were kept to a minimum. Once steady state was reached at an individual suction value, as indicated by a constant infiltration rate, the infiltration was halted at that suction and immediately resumed at the next (lower) suction value. In this way, the contact time between the PHCs and ethanol solution was minimized, thus reducing the opportunity for PHC solubilization and removal during infiltration measurements. All ethanol infiltrations were performed under pressure conditions equivalent to those of the water infiltrations, and were calculated as follows:

$$h_E = \frac{\rho_w h_w}{\rho_E} \tag{4.3}$$

where h_E and h_W are ethanol and water pressure heads (L), and ρ_E and ρ_W are ethanol and water densities (M L^{-3}).

Several analysis of variance (ANOVA) were used to examine differences in infiltration rates of the AOSM and surrounding soil matrix, and to determine whether changes in measurement depth, salvage depth, and water pressure head produce significant effects on the mean infiltration rates of AOSM, where differences were considered significant at $P < 0.05$. Additionally, Pearson's r was used to examine linear correlations between infiltration rate and WR (Contact angle [CA] and water drop penetration time [WDPT]).

4.5 Results

4.5.1 Material Characterization

Using the particle size classification system of the Canadian Soil Survey Committee (1982) and textural classification of the Canadian System of Soil Classification (Soil Classification Working Group, 1998), the AOSM and surrounding soil matrix of the ASCS are considered sand-textured, with the exception of two AOSM samples which were loamy sand. ANOVA revealed AOSM have a significantly ($P = 3 \times 10^{-6}$) lower quantity (i.e., mass) of clay sized particles than their respective host soils, although the total clay content is low in both the AOSM (0.0%) and soil matrix (0.4%) (Table C.1). In addition, ANOVAs also showed that the outer and inner potions of the AOSM are not significantly different ($P > 0.1$) in texture (soil separates) (Tables C.2, C.3, and C.4).

The TOC contents of the soil matrix and AOSM were determined for each of the soil salvage materials (Table 4.1). Rosso (2016) found similar mass-based TOC contents in the ASCS soil matrix, with means and standard deviations of 1.4 ± 0.2%, 0.8 ± 0.2%, and 0.5 ± 0.2% in the Bm, B/C, and SS salvages respectively. In addition, ANOVA showed that the TOC contents of the outer (7.6 ± 3.9%) and inner (9.6 ± 3.3%) portions of the AOSM are not significantly different ($P = 0.051$) (Table C.8); however, for the four AOSM samples tested on their inner portions, the TOC contents are significantly different ($P = 0.031$) (Table C.9), with less TOC in the outer material (7.4 ± 2.6%) than inner (9.6 ± 3.3%).

Table 4.1.
Mean and (standard deviation) of total organic carbon content in % by mass of soil matrix, outer AOSM, and inner AOSM from three soil salvage types.

Salvage Type	Depth (cm)	AOSM Weathering	Total Organic Carbon (%)		
			Soil Matrix	AOSM	
				Outer	Inner
Bm	15-50	Med-High	0.6 (0.09)	6.3 (2.1)	7.9 (2.1)
B/C	50-100	Low-Med	0.4 (0.03)	10.2 (5.6)	11.2 (3.1)
SS	15-200	Med-High	0.7 (0.06)	6.8 (2.1)	6.6 (1.0)

†AOSM = aggregated oil sand material

The low weathering class was composed of AOSM from the deep salvage types (B/C and SS); the medium class included all salvages (Bm, B/C, and SS); and the highly-weathered class included the salvage types with the shallowest materials (Bm and SS) (Fig. 4.1). ANOVA confirmed that AOSM from the low weathering class contains significantly greater TOC contents (13.0 ± 4.1%) than the highly-weathered (6.8 ± 2.8% TOC; $P = 5 \times 10^{-5}$) (Table C.10) and medium-weathered AOSM (6.4 ± 1.8% TOC; $P = 4 \times 10^{-15}$) (Table C.11).

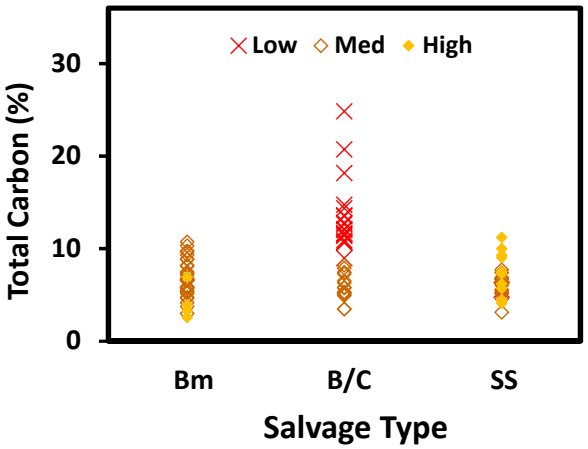

Figure 4.1. Total mass-based carbon content of AOSM from various weathering classes (low, medium, high) and soil salvage types: Bm (15-50 cm), B/C (50-100 cm), SS (15-200 cm).

4.5.2 Water Infiltration

In many cases, water infiltration into the AOSM began immediately upon contact with the infiltrometer, but in others it took up to several minutes. For many of the AOSM, once the flow of water began at a given suction, infiltration fluctuated through time. Infiltration rate was typically greatest during the initial several minutes of flow, and would then decrease rapidly through time. Due to this variability, the infiltration rates of individual tests were calculated as the mean of the readings from the first five minutes of measurements, taken at 10 s intervals. In addition to the temporal variability seen within individual infiltrations, there was also considerable variability between AOSM samples. The coefficients of variations (CV) in water infiltration rates were relatively high as well as suction dependent, ranging from 0.49 to 1.26 for outer material and from 0.40 to 1.01 for inner material.

Figure 4.2 shows examples of the various water infiltration–suction trends observed in the AOSM. Many of the individual samples did not show an exponential increase in infiltration rate with a decrease in suction (increase in water pressure head), but instead would experience a decrease in infiltration or no clear trend at all. Figure 4.2A and to some extent Figure 4.2E, show infiltration curves from AOSM sampling positions which display typical soil water infiltration curves, for which Eq. 4.2 can be successfully applied. The remaining examples in Figure 4.2 show infiltration curves which would be considered atypical for homogeneous soils.

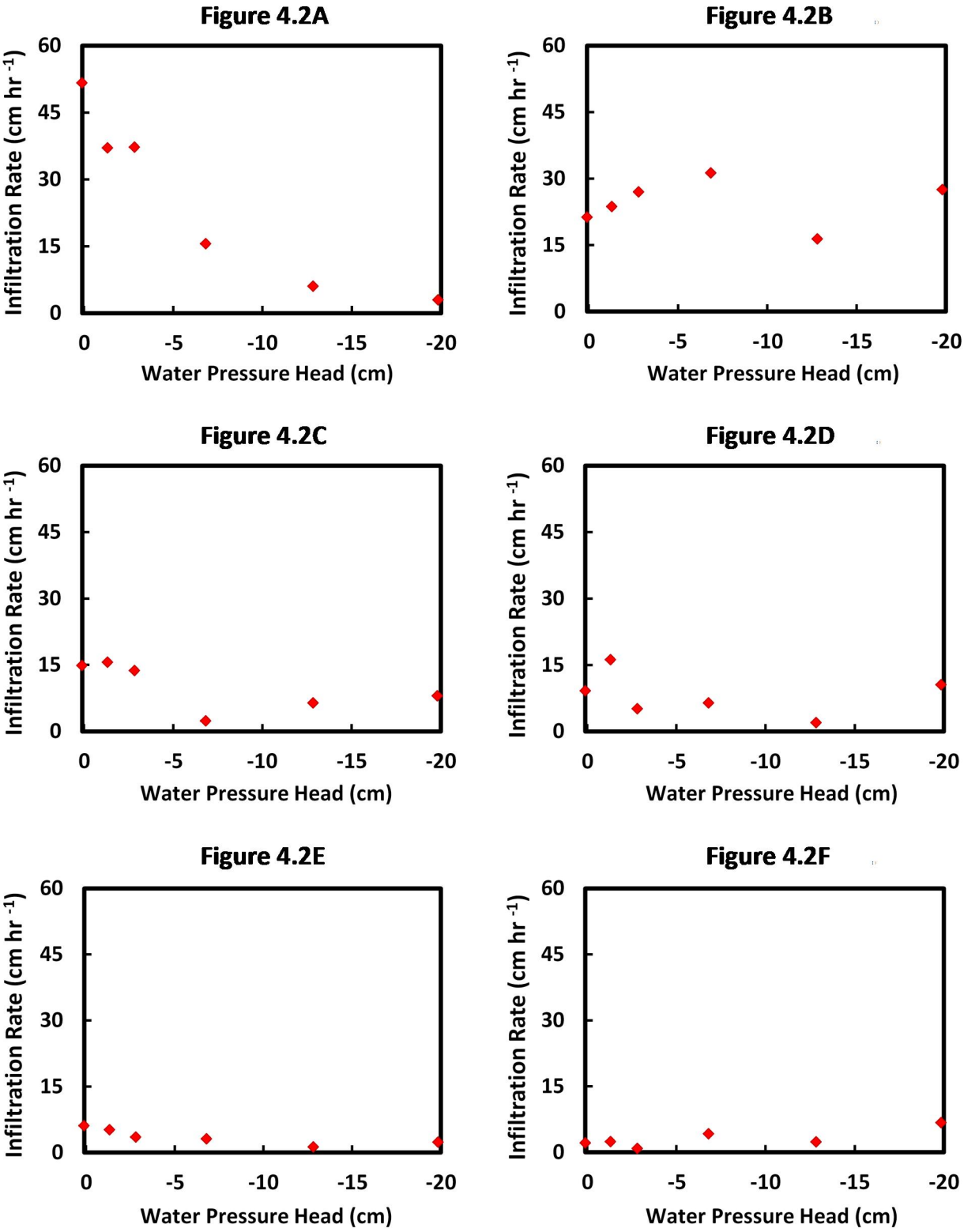

Figure 4.2. Water infiltration rates of AOSM, as a function of water pressure head. Figures 2A to 2F show the results from six samples which encompass the various infiltration trends observed in AOSM.

The mean water infiltration rates of the outer and inner portions of the AOSM are similar at each of the tested suctions (water pressure head values). The results of the water infiltrations confirmed the mean infiltration rates of the outer and inner portions, both separately and combined, did not significantly differ with suction (within or across individual AOSM samples or salvage types). Because the water infiltration rates of the outer and inner portions of AOSM were not significantly different, the results for these materials were combined prior to further data analysis. The mean water infiltration values of the AOSM (outer and inner combined) and soil matrix are presented in Figure 4.3. The mean water infiltration rates of the soil matrix differ significantly with suction (Table C.12), where a decrease in suction results in greater infiltration. The soil matrix values were used in conjunction with Eq. 4.2 to obtain hydraulic parameters for this material (Fig. 4.3). The AOSM; however, did not show the same exponential relationship and; therefore, Eq. 4.2 could not be applied with the same level of accuracy. ANOVAs show AOSM have significantly lower mean water infiltration rates than that of the soil matrix in the $\Psi \leq 7$cm suction range (Tables C.17, C.18, C.19, and C.20); however, no significant difference was found at higher suctions.

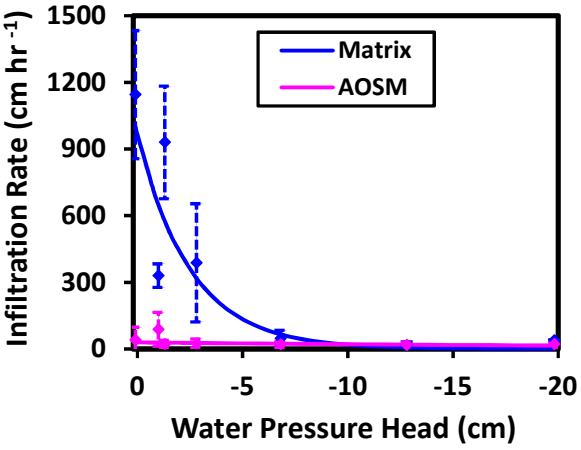

	α (cm^{-1})	K_{fs} ($cm\ hr^{-1}$)	r^2
Matrix	**0.39**	**31.1**	**0.81**
AOSM	**0.03**	**0.08**	**0.24**

Figure 4.3. Mean water infiltration rate as a function of water pressure head for soil matrix and AOSM. Solid lines (curves) are best-fit predictions obtained using Wooding's (1968) relationship; error bars display standard deviations of mean values. Tabled values show the predicted hydraulic parameters (field-saturated hydraulic conductivity, K_{fs}; inverse capillary length scale, α) and the fit of the predicted curves (Pearson's correlation coefficient, r^2).

According to the results of Neil and Si (2018a), the majority of the AOSM samples used in the current study express some level of water repellency. The mean CA of water on the surface of air-dry AOSM samples was 47° with a CV of 96%, and the mean WDPT was 824 s with a CV of 221% (Neil and Si, 2018a). While there may appear to be a relationship between infiltration rate and WR (CA and WDPT) for select AOSM samples and/or suctions, the majority did not show any predictable relationships. There is; however, a relationship between the AOSM weathering stage and mean water infiltration rates. Figure 4.4 shows the measured and predicted water infiltration values of AOSM from the three weathering classes.

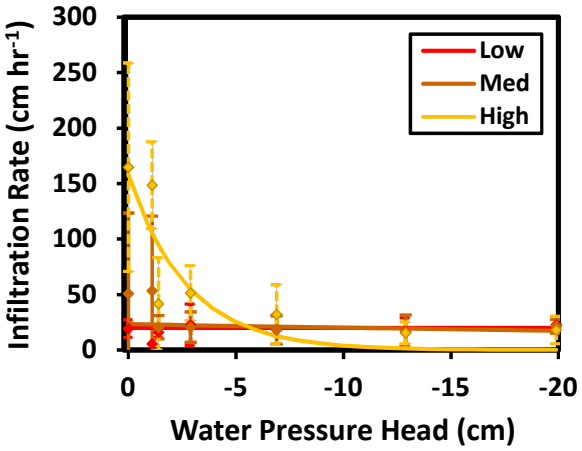

	α (cm^{-1})	K_{fs} (cm hr^{-1})	r^2
Low	0.0003	0.0004	0.35
Med	0.02	0.03	0.20
High	0.37	4.61	0.83

Figure 4.4. Mean water infiltration rates as a function of water pressure head for AOSM from three weathering stages. Solid lines (curves) are best-fit predictions obtained using Wooding's (1968) relationship; error bars display standard deviations of mean values. Tabled values show the predicted hydraulic parameters (field-saturated hydraulic conductivity, K_{fs}; inverse capillary length scale, α) and the fit of the predicted curves (Pearson's correlation coefficient, r^2).

The highly-weathered AOSM had the greatest water infiltration rates in the macropore range ($\Psi \leq 3$cm), of all weathering classes, and exhibited an exponential infiltration–suction trend. Consequently, Eq. 4.2 fit well to the measured data ($r^2 = 0.83$). In contrast, the low- and medium-weathered AOSM had relatively low water infiltration rates at all tested suctions, with a negligible increase or even a decrease in infiltration with decreasing suction. As a result, Eq. 4.2 provided a weaker fit to the low- ($r^2 = 0.35$) and medium-weathered ($r^2 = 0.20$) AOSM.

Three AOSM samples were tested on their outer surfaces to examine the effects of drying between infiltrations. Figure 4.5 includes the results from one of the samples, which showed a similar pattern to that of the other two samples. When water infiltration rate declined in response to a decrease in suction (purple line segments in Figure 4.5), the AOSM was air dried and the experiment resumed.

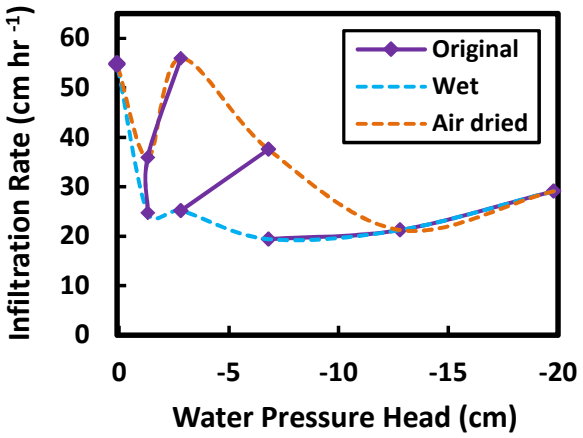

Figure 4.5. Mean water infiltration rates as a function of water pressure head for an AOSM sample. Each separate purple line segment represents infiltrations performed sequentially, with no drying time between measurements. The blue line represents the infiltration rates obtained when the sample was wet from previous infiltrations. The orange line shows the infiltration rates obtained when the sample was air dried between measurements.

Generally, once the AOSM was re-dried and re-tested, water infiltration rates were greater (orange dotted line in Figure 4.5) than when the material was wet (blue dotted line in Figure 4.5). However, this did not necessarily result in a more traditional trend, where an increase in infiltration occurs in response to a decrease in suction. As with the majority of the AOSM, in addition to the unusual mean infiltration–suction trends, there were fluctuating infiltration rates through time at individual suctions.

4.5.3 Ethanol Infiltration

To determine whether WR was contributing to the atypical trends seen in the water infiltration results, infiltrations were performed using 95% ethanol. Four AOSM samples, which showed considerable fluctuations in water infiltration rates through time as well as atypical infiltration–suction

trends, were tested with ethanol on their outer surfaces. The water and ethanol infiltration curves show clear differences in their magnitude and infiltration–suction relationships (Fig. 4.6), as is the case for all of the AOSM tested with ethanol. Ethanol infiltration did not occur in any of the AOSM or soil matrix samples at the 20 cm suction, but at all other suctions it was typically greater than that of its water counterpart.

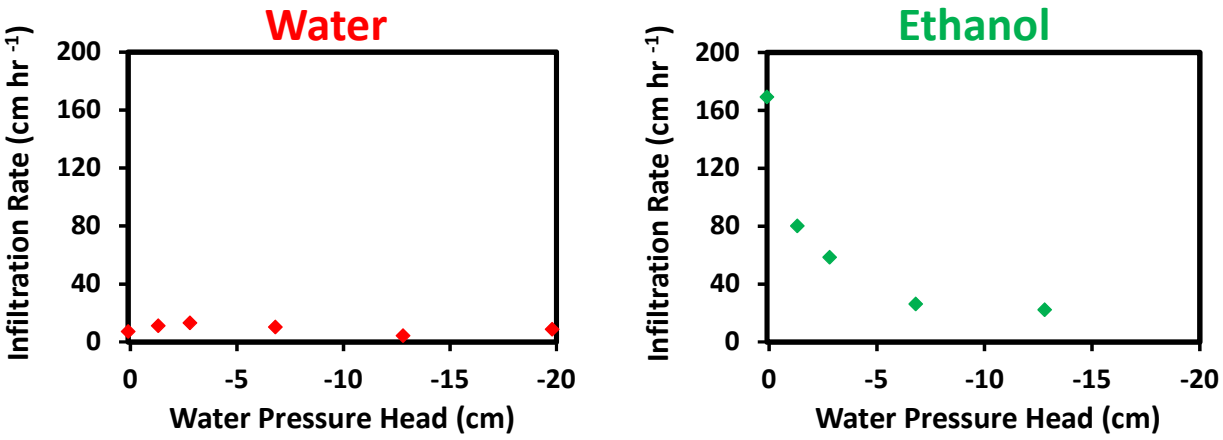

Figure 4.6. Mean infiltration rates of water and 95% ethanol as a function of water pressure head for an AOSM sample.

The AOSM infiltration rates of water and ethanol are significantly different at $\Psi < 3$ cm (Tables C.13 and C.14). Furthermore, the mean AOSM ethanol infiltration rates were at least 2 times greater, depending on suction, and generally displayed a more exponential relationship with suction than that of their water infiltrations (Fig. 4.7B). ANOVAs confirmed the water infiltration rates of AOSM were similar between suctions (Table C.15), but the ethanol infiltration rates differed significantly with suction (Table C.16) where a decrease in suction resulted in an increase in infiltration.

The soil matrix, which does not contain an abundance of PHCs (< 1% TOC), also showed some repellency, with ethanol infiltration rates of up to approximately 2.5 times greater in the macropore range, depending on suction, than its water infiltration rates. Unlike the AOSM, the soil matrix water infiltration significantly differed between suctions (Table C.12), where a decrease in suction resulted in an increased infiltration rate (Fig. 4.7A). The ethanol infiltration rates of the soil matrix also differed between suctions (Fig. 4.7A).

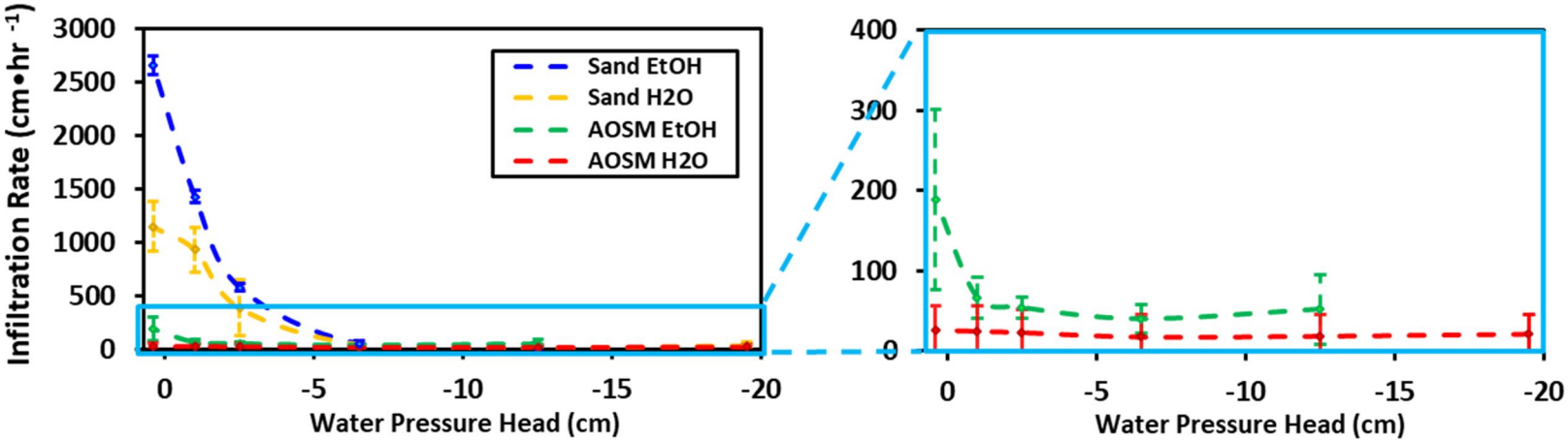

Figure 4.7. Mean infiltration rates of water (H_2O) and 95% ethanol (EtOH) as a function of water pressure head for AOSM and sandy soil matrix samples. Figure 7B shows a magnified view of the infiltration curves of the AOSM displayed in Figure 7A.2

4.6 Discussion

4.6.1 Water Infiltration

The results of the AOSM weathering classification are consistent with onion-skin weathering, where AOSM from shallow salvage depths are presumably more exposed to weathering agents and; thus, more degraded and contain less TOC (i.e., PHCs) than those found at greater depths. Additionally, the four samples tested on their inner portions contained significantly greater TOC contents on their inner portions than outer. These results are consistent with those of Neil and Si (2018a), who found that TOC content as well as WR (CA and WDPT) are negatively correlated to the extent of weathering of the AOSM and positively correlated to salvage depth and to depth within individual AOSM samples. However, the current study shows that water infiltration under negative pore water pressure is, at most, weakly correlated to WR. Although AOSM has the potential for WR, as is suggested by the maximum WDPT and CA values, it is not necessarily reflected in its actual ability to absorb and conduct water. Neil and Si (2018a) also showed that the majority of AOSM (> 80%) allowed some absorption to initiate within one minute of contact with water, and concluded that the WR was primarily subcritical in nature. Subcritical water repellency is the ability to alter surface chemistry, and change between hydrophobic and hydrophilic states, depending on moisture conditions (Doerr et al. 2000; Diehl 2013). Consequently, because water was being introduced into the AOSM during the infiltration measurements, the water content was increasing and; thus, the water repellency of the AOSM may have been actively changing (decreasing) during the experiment. This may partially explain why there is no correlation between the water infiltration rates and the WR values of the AOSM, which were tested under initially air-dry conditions.

Delay in the onset of flow in some samples during the initial several minutes of testing is likely due to the WR of the material. However, contrary to the results of Neil and Si (2018a), the water infiltrations performed in the current study indicate that AOSM does not behave like a typical subcritically water repellent soil. Typically, water infiltration into a homogeneously-subcritically water repellent soil is initially slow, then gradually increases with time as the soil is exposed to water and the

repellency is reduced (Tillman et al. 1989). According to the current water infiltration study these materials appear to behave purely hydrophobically upon contact with water, but hydrophilically after the sudden onset of infiltration, as opposed to subcritically water repellent. In many instances water infiltration did not commence upon contact between the infiltrometer tip and AOSM, and often required several minutes to establish flow, which resembles a hydrophobic material. Once flow commenced, infiltration rates were generally greatest at the onset of flow and then decreased or ceased as time proceeded, which resembles a hydrophilic material (Tillman et al. 1989). However, Neil and Si (2018a) also found that the WR in AOSM increased with depth into the samples. This increase in WR with depth into individual aggregates could also be contributing to the general decrease in water infiltration over time, by increasing the amount of time required to wet the material and allow further infiltration as the wetting front travels deeper into the AOSM. This may also be responsible for the temporally fluctuating water infiltration rates seen in many samples. It is possible that as the wetting front reaches new portions of the AOSM pore structure, it comes into contact with previously unexposed subcritically water repellent materials, which require contact time with water to reorient to a hydrophilic position before allowing further infiltration. In this way, the flow rate would fluctuate through time in response to the changing water repellent conditions at the wetting front.

Despite the observed decrease in infiltration over time, there is often still a surge of water during the initial stage (several seconds to minutes) when performing infiltrations at subsequently lower suctions. The relationship between pore suction and pore size may explain this. As previously mentioned, as pore water suction decreases (water pressure head increases), the maximum pore size participating in the infiltration increases (Luxmoore 1981). The equivalent pore diameter for a given pore water pressure may be determined using a form of the Young-Laplace equation applicable to capillary tubing, which is based on the original works of Laplace (1805) and Young (1805) later unified by Gauss (1830).

This relationship between pore diameter and pore water pressure is often referred to as the height of capillary rise equation or Jurin's Rule, in honour of James Jurin (1717) who was among the first to record observations of capillary rise phenomena:

$$h = \frac{2\gamma\, cos\theta}{\rho g r} \tag{4.4}$$

where h is the pore liquid pressure (L), γ is the surface tension of the liquid (M T^{-2}), θ is the contact angle between the liquid and material surfaces (°), ρ is the liquid density (M L^{-3}), g is the acceleration due to gravity (L T^{-2}), and r is the pore radius (L). If AOSM pores become filled under a previously tested (higher) suction condition, with water that cannot be redistributed away from the infiltration point and throughout the material within the time frame of the experiment, the only pores which are empty and available to take on water at a subsequently lower suction are the newly accessed, larger pores. These larger pores may then quickly fill with water during infiltration, causing a rapid reduction in pore suction, resulting in a decreased infiltration rate through time. Additionally, as pore size increases, flux also increases according to Poiseuille's (1847) Law for ideal fluids:

$$q = -\frac{r^2 \rho_f g}{8\eta} \cdot \frac{\Delta h}{\Delta x} \tag{4.5}$$

where q is the fluid flux (L^3 L^{-2} T^{-1}), r is the pore radius (L), ρ_f is the fluid density (M L^{-3}), g is the acceleration due to gravity (L T^{-2}), η is the fluid viscosity (M L^{-1} T^{-1}), Δh is the change in pressure head (L), and Δx is the change in distance in the direction of flow (L). Poiseuille's Law indicates that fluid flux is proportional to the square of the pore radius, so a small change in pore size can produce a large change in flux. Due to this relationship, the majority of the total hydraulic conductivity of a soil is produced from flow through large pores (macropores; ≥ 1 mm diameter) and very little from small pores (meso- and micro-pores). This would explain why the water infiltration rates of AOSM often increased significantly in response to an increase in pressure, even in samples that experienced a near cessation of flow over time under the previous (lower) pressure conditions.

Although ANOVAs indicate that the water infiltration rates of AOSM showed no statistically significant (α = 0.05) relationship with WR, they do appear to be related to the AOSM stage of weathering (Fig. 4.4). In the macropore suction range ($\Psi \leq 3$ cm), in contrast to the low- and medium-weathered AOSM, the highly-weathered material shows an increase in water infiltration with decreasing suction. Based on the infiltration–suction trends in Figure 4.4, it appears as though the low- and medium-weathered AOSM primarily contain pores that are smaller than 0.15 mm in diameter (equivalent to Ψ = 20 cm using Eq. 4.4). In other words, the majority of the pores are accessed when performing the infiltrations at Ψ = 20 cm and; therefore, when the suction is decreased, few or no additional (larger) pores are accessed. Consequently, identical pore sizes (≤ 0.15 mm) are being accessed throughout the Ψ = 20 to 0.1 cm range, producing a relatively uniform infiltration rate throughout this range. The highly-weathered AOSM; however, must contain a considerable portion of macropores (≥ 1 mm diameter; $\Psi \leq 3$ cm). As suction is decreased, additional (larger) pores are accessed and the highly-weathered AOSM experiences significantly increased infiltration rates. Similar trends can be observed in the mean AOSM and soil matrix water infiltration values. The mean AOSM infiltration rates are relatively constant throughout the range of tested suctions, similar to that of the low- and medium-weathered AOSM; whereas, the soil matrix shows an exponential infiltration–suction trend similar to that of the highly-weathered AOSM (Fig. 4.3). This suggests that in relation to the soil matrix, the highly-weathered AOSM generally have a lower proportion of macropores that are effectively conducting water, and the medium- and low-weathered AOSM have even less. Although there are differences in the macropore range, there are no significant differences among the various AOSM and soil matrix samples in the Ψ = 7 to 20 cm range. This indicates that these coarse textured materials have very few small pores which conduct water, regardless of their material type, the presence or amount of PHCs, or whether the PHCs are water repellent. It is only when accessing macropores ($\Psi \leq 3$ cm) that the mean infiltration rates of the various AOSM and soil matrix start to deviate from one another. This suggests that, unlike small pores, the macropores of these materials are substantially affected by interstitial PHCs, whether it be from WR or a reduction in the quantity and

connectivity of macropores. Furthermore, the macropores of the AOSM appear to be affected by the degradational histories and resultant PHC contents and distributions within the AOSM, as is suggested by the mean water infiltration–suction trends among the different weathering classes (Fig. 4.4). An important implication of these findings is that AOSM behaves like a compacted soil, where the presence of PHCs mimic that of compaction. Typically, as soils are compacted, there is a reduction in macroporosity and increases in meso- and micro-porosity (McNabb et al. 2001; Dec et al. 2008). Additionally, as compaction occurs and pore size distribution is modified, there is often a reduction in pore connectivity (McNabb et al. 2001). In the current study, as PHC content in AOSM increases, water infiltration in the macropore suction range decreases considerably, whereas meso- and micro-pore flow are relatively unaffected.

For the soil matrix, when using the fitted hydraulic parameter values of α = 0.39 cm^{-1} and K_{fs} = 31 cm hr^{-1}, the predicted water infiltration values fit well to the measured ones (r^2 > 0.80). These parameters can be used to predict infiltration rates under varying suction or moisture conditions, which may be subsequently encountered in the field. Due to the unpredictable nature of the infiltration–suction relationships seen in many of the AOSM, obtaining hydraulic parameters for individual samples was for the most part unsuccessful. In some cases, it was possible to fit the model (Eq. 4.2) to the measured data for individual sampling locations within a single AOSM sample, and even more rare to fit the model to the mean infiltration values, of all locations within a single AOSM sample. It is important to note that although hydraulic parameters have been successfully obtained from select AOSM infiltration tests, these values do not represent the entire or even typical range of AOSM, but rather only describe the samples which behave according to the exponential relationship typically seen in homogeneous soils as outlined by Wooding (1968) in Eq. 4.2. Therefore, these parameters would be of little use in future predictions or modelling. However, when fitting the mean infiltration values of multiple AOSM samples (Fig. 4.3), particularly for individual weathering classes (Fig. 4.4), Eq. 4.2 fits considerably better. It is important to note that although the model provides a statistically (r^2) weak fit to the measured data of the low- and medium-weathered AOSM (Fig. 4.4) as well as the mean values for all AOSM samples (Fig. 4.3), the difference in magnitude between the respective measured and

predicted values is quite small. In contrast, the highly-weathered AOSM has a statistically strong fit, but the magnitude difference between measured and predicted values is relatively large. This is due to the range of infiltration values from each of the classes. The highly-weathered AOSM show a relatively large range of water infiltration values. Therefore, when deviating from the mean by a given magnitude, there will be a larger impact proportionally on the fit (r^2) of the low- and medium-weathered AOSM and mean AOSM because their range of values is relatively small. Consequently, although the obtained hydraulic parameters produce a poor fit statistically, they provide a relatively good fit when considering the magnitude difference between the measured and predicted values and; therefore, they may still be of use in future prediction and modelling exercises.

The increased water infiltration rates of the AOSM that were air dried between tests, suggests that once soil pores are filled with water during the early part of a test, infiltration decreases considerably (Fig. 4.5). This also suggests that WR is not the only (nor primary) factor influencing the infiltration of water into AOSM. Generally, soil water repellency increases with increasing dryness of the soil (Tillman et al. 1989; Diehl 2013); and therefore, if WR were the primary factor impacting the infiltration of water into the AOSM, drying the material would result in significantly reduced infiltration rates. Although the water infiltration rates generally increased once air dried, flow still fluctuated through time. As mentioned, it is possible that as the wetting front travels deeper into the AOSM, portions which have been previously unexposed to water take substantial time to wet and allow further infiltration, and could explain the temporally fluctuating infiltration rates.

4.6.2 Ethanol Infiltration

The water infiltration rates in AOSM were smaller in magnitude and did not differ across suctions like that of the ethanol. This would indicate that WR within the AOSM is indeed producing a noticeable effect on water infiltration. The infiltration rates in the soil matrix did; however, differ with suction, but also showed differences between water and ethanol, indicating that repellency is also a factor in this material. The reduction in water infiltration due to repellency was similar in the AOSM and soil matrix, proportionally, according to their respective differences in water and ethanol infiltration rates (Fig. 4.7).

The water infiltration rates of the soil matrix were considerably greater than that of the AOSM in the macropore suction range. There are a number of potential causes for these reduced values in AOSM, including WR as well as a reduction in effective porosity due to interstitial PHCs. The ethanol infiltration rates of the soil matrix were also greater than those of the AOSM. Given what is known of these materials, the lower ethanol infiltration rates in the AOSM must be cause by interstitial PHCs which are reducing the volume and connectivity of pore spaces. This is suggested by the following: the AOSM and soil matrix are texturally similar, the soil matrix has relatively little or no pore plugging by PHCs, and the effects of WR are not present when using ethanol. Therefore, when using ethanol the only factor differing between the AOSM and soil matrix are the interstitial PHCs within the AOSM. This is further supported by the difference between the water infiltration rates of the low/medium-weathered (high PHC content; low infiltration rates) and highly-weathered (low PHC content; high infiltration rates) AOSM (Fig. 4.4). This suggests that water infiltration rate decreases with increasing PHC content in these coarse-textured soil materials. Similarly, Pernitsky et al. (2016) found that increasing bulk density and PHC concentration within lean oil sand overburden materials resulted in a decrease in hydraulic conductivity of the lean oil sand and an increase in water storage in the overlying coarse-textured soils. In addition, Neil and Si (2018a) found that PHC content increases with depth into individual AOSM samples. This suggests that the further the wetting front of a probing liquid travels into individual AOSM, the greater the potential for reduced infiltration due to a reduction in pore volume and connectivity resulting from the increased presence of interstitial PHCs.

4.6.3 Implications for Water Storage

It would appear that AOSM have the potential to decrease the infiltration and storage of water due to the presence of interstitial PHCs. The PHCs within AOSM occupy space and interrupt the continuity of pores, impeding water from entering and occupying these materials. This effect would likely become more pronounced as the PHC content of the AOSM increased, as is suggested by the water infiltration rates of the AOSM of different weathering stages. As part of a reclamation soil profile the interstitial PHCs in the low-weathered AOSM (i.e., high PHC content) would produce the greatest

decrease in the soil water storage, followed by the medium- and highly-weathered AOSM (i.e., lower PHC contents). However, the reduced infiltration rates of the AOSM in comparison to the surrounding soils may also slow the vertical flow of water, causing an increase in the residence time of water within the soil profile. Keeping water in the soil for a longer period of time provides vegetation with more time to access water, essentially increasing the soil water storage over relatively long time spans. In reclamation soils that contain considerable quantities of coarse-textured materials, which naturally have low water and nutrient holding capacities, an increase in the water residence time may be beneficial to emerging and stable ecosystems as it provides additional plant-available water to a soil which is already relatively susceptible to drought stress. It is likely that the PHC content of the AOSM would impact how pronounced this residence time effect would be. Based on the infiltration rates obtained in this study, it is likely that the low-weathered AOSM would produce the greatest reduction in the flow of water and hence the greatest increase in residence time within the soil. However, the low-weathered material may more or less act as an impermeable object, causing water to rapidly flow around it, which would have little effect on the residence time. It is possible that the medium- or highly-weathered ASOM would result in a greater increase in the residence time of water because more of the water flows through the pore structure of the AOSM, at a reduced rate, before continuing downward through the soil profile.

Based on the results of this study, it is difficult to predict which mechanism (reduced volume of soil capable of water storage; increased residence time) will have a greater effect on the soil water balance and amount of plant-available water within the soil profile. It is possible that the two effects will offset one another, resulting in a null net effect to the soil water balance. Future modelling studies, using the hydraulic parameters obtained in this study and others, could provide an improved understanding of the effects of AOSM inclusions on the soil water dynamics of reclamation soil profiles.

4.7 Conclusions

The AOSM weathering classification is consistent with onion-skin weathering: AOSM originating from the near-surface of the soil profile is weathered to a greater extent, and consequently contains less TOC (i.e., PHCs) and has greater water infiltration rates in the macropore suction range, than AOSM from at depth and; PHC content increases with depth into individual aggregates, but mean water infiltration rate is not affected by measurement depth.

The paired water and ethanol infiltrations confirmed that some form of WR is present in the pore structure of the AOSM. Ethanol infiltration rates were greater and showed a pronounced increase with decreasing suction, as opposed to water which was reduced in magnitude and frequently did not show any significant change with suction. The ethanol measurements revealed that WR is also present in the soil matrix, which showed greater infiltration rates for ethanol than water. The difference in the water and ethanol infiltrations were approximately the same for both the soil matrix and AOSM, suggesting similar levels of WR. The ethanol infiltration rates of the soil matrix were significantly greater than that of the AOSM. These results also indicate that WR is not solely responsible for the reduced water infiltration in the AOSM, and suggests that a difference in effective (i.e., conducting) porosity may also be contributing. Since we know that the soil matrix and AOSM in this study are nearly texturally identical and have approximately the same WR, it seems likely that differences in infiltration are due to differences in porosity resulting from interstitial PHCs. While the water infiltration trends may reflect a hydrophilic or subcritically water repellent soil as opposed to a truly hydrophobic soil, the difference in magnitude between the ethanol and water infiltrations indicates that WR was present to some extent. Based on these results, it seems likely that water flow in AOSM is affected by both WR and a reduction in porosity due to interstitial PHCs.

As AOSM is further weathered and degraded through time, interstitial PHCs which can potentially cause WR as well as a reduction in effective porosity may be removed, leaving behind a coarse textured material similar to the surrounding soil matrix. As these chemical and physical changes occur, the hydraulic properties of the AOSM will become more similar to that of the surrounding soils. Furthermore, it appears as though PHCs have a greater effect on larger sized pores, and as PHC

content increases, infiltration in the macropore range decreases considerably. In this way, the interstitial PHCs in AOSM produce an effect similar to that of compaction, by reducing macroporosity and pore connectivity.

Water infiltration rates of AOSM were significantly lower than the soil matrix in the macropore suction range. Because the majority of a soils hydraulic conductivity is attributed to macropore flow, the difference between the AOSM and soil matrix macropore flows suggests that the soil water dynamics in these coarse textured soils would be significantly affected by AOSM inclusions. The space that is occupied by AOSM causes a reduction in the volume of soil capable of storing water, potentially resulting in decreased water storage. However, as water travels through the soil profile and reaches portions of AOSM, flow rate will decrease, which may result in an increase in residence time and; therefore, an increase in water storage, in the soils located above. This may explain the previous observations of increased water contents in soils overlying oil sand. Consequently, depending on its location within the soil profile, AOSM has the potential to modify water content and alter the soil moisture regime and ecosite. If AOSM is present just beneath the rooting zone, there is potential to increase the soil water storage within the rooting zone and allow for the establishment of relatively productive ecosites with wet moisture regimes. However, if AOSM is located deeper in the profile where it does not produce a significant effect on the soil water storage in the rooting zone, relatively dry ecosites may develop. Therefore, AOSM-affected soils may provide another tool with which to influence the soil water regimes of reclaimed sites, in order to customize them to support a range of desired ecosites.

5. SYNTHESIS AND CONCLUSIONS

Surface mining activities in the oil sands region of Northern Alberta result in the removal of vegetation, soils, and landform features, causing a disruption to normal ecosystem functions. In order to reclaim the affected areas, soil prescriptions which are capable of providing the necessary conditions to support a target ecosystem are required. Properties such as water and nutrient retention will largely determine the possible ecosystems which are capable of developing. Many of the materials available for reclamation throughout the region are coarse-textured soils, which have relatively low water and nutrient holding capacities. Nevertheless, these soils naturally supported a range of moisture and nutrient regimes, and associated ecosite phases, from dry to relatively wet. The natural layering of soil and sediment horizons is known to result in a greater available water holding capacity than that of texturally-homogeneous soil profiles. However, these soils are also known to contain portions of oil sand in the form of aggregates and layers, and it has been observed that soil water content is frequently greater directly above these materials than in the surrounding soils. In order to prepare effective soil reclamation prescriptions which are capable of supporting target ecosystems, the hydraulic properties of oil sand inclusions must be investigated.

The overarching objective of this thesis work was to evaluate the potential for oil sand inclusions (i.e. AOSM) to modify the soil water dynamics of coarse-textured reclamation soil profiles. Two main studies were performed to address this objective. The first study provided an indication of the maximum hydrophobicity, or soil water repellency, of AOSM, as well as it's persistence with time and with increasing water content. The study was performed to understand the potential for AOSM hydrophobicity to modify the soil water dynamics of its host soil profile through reduced absorption and flow. The second study examined the tension-dependent infiltration rates of AOSM and surrounding coarse-textured soil materials, to support the findings of the first study and to further evaluate the potential for AOSM to modify the soil water dynamics of reclamation soils.

Chapter 3 addressed the first objective, where measurements of sessile drop contact angle and water drop penetration time provided indications of the degree and persistence of WR of AOSM.

Testing occurred on AOSM from various salvage depths and at multiple sampling depths within individual aggregates. The results were highly variable, showing a wide range of WR in terms of both degree and persistence, with values spanning nearly the entire spectrum typically observed in natural soil materials. However, despite the excessive levels of WR found in many of the AOSM, the majority allowed water infiltration to commence within a reasonable time, typically within one minute of contact with water. This indicates that although AOSM has the potential for WR, it will likely persist after wetting only in the materials which are highly hydrophobic, minimizing the potential for associated negative effects to the soil profile. Furthermore, it was found that with increasing salvage depth, the apparent stage of weathering of AOSM decreased, while the PHC content (measured as TOC content) and WR increased. Similarly, the PHC content and WR increased with increasing depth into individual AOSM. This suggests that AOSM undergo onion-skin weathering, where near-surface deposits and the surfaces of individual aggregates experience greater exposure to weathering and degradation. The relatively high levels of oxygen, heat, and microbes, as well as the frequent occurrence of wetting and drying cycles of these surface materials may promote weathering and degradation of the PHCs in AOSM. This breakdown of hydrophobic interstitial material may then result in a reduction in WR and increases in absorption and flow.

In Chapter 4, the potential for AOSM to modify soil water dynamics was further evaluated by determining the infiltration rates, of water and 95% ethanol, of AOSM and surrounding coarse-textured soils using a miniaturized infiltrometer. The results of the study are consistent with onion-skin weathering of AOSM throughout the depth of the profile, where AOSM from the near-surface appeared to be more highly weathered, contain less PHCs, and consequently had greater water infiltration rates than deeper materials. Similarly, PHC content increased with increasing depth into individual AOSM, but water infiltration rate was not significantly affected. The paired water and ethanol infiltrations indicated that WR was present in both the AOSM and surrounding soils, with approximately equal reductions in water infiltration rates as compared to ethanol for both materials. The water infiltration of AOSM was significantly lower than that of the surrounding soil throughout the macropore suction range. Because we know that the AOSM and surrounding soil are nearly texturally identical, and

express approximately equal levels of WR, the differences in their infiltration rates are likely the result of differences in conducting porosity due to interstitial PHCs within the pore structure of the AOSM. The difference observed in AOSM from different stages of weathering also suggests this is the case, where the water infiltration rates of the highly weathered AOSM were significantly greater than that of the medium- and low-weathered AOSM throughout the macropore suction range.

The differences in infiltration rates of the AOSM and surrounding soil suggests that water flow through coarse-textured soil profiles may be considerably affected by AOSM inclusions. If AOSM is present in the near-surface, there is the potential for reduced absorption and downward flow of water through the AOSM into the underlying soil, resulting in reduced soil water storage. Conversely, the reduced infiltration rates and conducting porosity of the AOSM could result in the formation of flow barriers at the interfaces between the AOSM and surrounding soils. Therefore, if AOSM is located below the surface, there is an opportunity to slow the flow of water through the profile and increase the soil water storage in the soil above AOSM.

In summary, as salvage depth increased, weathering of AOSM decreased, resulting in increases in PHC content and WR, and a decrease in infiltration rate. These results imply the benefit of performing discreet salvage and replacement of soil layers during mining and reclamation activities. Through the separation of deep and shallow soil materials, deep deposits which have relatively great hydrophobicity remain at depth where water content is generally greater and; therefore, the expression of hydrophobicity is minimal. In addition, deep deposits have relatively low infiltration rates, and if placed in the near-surface, could result in a reduction in water infiltration into the soil profile and an associated reduction in soil water storage. However, particularly in coarse-textured soils, it may be advantageous to place AOSM in the near-surface, within or directly beneath the rooting zone, where it’s WR and/or low infiltration capability allow it to slow the downward flow of water and increase plant available soil water storage. Ultimately, the ability of AOSM inclusions to modify soil water storage provides an additional tool with which to customize reclamation soil prescriptions and create the conditions necessary to support target ecosystems.

It is apparent that AOSM have the capability to alter the hydrology of their host soils. According to previous surveys, approximately 70% of the soils in the top 3 meters of the oil sands region contain < 5% oil sand by volume. For these reclamation soils, because the oil sand is present in relatively small quantities, there may not be a significant effect on the hydrology of the reclamation soil profiles. However, approximately 15% of the soils were found to contain between 5% and 25% oil sand by volume, and the remaining soils contain > 25%. In the soil materials which contain higher quantities of oil sand, there may be a considerably greater effect to the soil hydrology. As such, the oil sand quantity of reclamation soils should be assessed prior to reclamation. When using soil materials containing greater quantities of oil sand, soil profiles should be carefully constructed in order to minimize the expression of WR and the associated reductions in water infiltration and soil water storage in the near-surface. However, as previously mentioned, the presence of oil sand material in the near-surface may not pose a threat to soil water storage, but may in fact increase water residence time and soil water storage, providing a strategy with which to control the soil moisture regime of reclaimed sites, Future modelling studies, using the hydraulic parameters obtained in this and other research, will improve our understanding of the soil water dynamics of AOSM-affected reclamation soils. Modelling is a quantitative tool with which to evaluate the effects of AOSM on entire soil profiles, over long time spans. By modelling various prescriptions or combinations of AOSM-affected soils, multiple reclamation scenarios may be evaluated and compared, providing an indication of their ability's to support target ecosystems. By modelling the soil water dynamics over long time spans, the sustainability's of the various reclamation prescriptions may be assessed. Furthermore, the effects of ecological succession may also be examined, providing further indication of the interactions between the reclaimed soils and ecosystems. Through such modelling studies, the design of AOSM-affected reclamation soil prescriptions can be further optimized to sustainably support target ecosystems and promote reclamation success.

6. REFERENCES

Adams, R.H., Cerecedo-Lopez, R.A., Alejandro-Alvarez, L.A., Dominguez-Rodriguez, V.I., and Nieber, J.L. 2016. Treatment of water-repellent petroleum-contaminated soil from Bemidji, Minnesota, by alkaline desorption. Int. J. Environ. Sci. Technol. **13**: 2249–2260. doi:10.1007/s13762-016-1058-4.

Bachmann, J., Deurer, M., and Arye, G. 2007. Modeling water movement in heterogeneous water-repellent soil: 1. Development of a contact angle-dependent water-retention model. Vadose Zone J. **6**: 436–445. doi:10.2136/vzj2006.0060.

Bauters, T.W.J., Steenhuis, T.S., Dicarlo, D.A., Nieber, J.L., Dekker, L.W., Ritsema, C.J., Parlange, J.-Y., and Haverkamp, R. 2000. Physics of water repellent soils. J. Hydrol. **231**–**232**: 233–243. doi:10.1016/S0022-1694(00)00197-9.

Beckingham, J.D., and Archibald, J.H. 1996. Field guide to ecosites of northern Alberta. Natural Resources Canada, Canadian Forest Service, Northern Forestry Centre, Edmonton, Alberta. Special Report 5.

Behrens, R., Bouchez, J., Schuessler, J.A., Dultz, S., Hewawasam, T., and von Blanckenburg, F. 2015. Mineralogical transformations set slow weathering rates in low-porosity metamorphic bedrock on mountain slopes in a tropical climate. Chem. Geol. **411**: 283–298. doi:10.1016/j.chemgeo.2015.07.008.

Bisdom, E.B.A., Dekker, L.W., and Schoute, J.F.T. 1993. Water repellency of sieve fractions from sandy soils and relationships with organic material and soil structure. Geoderma **56**: 105–118. doi:10.1016/0016-7061(93)90103-R.

Brassington, K.J., Hough, R.L., Paton, G.I., Semple, K.T., Risdon, G.C., Crossley, J., Hay, I., Askari, K., and Pollard, S.J.T. 2007. Weathered hydrocarbon wastes: A risk management primer. Crit. Rev. Environ. Sci. Technol. **37**: 199–232. doi:10.1080/10643380600819625.

Brunner, C., Wolf, M., and Bachofen, R. 1987. Enrichment of bitumen-degrading microorganisms. FEMS Microbiol. Lett. **43**: 337–344.

Buczko, U., Bens, O., and Durner, W. 2006. Spatial and temporal variability of water repellency in a sandy soil contaminated with tar oil and heavy metals. J. Contam. Hydrol. **88**: 249–268. doi:10.1016/j.jconhyd.2006.07.002.

Canadian Council of Ministers of the Environment (CCME) 2008. Canada-wide standards for petroleum hydrocarbons (PHC) in soil. [Online] Available: http://www.ccme.ca/files/Resources/csm/phc_cws/%0Aphc_standard_1.0_e.pdf (accessed 17.02.21).

Canadian Soil Survey Committee 1982. Expert Committee on Soil Survey: The Canada Soil Information System (CanSIS): Manual for describing soils in the field.

Cerniglia, C.E. 1992. Biodegradation of polycyclic aromatic hydrocarbons. Biodegradation **3**: 351–368. doi:10.1007/BF00129093.

Chau, H.W., Biswas, A., Vujanovic, V., and Si, B.C. 2014. Relationship between the severity, persistence of soil water repellency and the critical soil water content in water repellent soils. Geoderma **221**–**222**: 113–120. doi:10.1016/j.geoderma.2013.12.025.

Chau, H.W., Goh, Y.K., Vujanovic, V., and Si, B.C. 2012. Wetting properties of fungi mycelium alter soil infiltration and soil water repellency in a γ-sterilized wettable and repellent soil. Fungal Biol. **116**: 1212–1218. doi:10.1016/j.funbio.2012.10.004.

Cumulative Environmental Management Association (CEMA) 2006. Land capability classification system for forest ecosystems in the oil sands, 3rd edition. Volume 1: Field manual for land capability determination. [Online] Available: http://cemaonline.ca/index.php/administration/doc_download/90-land-capability-classification-system-for-forest-ecosystems-manual-lccs (accessed 17.02.21).

Dane, J.H., and Topp, G.C. (eds.) 2002. Methods of soil analysis: Part 4 - Physical methods. SSSA Book Series 5, Madison, WI.

Dang-Vu, T., Jha, R., Wu, S.Y., Tannant, D.D., Masliyah, J., and Xu, Z. 2009. Wettability determination of solids isolated from oil sands. Colloids Surfaces A: Physiochem. Eng. Asp. **337**: 80–90.

Dec, D., Dörner, J., Becker-Fazekas, O., and Horn, R. 2008. Effect of bulk density on hydraulic properties of homogenized and structured soils. J. Soil Sc. Plant Nutr. **8**: 1–13. [Online] Available: http://www.scielo.cl/pdf/rcsuelo/v8n1/art01.pdf.

Dekker, L.W., and Ritsema, C.J. 1994. How water moves in a water repellent soil 1. Potential and actual water repellency. Water Resour. Res. **30**: 2507–2517.

Diehl, D. 2013. Soil water repellency: Dynamics of heterogeneous surfaces. Colloids Surfaces A Physicochem. Eng. Asp. **432**: 8–18. doi:10.1016/j.colsurfa.2013.05.011.

Doerr, S.H., Shakesby, R.A., and Walsh, R.P.D. 2000. Soil water repellency: Its causes, characteristics and hydro-geomorphological significance. Earth Sci. Rev. **51**: 33–65. doi:10.1016/S0012-8252(00)00011-8.

Eastcott, L., Shiu, W.Y., and Mackay, D. 1988. Environmentally relevant physical-chemical properties of hydrocarbons: A review of data and development of simple correlations. Oil Chem. Pollut. **4**: 191–216. doi:10.1016/S0269-8579(88)80020-0.

Fleming, M. 2012. Petroleum hydrocarbon content, leaching and degradation from surficial bitumens in the Athabasca oil sands region. M.Sc. thesis, University of Saskatchewan.

Frontera-Suau, R. 2000. Impact of microbial community structure on crude oil biodegradation. Ph.D. Dissertation, Medical University of South Carolina. doi:10.16953/deusbed.74839.

Gauss, C.F. 1830. Principia generalia theoriae figurae fluidorum in statu aequilibrii. Sumtibus Dieterichianis, Göttingen, Germany.

Gerke, H.H., and Köhne, J.M. 2002. Estimating Hydraulic Properties of Soil Aggregate Skins from Sorptivity and Water Retention. Soil Sci. Soc. Am. J. **66**: 26–36.

González-Delgado, A.M. 2011. Effect of hydraulic properties of porous media on solute transport under variable saturated flow conditions in repacked columns. Ph.D. Dissertation, New Mexico State University.

Gosselin, P., Hrudey, S.E., Naeth, M.A., Plourde, A., Therrien, R., Van Der Kraak, G., and Xu, Z. 2010. The Royal Society of Canada Expert Panel: Environment and health impacts of Canada's oil sands industry. The Royal Society of Canada, Ottawa, ON, Canada.

Government of Alberta (GOA) 2009. Environmental management of Alberta's oil sands. [Online] Available: http://environment.gov.ab.ca/info/library/8042.pdf (accessed 13.08.15).

Government of Alberta (GOA) 2016. Introduction to oil sands. [Online] Available: http://www.capp.ca/publications-and-statistics/publications/287586 (accessed 17.02.21).

Gray, D.M. 1970. Handbook of the principles of hydrology. National Research Council of Canada.

Gu, Y. 2006. Oil sands weathering. M.Sc. thesis, University of Alberta.

Hamlett, C.A.E., Shirtcliffe, N.J., McHale, G., Ahn, S., Bryant, R., Doerr, S.H., and Newton, M.I. 2011. Effect of particle size on droplet infiltration into hydrophobic porous media as a model of water repellent soil. Environ. Sci. Technol. **45**: 9666–9670.

Hein, F.J. 2006. Heavy oil and oil (tar) sands in North America: An overview & summary of contributions. Nat. Resour. Res. **15(2)**: 67–84. doi:10.1007/s11053-006-9016-3.

Hirata, Y., Chigira, M., and Chen, Y. 2016. Spheroidal weathering of granite porphyry with well-developed columnar joints by oxidation, iron precipitation, and rindlet exfoliation. Earth Surf. Process. Landforms. doi:10.1002/esp.4008.

Huang, M., Barbour, S.L., Elshorbagy, A., Zettl, J.D., and Si, B.C. 2011a. Infiltration and drainage processes in multi-layered coarse soils. Can. J. Soil Sci. **91**: 169–183. doi:10.4141/cjss09118.

Huang, M., Barbour, S.L., Elshorbagy, A., Zettl, J.D., and Si, B.C. 2011b. Water availability and forest growth in coarse-textured soils. Can. J. Soil Sci. **91**: 199–210. doi:10.4141/cjss10012.

Hudson, B.D. 1994. Soil organic matter and available water capacity. J. Soil and Water Cons. **49(2)**: 189–194.

Hunter, A. 2011. Investigation of water repellency and critical water content in undisturbed and reclaimed soils from the Athabasca oil sands region of Alberta, Canada. M.Sc. thesis, University of Saskatchewan. [Online] Available:http://library2.usask.ca/theses/available/etd-07072011-112233/unrestricted/HunterMSCThesis.pdf.

Jafvert, C.T., and Heath, J.K. 1991. Sediment- and saturated-soil-associated reactions involving an anionic surfactant (dodecylsulfate). 1. Precipitation and micelle formation. Environ. Sci. Technol. **25**: 1031–1038. doi:10.1021/es00018a003.

Johnson, E.A., and Miyanishi, K. 2008. Creating new landscapes and ecosystems: The Alberta oil sands. Ann. N. Y. Acad. Sci. **1134**: 120–145. doi:10.1196/annals.1439.007.

Jurin, J. 1717. An account of some experiments shown before the Royal Society; with an enquiry into the cause of the ascent and suspension of water in capillary tubes. Philisophical Transactions **30:** 739–747.

Laplace, P.S. 1805. Traité de Mécanique Céleste, Supplément a la théorie de l'action capillaire. Chez Courcier, Paris, France.

Leatherdale, J., Chanasyk, D.S., and Quideau, S. 2012. Soil water regimes of reclaimed upland slopes in the oil sands region of Alberta. Can. J. Soil Sci. **92**: 117–129. doi:10.4141/cjss2010-027.

Leeds-Harrison, P.B., Youngs, E.G., and Uddin, B. 1994. A device for determining the sorptivity of soil aggregates. Eur. J. Soil Sci. **45**: 269–272.

Leskiw, L.A. 2005. Hydrocarbons in natural soils: literature review. Report prepared for the Cumulative Environmental Management Association (CEMA) by Paragon Soil and Environmental Consulting Inc.

Leskiw, L.A., Arregoces, C., Boorman, S., Zakele, T., and Startsev, A. 2006. Hydrocarbons in natural oil sands soils: Field survey. Report prepared for the Cumulative Environmental Management Association (CEMA) by Paragon Soil and Environmental Consulting Inc. [Online] Available:http://library.cemaonline.ca/ckan/dataset/2006-0031/resource/651a3c32-80e7-462d-94d9-839a361598cf (accessed 17.02.21).

Liu, H., Lei, T. W., Zhao, J., Yuan, C. P., Fan, Y. T., Qu, L. Q. 2011. Effects of rainfall intensity and antecedent soil water content on soil infiltrability under rainfall conditions using the run off-on-out method. Journal of Hydrology **396**: 24–32.

Luxmoore, R.J. 1981. Micro-, meso-, and macroporosity of soil. Soil Sci. Soc. Am. J. **45**: 671. doi:10.2136/sssaj1972.03615995003600030047x.

McCarthy, E.L. 1934. Mariotte’s bottle. Science **80**: 100.

McNabb, D.H., Startsev, A.D., and Nguyen, H. 2001. Soil wetness and traffic level effects on bulk density and air-filled porosity of compacted boreal forest soils. Soil Sci. Soc. Am. J. **65**: 1238–1247. doi:10.2136/sssaj2001.6541238x.

Meyer, R.F., Attanasi, E.D., and Freeman, P.A. 2007. Heavy oil and natural bitumen resources in geological basins of the world. U.S. Geological Survey Open-File Report 2007-1084. [Online] Available: https://pubs.usgs.gov/of/2007/1084/OF2007-1084v1.pdf (accessed 17.02.21).

Mossop, G.D. 1980. Geology of the Athabasca oil sands. Science **207**: 145–152.

Müller, K., and Deurer, M. 2011. Review of the remediation strategies for soil water repellency. Agric. Ecosyst. Environ. **144**: 208–221. doi:10.1016/j.agee.2011.08.008.

Naeth, M.A., Chanasyk, D.S., and Burgers, T.D. 2011. Vegetation and soil water interactions on a tailings sand storage facility in the Athabasca oil sands region of Alberta Canada. Physics and Chemistry of the Earth **36**: 19–30.

Natural Regions Committee 2006. Natural regions and subregions of Alberta. Compiled by D.J. Downing and W.W. Pettapiece. Government of Alberta. Pub. No. T/852. [Online] Available: http://www.albertaparks.ca/media/2942026/nrsrcomplete_may_06.pdf (accessed 17.02.21).

Neil, E.J., and Si, B.C. (2018a). Exposure to weathering reduces the water repellency of aggregated oil sand material from subsoils of the Athabasca region. Published in Can. J. Soil Sci. doi:10.1139/CJSS-2017-0087.

Neil, E.J., and Si, B.C. (2018b). Interstitial hydrocarbons reduce the infiltration rates of coarse-textured reclamation materials from the Athabasca oil sands. Accepted in Catena.

Nicot, J.-P., Gross, B. 2009. Self-sealing evaporation ponds for small inland desalination facilities and containment equivalence concepts in Texas. Desalination and Water Treatment **3**: 1–3, 29–42. doi:10.5004/dwt.2009.436.

Oil Sands Vegetation Reclamation Committee 1998. Guidlines for reclamation to forest vegetation in the Athabasca oil sands region. [Online] Available: https://extranet.gov.ab.ca/env/infocentre/info/library/6869.pdf (accessed 17.02.21).

Page, C.A., Bonner, J.S., Sumner, P.L., and Autenrieth, R.L. 2000. Solubility of petroleum hydrocarbons in oil/water systems. Mar. Chem. **70**: 79–87. doi:10.1016/S0304-4203(00)00016-5.

Peak, D., Ford, R.G., and Sparks, D.L. 1999. An in situ ATR-FTIR investigation of sulfate bonding mechanisms on goethite. J. Colloid Interface Sci. **218**: 289–299. doi:10.1006/jcis.1999.6405.

Pernitsky, T., Hu, W., Si, B.C., Barbour, L. 2016. Effects of petroleum hydrocarbon concentration and bulk density on the hydraulic properties of lean oil sand overburden. Can. J. Soil Sci. **96**: 435–446.

Poiseuille, J.L.M. 1847. Sur le mouvement des liquides de nature differente dans les tubes de tres petits diametres. Ann. Chim. Phys., 3rd series, 21: 76-110 (plus Plate II).

Quyum, A., Achari, G., and Goodman, R.H. 2002. Effect of wetting and drying and dilution on moisture migration through oil contaminated hydrophobic soils. Sci. Total Environ. **296**: 77–87. doi:10.1016/S0048-9697(02)00046-3.

Rasband, W. (1997-2012). ImageJ, U.S. National Institutes of Health, Bethesda, Maryland, USA. [Online] Available: http://rsbweb.nih.gov/ij/docs/guide/user-guide.pdf (accessed 17.02.21).

Reid, B.J., Jones, K.C., and Semple, K.T. 2000. Bioavailability of persistent organic pollutants in soils and sediments—a perspective on mechanisms, consequences and assessment. Environ. Pollut. **108**: 103–112. doi:10.1016/S0269-7491(99)00206-7.

Rooney, R.C., and Bayley, S.E. 2011. Setting reclamation targets and evaluating progress: Submersed aquatic vegetation in natural and post-oil sands mining wetlands in Alberta, Canada. Ecol. Eng. **37**: 569–579. doi:10.1016/j.ecoleng.2010.11.032.

Rosso, M.E.M. 2016. Observations of soil moisture dynamics associated with hydrocarbon affected and layered coarse textured soils. M.Sc. thesis, University of Saskatchewan.

Roy, J.L., and McGill, W.B. 2000. Investigation into mechanisms leading to the development, spread and persistence of soil water repellency following contamination by crude oil. Can. J. Soil Sci. **80(4)**: 595–606. doi:10.4141/S99-091.

Roy, J.L., Mcgill, W.B., Lowen, H.A., and Johnson, R.L. 2003. Relationship between water repellency and native and petroleum-derived organic carbon in soils. J. Environ. Qual. **32**: 583–590.

Scott, H.D. 2000. Soil physics. Agricultural and environmental applications. 1st ed. Iowa State University Press, Ames, Iowa, USA.

Shirtcliffe, N.J., McHale, G., Atherton, S., Newton, M.I. 2010. An introduction to superhydrophobicity. Advances in Colloid and Interface Science. **161**: 124–138.

Si, B.C., Dyck, M., and Parkin, G. 2011. Flow and transport in layered soils. Can. J. Soil Sci. **91**: 127–132.

Soil Classification Working Group 1998. The Canadian system of soil classification, 3rd edition. Agric. Agri-Food Canada Publ. 1646 (Revised). [Online] Available: http//sis.agr.gc.ca/ cansis/publications/manuals/1998-cssc-ed3/cssc3_manual.pdf (accessed 17.02.21).

Stalder, A.F., Melchior, T., Müller, M., Sage, D., Blu, T., and Unser, M. 2010. Low-bond axisymmetric drop shape analysis for surface tension and contact angle measurements of sessile drops. Colloids Surfaces A Physicochem. Eng. Asp. **364**: 72–81. doi:10.1016/j.colsurfa.2010.04.040.

Takamura, K. 1982. Microscopic structure of Athabasca oil sand. Can. J. Chem. Eng. **60**: 538–545. doi:10.1002/cjce.5450600416.

Tillman, R.W., Scotter, D.R., Wallis, M.G., and Clothier, B.E. 1989. Water-repellency and its measurement by using intrinsic sorptivity. Aust. J. Soil Res. **27**: 637–644.

Visser, S. 2008a. Petroleum hydrocarbons (PHCs) in lean oil sand (LOS): degradation potential and toxicity to ecological receptors. Report prepared for the Cumulative Environmental Management Association (CEMA). [Online] Available: http://library.cemaonline.ca/ckan/dataset/2890be17-e1bb-4967-8ba4-d216cb4b4066/resource/2f217cde-af5f-4298-9252-fbe547a10534/download/s.visserleanoilsands.pdf (accessed 17.08.14).

Visser, S. 2008b. Petroleum hydrocarbons (PHCs) in tar balls: degradation potential, leaching potential and toxicity to ecological receptors. Report prepared for the Cumulative Environmental Management Association (CEMA). [Online] Available: http://library.cemaonline.ca/ckan/dataset/95718b17-d8f3-4247-8eb4-6b4385862646/resource/02ebd1b3-8d4a-48ce-b5e2-88ed8fae41f6/download/svisse1.pdf (accessed 17.02.21).

Walker, J.D., Colwell, R.R., and Petrakis, L. 1976. Biodegradation rates of components of petroleum. Can. J. Microbiol. **22**: 1209–1213. doi:10.1139/m76-179.

Wang, D.L., and Anderson, D.W. 1998. Direct measurement of organic carbon content in soils by the Leco CR-12 carbon analyzer. Commun. Soil Sci. Plant Anal. **29**: 15–21. doi:10.1080/00103629809369925.

Wooding, R.A. 1968. Steady infiltration from a shallow circular pond. Water Resour. Res. **4**: 1259–1273.

Young, T. 1805. An essay on the cohesion of fluids. Philosophical Transactions of the Royal Society of London. W. Bulmer and Co., Cleveland-Row, St. James's, London, England.

Zettl, J.D., Barbour, S.L., Huang, M., Si, B.C., and Leskiw, L.A. 2011. Influence of textural layering on field capacity of coarse soils. Can. J. Soil Sci. **91**: 133–147. doi:10.4141/cjss09117.

Zhao, Y., and Machel, H.G. 2011. Biodegradation characteristics of bitumen from the Upper Devonian Grosmont reservoir , Alberta , Canada. Bull. Can. Pet. Geol. **59**: 112–130. doi:10.2113/gscpgbull.59.2.112.

Zhou, W., and Zhu, L. 2005. Solubilization of polycyclic aromatic hydrocarbons by anionic-nonionic mixed surfactant. Colloids Surfaces A Physicochem. Eng. Asp. **255**: 145–152. doi:10.1016/j.colsurfa.2004.12.039.

APPENDICES

APPENDIX A. ATTENUATED TOTAL REFLECTANCE FOURIER TRANSFORM INFRARED SPECTROSCOPIC MEASUREMENT OF AGGREGATED OIL SAND MATERIAL

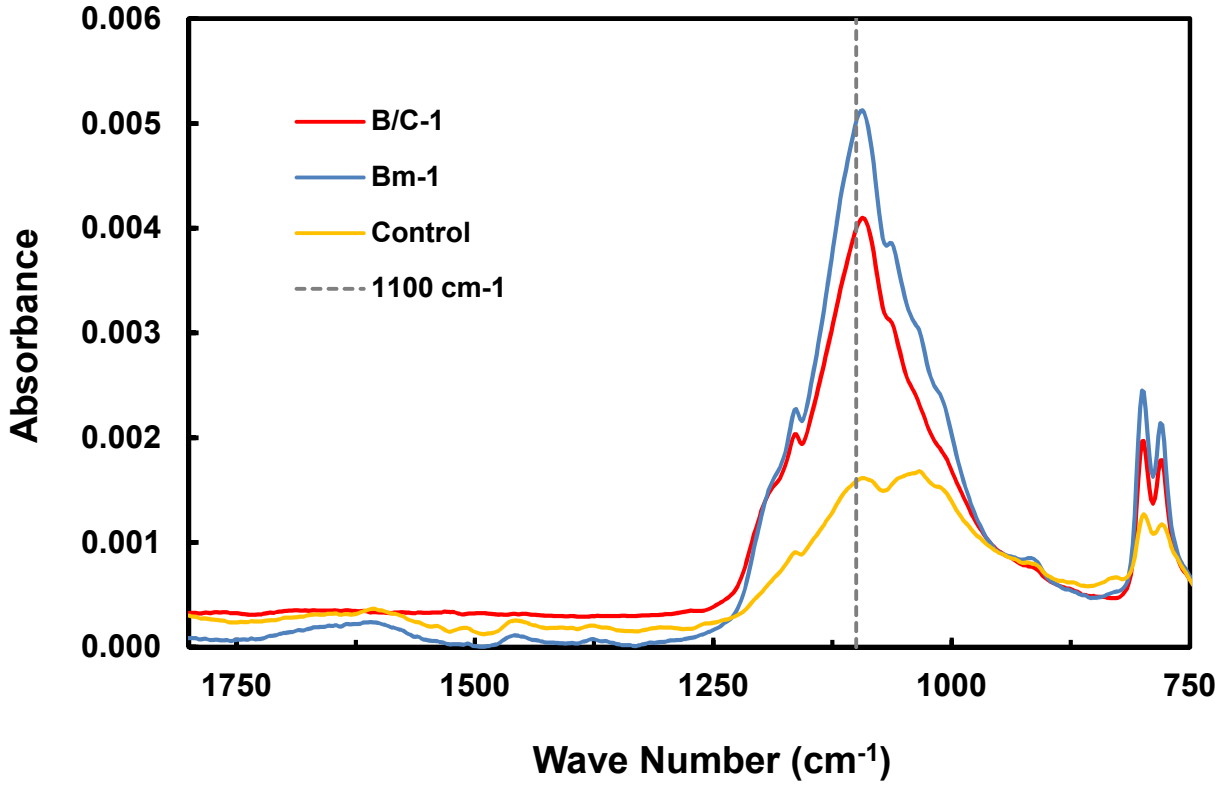

Figure A.1. ATR-FTIR absorbance spectra of AOSM samples with surface precipitate.

APPENDIX B. THE EFFECTS OF AGGREGATED OIL SAND MATERIAL ON THE SATURATION, DRAINAGE, AND FIELD CAPACITY OF RECLAMATION SOILS

B.1 Introduction

The results of Chapter 4 indicate that, regardless of the cause(s), water infiltration rates of air dry aggregated oil sand materials (AOSM) are generally lower than that of their surrounding sandy soil matrix. To further assess the potential effects of AOSM inclusions on the soil moisture dynamics of reclamation profiles, a soil column study was designed. A set of experiments examining the saturation, drainage, and soil water content at field capacity (FC) of pure soil and AOSM/soil combinations were conducted.

B.2 Materials and Methods

This study utilized the same materials of the Aurora Soil Capping Study (ASCS) site, located north of Fort McMurray, AB, that were examined in Chapters 3 and 4. The experiment utilized a set of two acrylic soil columns, with inner diameters of 12.7 cm, and heights of 20 cm and 40 cm for the upper and lower columns respectively. The two columns were stacked vertically, containing at their interface a selectively-permeable nylon membrane with an air-entry value of –3 kPa. Under atmospheric pressure conditions, the nylon membrane allows the passage of water, but not air. This prevents air within the columns from becoming trapped at the interface and affecting the lower boundary condition of the upper column during the saturation and drainage procedures. Any trapped air in the upper column will exit through the top of the column which is open to atmosphere, or through one of the four breather holes (3/16” dia.) that were placed equidistantly along the circumference of the column at a height of 1 cm from its bottom. Air within the lower column must exit through the bottom of the column which is open to atmosphere, or through one of two sets of four breather holes located at heights of 3 cm and 20 cm.

The study design consisted of paired experiments with one control and one AOSM-affected treatment per pair. The first experiment served as the control and contained pure sand in both the

lower and upper soil columns. The second experiment contained the same lower column used in the first treatment (no re-packing), but the upper column was re-packed to contain an air-dry AOSM sample approximately centered within the column. Each paired set of experiments were performed in triplicate with three separate sets of control columns and AOSM samples. The samples were chosen based on their total organic carbon (TOC) contents (i.e., PHC contents) and visual signs of weathering, and were intended to represent three different stages, or extents, of weathering and degradation. The known physical and water repellent properties of the AOSM samples are displayed in Table B.1.

Table B.1.
Physical properties of the aggregated oil sand materials included in upper soil columns.

Soil Columns	AOSM Sample	Stage of Weathering	TOC§ (g 100g^{-1})	CA§ (°)	WDPT§ (s)	Volume (cm^3)	ρ_b (g cm^{-3})
1	A	4	9.6 ± 0.2	128	2010	63	2.05
2	B	1	21.3 ± 3.4	104 ± 20	606 ± 725	164	1.74
3	C	5	5.1 ± 0.1	0 ± 0	1 ± 0	81	1.76

† AOSM = aggregated oil sand material
‡ Stage of weathering of AOSM ranges from 1 (low) to 7 (highly weathered)
§ Values are reported as mean ± standard deviation
¶ TOC = total organic carbon
# CA = contact angle
†† WDPT = water drop penetration time
‡‡ ρ_b = bulk density

All upper and lower soil columns were packed at bulk densities of approximately 1.6 g cm^{-3}, which is somewhat higher than the range of bulk densities observed by Zettl et al. (2011) in natural, coarse-textured soil profiles of the region, and equivalent to the average reclaimed bulk density of the texturally-similar lean oil sand overburden included in the soil profiles of the ASCS site (Pernitsky et al., 2016). A bulk density slightly greater than that of the natural soils was chosen, in order to represent the worst case scenario in terms of reduced porosity due to compaction from heavy machinery during the replacement and reconstruction of the reclaimed soil profiles.

The lower column was packed to its maximum height of 40 cm, in order to ensure a continuum of soil and good contact between the lower and upper columns. The upper column was packed to a height of 18 cm, leaving 2 cm of head space in the top of the column for ponded water application. Once the upper and lower columns were packed and vertically affixed, de-aired tap water was introduced to the top of the upper column. Water was ponded and maintained at an average height of 1.75 cm above the soil surface until approximately 3 pore volumes (9L) of water were introduced. After the disappearance of the ponded water, the columns were left to drain for 48 hours to achieve FC.

During the experiment a time domain reflectometry (TDR) device was used to monitor the volumetric soil water content (θ_v) in the top 6.5 cm of the upper soil column while it was brought to saturation and drained to FC. Triplicate sets of TDR probes were installed to account for variability within each of the columns. After 48 hrs of drainage the columns were assumed to be at FC, which was confirmed by a relatively constant water content through time as revealed by TDR (Fig. B.1). Once FC was reached, the soil columns were detached and their masses recorded. The contents of the upper column were then sampled to determine the water content of the soil profile and its relationship with depth. Sand was removed from the upper column in 2 cm vertical lifts. Each lift was sampled six times (spaced equidistantly within the horizontal cross section of the column), where each sample was composed of approximately 20 to 30 g of wet sand. In order to obtain the gravimetric soil water contents, the wet samples were then dried at 105 °C for 24 hrs and their masses re-determined.

Analysis of variance (ANOVA) were performed on the volumetric water content results obtained from the TDR in order to explore potential differences between probes, as well as differences through time, as drainage occurred. ANOVAs were also used to examine differences in post-drainage (FC) water contents between the pure sand and sand/AOSM columns. Differences were considered significant when $P < 0.05$.

B.3 Results and Discussion

ANOVAs revealed that during the 48 hr drainage period the mean θ_v of the top 6.5 cm of the upper columns were not significantly different, with the exception of control column 1 (Sand 1 in Figure B.1)

which was significantly different than all other control and AOSM treatments. The TDR probes in the upper column of control column 1 were installed immediately after saturation prior to drainage, whereas the probes for all other columns were installed prior to saturation. It is possible that the contact between the probe bodies and soil particles was more effective when installed prior to saturation, because the saturation process allows particles which are disturbed during probe installation to resettle tightly around the probe, resulting in a higher observed water content.

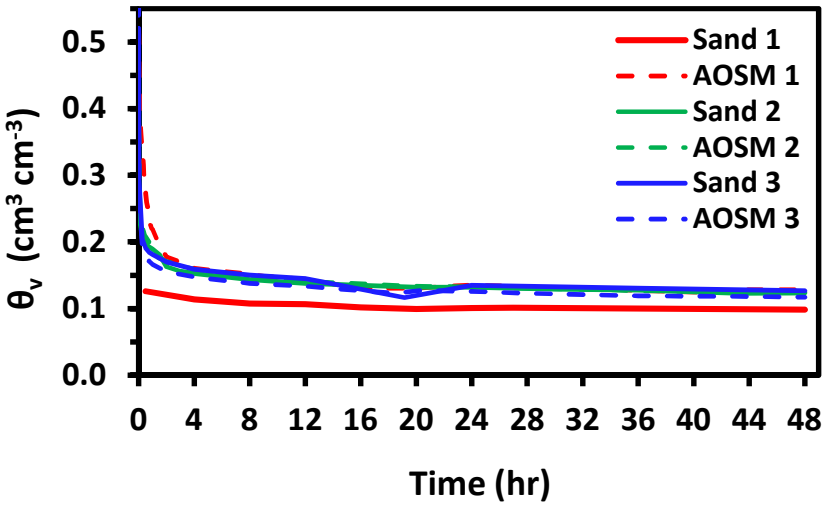

Figure B.1. Post-saturation (drainage) volumetric water content of sand from the upper soil columns. Solid lines are treatments with pure sand; dotted lines are treatments with sand and AOSM.

During drainage, TDR revealed that > 90% of the total water loss in the top 6.5 cm of the upper columns occurred in the first 4 hrs (with the exception of control column 1, which due to its installation method has no saturated water content value for comparison) (Fig. B.1). The θ_v of the top 6.5 cm of the upper columns 48 hrs after drainage (excluding control column 1, θ_v = 0.098 $cm^3\ cm^{-3}$) were fairly consistent with a mean θ_v of 0.124 $cm^3\ cm^{-3}$ and standard deviation of 0.004 $cm^3\ cm^{-3}$.

The results for the gravimetric water content sampling of the upper columns were converted to volumetric water contents, and displayed in Figures B.2A, B.2B, and B.2C. Two of the paired experiments (columns 1 and 3; Figs. B.2A and B.2C) showed lower water contents throughout the majority of the column when AOSM was present, and one (column 2; Fig. B.2B) showed no significant difference between that of the pure sand and AOSM/sand treatments.

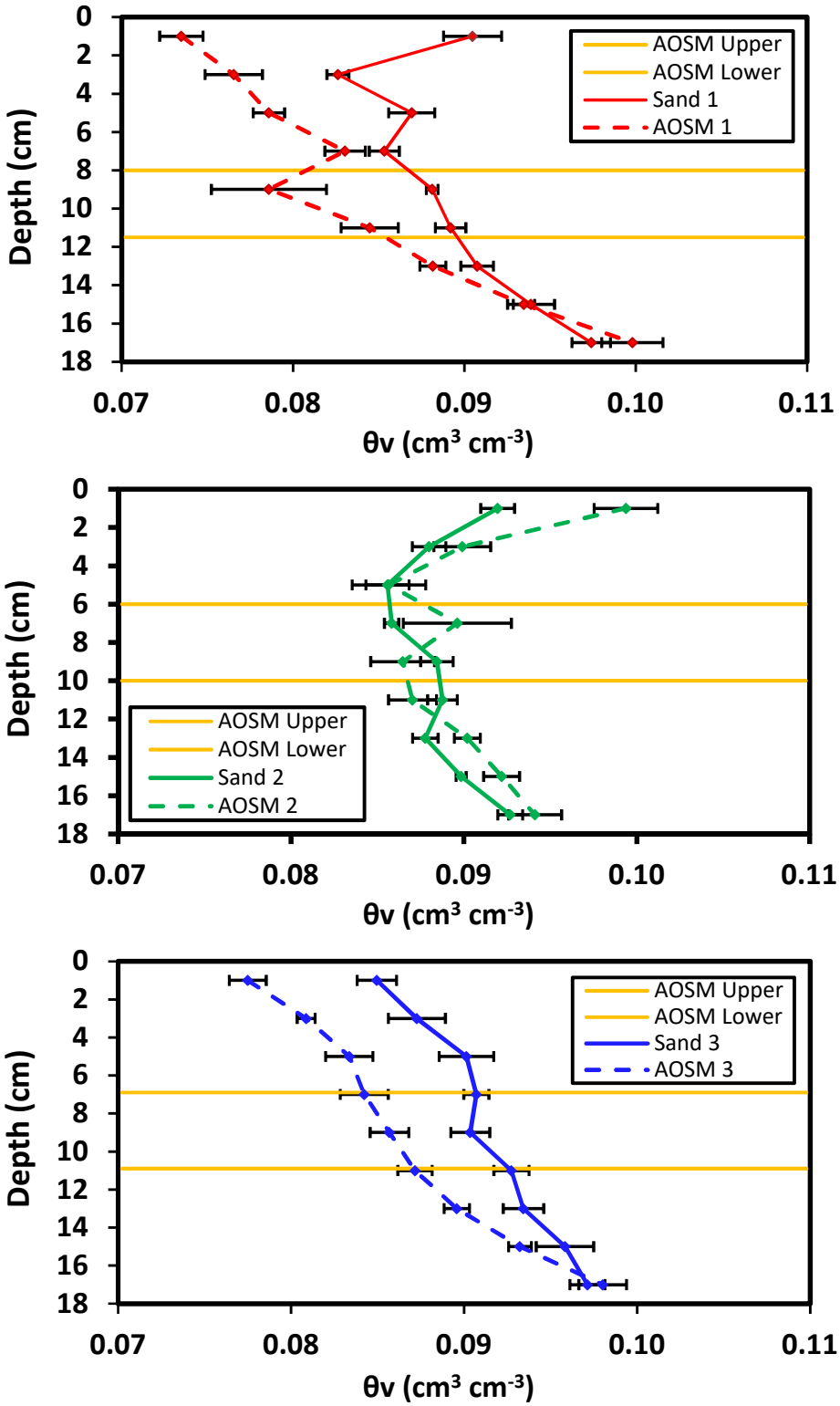

Figure B.2 (A, B, and C). Volumetric water contents with standard deviations, at FC, of sand from the upper soil columns of paired Columns 1, 2, and 3. Solid lines are treatments with pure sand; dotted lines are treatments with sand and AOSM; yellow horizontal lines are the upper and lower depth boundaries of the AOSM inclusions.

It is possible that, due to the significantly lower infiltration capability of the AOSM in comparison to the surrounding soil, air was entrapped above and/or below the inclusions. During saturation, the wetting front should be relatively uniform as it vertically advances through the homogenously packed sand. Once the wetting front reaches the AOSM inclusion, it encounters a flow barrier because the hydraulic conductivity of the AOSM is significantly lower than that of the surrounding sand. As it reaches this hydraulic barrier, water will take the path of least resistance and consequently flow preferentially through the sand surrounding the AOSM inclusion. As the water continues to flow through the sand it will do so in a more or less vertical direction, due to the coarse pore-size distribution and strong influence of gravity on water movement in pores of this size. Therefore, as the wetting front passes the bottom boundary of the AOSM, there may be limited lateral flow, resulting in a dry region directly below the AOSM inclusion.

Similarly, during saturation, air which is occupied in the soil pores must be displaced in order for water to enter the pores. In the current study, as water enters pore spaces, air must exit the column through the breather holes located near its bottom edge. It is possible that, due to the limited porosity and/or pore connectivity of AOSM, the air permeability (in addition to the hydraulic conductivity) may be significantly reduced in AOSM compared to the surrounding sand. This would indicate that as the soil column is being saturated, air is being displaced through the sand portions more rapidly than through the AOSM. This arrangement would enable water to fill the pore spaces of the portions of the column which contained a vertical continuum of sand throughout the height of the column, more rapidly than the portions located above the AOSM. This would create a non-uniform wetting front, allowing water in the portions of sand surrounding the AOSM to reach the depth of the AOSM more rapidly than the water travelling through portions of sand directly above AOSM. Once the wetting front surrounds the lateral surfaces of the AOSM, there are no empty (air-filled) pore spaces connecting the empty pores of the sand above the AOSM to the breather holes at the base of the column. Therefore, the air in the empty pore spaces above the AOSM becomes trapped, limiting the amount of water that can enter these pores, and resulting in comparably lower water contents above the AOSM than in the surrounding soil.

As mentioned, unlike that of Columns 1 and 3, Column 2 showed no significant difference in soil water contents when AOSM was included. To further explore this inconsistency, the experiment for the AOSM/sand treatment for column 2 was repeated. The repeated experiment resulted in significantly greater soil water contents in the AOSM-affected sand than in that of the pure sand treatment, for the soils located at depths below the depth of the AOSM inclusion.

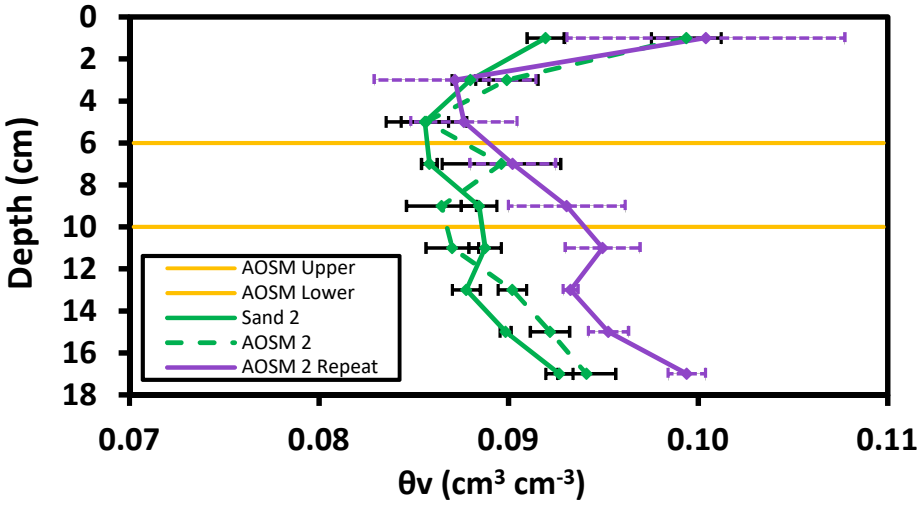

Figure B.3. Volumetric water contents with standard deviations, at FC, of sand from the upper soil columns of the Column 2 measurements. Solid lines are treatments with pure sand; the dotted line is the treatment with sand and AOSM; yellow horizontal lines are the upper and lower depth boundaries of the AOSM inclusion.

The results of this study suggest that AOSM do have the ability to modify the soil water storage in coarse-textured reclamation soils of the region. At equivalent depths, the differences in the soil water contents of the pure sand and AOSM-affected sand treatments are typically less than 1% volumetric water content (0.01 $cm^3 \cdot cm^{-3}$). While this may seem like a relatively small difference, it resulted in considerable differences in the total soil water storage (up to 9%; 9 cm of water in a 1 m soil profile).

B.4 Conclusions

The study outlined in Chapter 4 suggests that due to relatively low infiltration rates, AOSM have the potential to increase soil water storage in overlying soils via the creation of flow barriers, which slow the downward flow of water. The study summarized in this current appendix suggests this isn't always the case and that, due to the wetting patterns experienced in AOSM-affected soils, AOSM may also decrease or have no effect on, the water storage of the overlying soils. These results re-illustrate the variability of the hydraulic properties of AOSM, and imply that additional testing would be beneficial, particularly at the field scale. Nevertheless, this study provides additional confirmation that the presence of AOSM can considerably alter the soil water dynamics of coarse-textured AOSM-affected reclamation soils.

APPENDIX C. ANALYSIS OF VARIANCE OUTPUTS

Table C.1. Analysis of variance (ANOVA) of clay content ($g \bullet 100\ g^{-1}$) of aggregated oil sand material (AOSM) and surrounding soil matrix.

Groups	*Count*	*Sum* ($g \bullet 100\ g^{-1}$)	*Mean* ($g \bullet 100\ g^{-1}$)	*Variance* ($g \bullet 100\ g^{-1}$)
AOSM	41	0.116	0.003	0.000
Soil Matrix	8	3.377	0.422	0.277

Source of Variation	*SS*	*df*	*MS*	*F*	*P-value*	*F critical*
Between Groups	1.177	1	1.177	28.353	2.784×10^{-6}	4.047
Within Groups	1.951	47	0.042			
Total	3.128	48				

Table C.2. Analysis of variance (ANOVA) of sand content ($g \bullet 100\ g^{-1}$) of outer and inner portions of aggregated oil sand material (AOSM).

Groups	*Count*	*Sum* ($g \bullet 100\ g^{-1}$)	*Mean* ($g \bullet 100\ g^{-1}$)	*Variance* ($g \bullet 100\ g^{-1}$)
Outer AOSM	24	2218.556	92.440	19.347
Inner AOSM	17	1601.453	94.203	4.428

Source of Variation	*SS*	*df*	*MS*	*F*	*P-value*	*F critical*
Between Groups	30.940	1	30.940	2.339	0.134	4.091
Within Groups	515.834	39	13.227			
Total	546.774	40				

Table C.3. Analysis of variance (ANOVA) of silt content ($g \bullet 100\ g^{-1}$) of outer and inner portions of aggregated oil sand material (AOSM).

Groups	*Count*	*Sum* ($g \bullet 100\ g^{-1}$)	*Mean* ($g \bullet 100\ g^{-1}$)	*Variance* ($g \bullet 100\ g^{-1}$)
Outer AOSM	24	181.328	7.555	19.351
Inner AOSM	17	98.547	5.797	4.428

Source of Variation	*SS*	*df*	*MS*	*F*	*P-value*	*F critical*
Between Groups	30.770	1	30.770	2.326	0.135	4.091
Within Groups	515.927	39	13.229			
Total	546.697	40				

Table C.4. Analysis of variance (ANOVA) of clay content ($g \bullet 100\ g^{-1}$) of outer and inner portions of aggregated oil sand material (AOSM).

Groups	*Count*	*Sum* ($g \bullet 100\ g^{-1}$)	*Mean* ($g \bullet 100\ g^{-1}$)	*Variance* ($g \bullet 100\ g^{-1}$)
Outer AOSM	24	0.116	0.005	0.001
Inner AOSM	17	0.000	0.000	0.000

Source of Variation	*SS*	*df*	*MS*	*F*	*P-value*	*F critical*
Between Groups	0.0002	1	0.0002	0.7031	0.4069	4.0913
Within Groups	0.0129	39	0.0003			
Total	0.0131	40				

Table C.5. Analysis of variance (ANOVA) of total organic carbon content ($g \bullet 100\ g^{-1}$) of outer and inner portions of aggregated oil sand material (AOSM) used in the water repellency study (Chapter 3).

Groups	*Count*	*Sum* ($g \bullet 100\ g^{-1}$)	*Mean* ($g \bullet 100\ g^{-1}$)	*Variance* ($g \bullet 100\ g^{-1}$)
Outer AOSM	76	566.308	7.451	14.114
Inner AOSM	19	181.566	9.556	10.623

Source of Variation	*SS*	*df*	*MS*	*F*	*P-value*	*F critical*
Between Groups	67.331	1	67.331	5.011	0.028	3.943
Within Groups	1249.732	93	13.438			
Total	1317.063	94				

Table C.6. Analysis of variance (ANOVA) of total organic carbon content ($g \bullet 100\ g^{-1}$) of low- and highly-weathered aggregated oil sand material (AOSM) used in the water repellency study (Chapter 3).

Groups	*Count*	*Sum* ($g \bullet 100\ g^{-1}$)	*Mean* ($g \bullet 100\ g^{-1}$)	*Variance* ($g \bullet 100\ g^{-1}$)
Low	21	273.306	13.015	16.740
High	14	91.594	6.542	7.195

Source of Variation	*SS*	*df*	*MS*	*F*	*P-value*	*F critical*
Between Groups	351.866	1	351.866	27.109	1.003×10^{-5}	4.139
Within Groups	428.336	33	12.980			
Total	780.202	34				

Table C.7. Analysis of variance (ANOVA) of total organic carbon content (g•100 g^{-1}) of low- and medium-weathered aggregated oil sand material (AOSM) used in the water repellency study (Chapter 3).

Groups	*Count*	*Sum* (g•100 g^{-1})	*Mean* (g•100 g^{-1})	*Variance* (g•100 g^{-1})
Low	21	273.306	13.015	16.740
Medium	60	382.974	6.383	2.976

Source of Variation	*SS*	*df*	*MS*	*F*	*P-value*	*F critical*
Between Groups	684.120	1	684.120	105.896	3.030×10^{-16}	3.962
Within Groups	510.364	79	6.460			
Total	1194.484	80				

Table C.8. Analysis of variance (ANOVA) of total organic carbon content (g•100 g^{-1}) of all outer and inner portions of aggregated oil sand material (AOSM) used in the infiltration study (Chapter 4).

Groups	*Count*	*Sum* (g•100 g^{-1})	*Mean* (g•100 g^{-1})	*Variance* (g•100 g^{-1})
Outer AOSM	69	526.287	7.627	15.085
Inner AOSM	19	181.566	9.556	10.623

Source of Variation	*SS*	*df*	*MS*	*F*	*P-value*	*F critical*
Between Groups	55.422	1	55.422	3.916	0.051	3.952
Within Groups	1216.977	86	14.151			
Total	1272.398	87				

Table C.9. Analysis of variance (ANOVA) of total organic carbon content (g•100 g^{-1}) of the outer and inner portions of aggregated oil sand material (AOSM) that were tested at multiple depths in the infiltration study (Chapter 4).

Groups	*Count*	*Sum* (g•100 g^{-1})	*Mean* (g•100 g^{-1})	*Variance* (g•100 g^{-1})
Outer AOSM	18	132.737	7.374	6.642
Inner AOSM	19	181.566	9.556	10.623

Source of Variation	*SS*	*df*	*MS*	*F*	*P-value*	*F critical*
Between Groups	44.000	1	44.000	5.064	0.031	4.121
Within Groups	304.119	35	8.689			
Total	348.119	36				

Table C.10. Analysis of variance (ANOVA) of total organic carbon content (g•100 g^{-1}) of low- and highly-weathered aggregated oil sand material (AOSM) used in the infiltration study (Chapter 4).

Groups	*Count*	*Sum* (g•100 g^{-1})	*Mean* (g•100 g^{-1})	*Variance* (g•100 g^{-1})
Low	21	273.306	13.015	16.740
High	12	81.305	6.775	7.887

Source of Variation	*SS*	*df*	*MS*	*F*	*P-value*	*F critical*
Between Groups	297.263	1	297.263	21.860	5.433×10^{-5}	4.160
Within Groups	421.553	31	13.598			
Total	718.816	32				

Table C.11. Analysis of variance (ANOVA) of total organic carbon content (g•100 g^{-1}) of low- and medium-weathered aggregated oil sand material (AOSM) used in the infiltration study (Chapter 4).

Groups	*Count*	*Sum* (g•100 g^{-1})	*Mean* (g•100 g^{-1})	*Variance* (g•100 g^{-1})
Low	21	273.306	13.015	16.740
Medium	55	353.242	6.423	3.113

Source of Variation	*SS*	*df*	*MS*	*F*	*P-value*	*F critical*
Between Groups	660.394	1	660.394	97.175	4.062×10^{-15}	3.970
Within Groups	502.897	74	6.796			
Total	1163.291	75				

Table C.12. Analysis of variance (ANOVA) of mean water infiltration rates ($cm \bullet hr^{-1}$) of soil matrix at different water pressure head (h) values.

Groups	*Count*	*Sum* ($cm \bullet hr^{-1}$)	*Mean* ($cm \bullet hr^{-1}$)	*Variance* ($cm \bullet hr^{-1}$)
h = – 20 cm	2	77.412	38.706	3.389
h = – 13 cm	6	95.494	15.916	255.991
h = – 7 cm	6	284.948	47.491	1309.317
h = – 3 cm	6	2324.351	387.392	70848.418
h = – 1.5 cm	2	1859.680	929.840	64301.623
h = – 0.1 cm	2	2289.426	1144.713	83060.362

Source of Variation	*SS*	*df*	*MS*	*F*	*P-value*	*F critical*
Between Groups	3266630	5	653326	23.084	3.008×10^{-7}	2.773
Within Groups	509434	18	28302			
Total	3776064	23				

Table C.13. Analysis of variance (ANOVA) of mean water and ethanol infiltration rates ($cm \bullet hr^{-1}$) of aggregated oil sand material at a pressure head value of – 1.5 cm H_2O.

Groups	*Count*	*Sum* ($cm \bullet hr^{-1}$)	*Mean* ($cm \bullet hr^{-1}$)	*Variance* ($cm \bullet hr^{-1}$)
Ethanol	4	265.349	66.337	663.547
Water	4	76.963	19.241	171.595

Source of Variation	*SS*	*df*	*MS*	*F*	*P-value*	*F critical*
Between Groups	4436.131	1	4436.131	10.624	0.017	5.987
Within Groups	2505.427	6	417.571			
Total	6941.558	7				

Table C.14. Analysis of variance (ANOVA) of mean water and ethanol infiltration rates ($cm \bullet hr^{-1}$) of aggregated oil sand material at a pressure head value of – 0.1 cm H_2O.

Groups	*Count*	*Sum* ($cm \bullet hr^{-1}$)	*Mean* ($cm \bullet hr^{-1}$)	*Variance* ($cm \bullet hr^{-1}$)
Ethanol	4	754.846	188.711	12735.441
Water	4	122.577	30.644	304.354

Source of Variation	*SS*	*df*	*MS*	*F*	*P-value*	*F critical*
Between Groups	49970.473	1	49970.473	7.664	0.032	5.987
Within Groups	39119.384	6	6519.897			
Total	89089.858	7				

Table C.15. Analysis of variance (ANOVA) of mean water infiltration rates ($cm \bullet hr^{-1}$) of aggregated oil sand material at different water pressure head (h) values.

Groups	*Count*	*Sum* ($cm \bullet hr^{-1}$)	*Mean* ($cm \bullet hr^{-1}$)	*Variance* ($cm \bullet hr^{-1}$)
h = – 20 cm	61	1279.394	20.974	164.188
h = – 13 cm	61	1215.648	19.929	222.268
h = – 7 cm	61	1186.960	19.458	131.362
h = – 3 cm	61	1347.886	22.096	268.236
h = – 1.5 cm	61	1281.923	21.015	305.225
h = – 0.1 cm	60	1524.945	25.416	307.867

Source of Variation	*SS*	*df*	*MS*	*F*	*P-value*	*F critical*
Between Groups	1377.495	5	275.499	1.182	0.317	2.239
Within Groups	83640.880	359	232.983			
Total	85018.375	364				

Table C.16. Analysis of variance (ANOVA) of mean ethanol infiltration rates ($cm \bullet hr^{-1}$) of aggregated oil sand material at different water pressure head (h) values.

Groups	*Count*	*Sum* ($cm \bullet hr^{-1}$)	*Mean* ($cm \bullet hr^{-1}$)	*Variance* ($cm \bullet hr^{-1}$)
h = – 13 cm	4	208.121	52.030	1889.316
h = – 7 cm	4	159.662	39.915	325.668
h = – 3 cm	4	216.041	54.010	157.316
h = – 1.5 cm	4	265.349	66.337	663.547
h = – 0.1 cm	4	754.846	188.711	12735.441

Source of Variation	*SS*	*df*	*MS*	*F*	*P-value*	*F critical*
Between Groups	60276.803	4	15069.201	4.777	0.011	3.056
Within Groups	47313.864	15	3154.258			
Total	107590.67	19				

Table C.17. Analysis of variance (ANOVA) of mean water infiltration rates ($cm \bullet hr^{-1}$) of aggregated oil sand material (AOSM) and surrounding soil matrix at a pressure head value of – 7 cm H_2O.

Groups	*Count*	*Sum* ($cm \bullet hr^{-1}$)	*Mean* ($cm \bullet hr^{-1}$)	*Variance* ($cm \bullet hr^{-1}$)
AOSM	61	1186.960	19.458	131.362
Soil Matrix	6	284.948	47.491	1309.317

Source of Variation	*SS*	*df*	*MS*	*F*	*P-value*	*F crit*
Between Groups	4293	1	4292.855	19.339	4.146×10^{-5}	3.989
Within Groups	14428	65	221.974			
Total	18721	66				

Table C.18. Analysis of variance (ANOVA) of mean water infiltration rates ($cm \bullet hr^{-1}$) of aggregated oil sand material (AOSM) and surrounding soil matrix at a pressure head value of – 3 cm H_2O.

Groups	*Count*	*Sum* ($cm \bullet hr^{-1}$)	*Mean* ($cm \bullet hr^{-1}$)	*Variance* ($cm \bullet hr^{-1}$)
AOSM	61	1347.886	22.096	268.236
Soil Matrix	6	2324.351	387.392	70848.418

Source of Variation	*SS*	*df*	*MS*	*F*	*P-value*	*F critical*
Between Groups	728945	1	728945	127.942	5.286×10^{-17}	3.989
Within Groups	370336	65	5697			
Total	1099281	66				

Table C.19. Analysis of variance (ANOVA) of mean water infiltration rates ($cm \bullet hr^{-1}$) of aggregated oil sand material (AOSM) and surrounding soil matrix at a pressure head value of – 1.5 cm H_2O.

Groups	*Count*	*Sum* ($cm \bullet hr^{-1}$)	*Mean* ($cm \bullet hr^{-1}$)	*Variance* ($cm \bullet hr^{-1}$)
AOSM	61	1281.923	21.015	305.225
Soil Matrix	2	1859.680	929.840	64301.623

Source of Variation	*SS*	*df*	*MS*	*F*	*P-value*	*F critical*
Between Groups	1599483	1	1599483	1181	1.259×10^{-41}	3.998
Within Groups	82615	61	1354			
Total	1682099	62				

Table C.20. Analysis of variance (ANOVA) of mean water infiltration rates ($cm \bullet hr^{-1}$) of aggregated oil sand material (AOSM) and surrounding soil matrix at a pressure head value of – 0.1 cm H_2O.

Groups	*Count*	*Sum* ($cm \bullet hr^{-1}$)	*Mean* ($cm \bullet hr^{-1}$)	*Variance* ($cm \bullet hr^{-1}$)
AOSM	60	1524.945	25.416	307.867
Soil Matrix	2	2289.426	1144.713	83060.362

Source of Variation	*SS*	*df*	*MS*	*F*	*P-value*	*F critical*
Between Groups	2424825	1	2424825	1437	1.273×10^{-43}	4.001
Within Groups	101225	60	1687			
Total	2526050	61				